Characterizing the Role of Paraoxonase 2 (PON2) in the Brain: Phenotypic Analysis and Modulating Factors

Jacqueline M. Garrick

A dissertation

submitted in partial fulfillment of

requirements for the degree of

Doctor of Philosophy

University of Washington

2021

Reading Committee:

Lucio G. Costa, Chair

Clement E. Furlong

Terrance J. Kavanagh

Program Authorized to Offer Degree:

Environmental & Occupational Health Sciences

University of Washington

Abstract

Characterizing the Role of Paraoxonase 2 (PON2) in the Brain: Phenotypic Analysis and Modulating Factors

Jacqueline M. Garrick

Chair of Supervisory Committee:

Professor Lucio G. Costa

Department of Environmental and Occupational Health Sciences, Toxicology

Paraoxonase 2 (PON2), one of three members of the paraoxonase gene family, is a ubiquitously expressed intracellular antioxidant enzyme. Primarily located at the inner mitochondrial membrane, it is thought to maintain redox homeostasis at the mitochondrial level and support proper cellular function. In the brain, PON2 is expressed highest in dopaminergic regions, such as the striatum and substantia nigra. *In-vitro* experiments with PON2 deficient primary cells have demonstrated it to be an important antioxidant in the brain, with deficient neural cells more sensitive to oxidative damage. In the general population, common polymorphisms known to affect the enzymatic activity of PON2 have been associated with increased risk for myocardial infarction as well as Alzheimer's disease, highlighting a direct impact on human health. Despite evidence for PON2 as an important antioxidant in the brain with human health impacts, little attention has focused on the role of PON2 in the brain and what global effects deficiency may have.

In my dissertation work, I further characterized PON2 deficiency in the brain to address important knowledge gaps. First, I characterized the developmental expression of PON2, demonstrating that PON2 is differentially expressed over early life development and suggests potential windows of susceptibility to oxidative damage in the developing and aging nervous system when PON2 expression is lowest. Second, I evaluated behavioral endpoints and transcript changes with RNA-Seq of three discrete regions (cerebral cortex, striatum, cerebellum) with PON2 deficiency, finding that PON2 deficient mice have motor deficits and significant changes to many RNA processing pathways. Additionally, PON2 deficiency abolishes sex-specific expression patterns observed in the brain. Building on previous work showing PON2 expression is highest in the dopaminergic regions and may play a role in the dopaminergic system, I compared the expression of key dopaminergic genes in wild type (WT) and PON2 deficient striatal tissue, finding that multiple dopaminergic pathway genes were impacted by PON2 deficiency at the transcript level. Quinpirole, a dopamine receptor 2 (DRD2) agonist, was able to significantly increase the expression of PON2 *in-vitro*, while fenoldopam, a dopamine receptor 1/5 (DRD1/5) agonist did not, suggesting PON2 plays a role in DRD2-specific signaling. Finally, I collected preliminary data suggesting PON2 deficiency impacts numerous targets relevant to neurodegenerative disease, supporting additional research in the aging nervous system.

Taken together, the findings of this dissertation identify that PON2 deficiency has significant impacts on the brain at both a biochemical and phenotypic level. These results address important gaps in the literature regarding PON2 deficiency in the central nervous system and supports further avenues of study to analyze additional pathways and behavioral endpoints, as well as further investigation of PON2 polymorphisms in the population.

Table of Contents

List of Figures and Tables

Acknowledgements

First, I would like to thank my doctoral advisor, Lucio G. Costa, for his mentorship and support. I would also like to thank Khoi Dao, my lab mom and the heart of the Costa lab, for her invaluable help over the years. I am grateful to the other members of the Costa lab as well, both past and present, for their encouragement and guidance.

This work was also supported by members of the Furlong lab, who assisted me with troubleshooting and served as an excellent resource for this project. Thank you, Clem, and Judit for your additional mentorship and being great collaborators.

Thank you to my dissertation committee members, Drs. Toby B. Cole, Lucio G. Costa, Clement E. Furlong, Terrance J. Kavanagh, Dianne F. Lattemann, and Robert A. Steiner for your helpful suggestions and patience throughout the years.

Finally, I would like to recognize the organizations that funded my work and allowed me to continue my studies:

National Institute of Environmental Health Sciences

ARCS Foundation

UW Department of Environmental and Occupational Health Sciences

Dedication

I would not be here without the loving support of my husband, Jon, who has been the best traveling companion for this whacky life adventure. Thanks for keeping me (relatively) sane and doing all the housework while I wrote this dissertation. I cannot wait to see where the next adventure takes us, and I am beyond fortunate to have found my soulmate. I must also give recognition to my two old lady cats, Piglet and Pancake, who have helped in their own special way—mostly by begging for food at the worst possible times. I miss you Piggy!

To my parents, Kerry and Steve: thank you for supporting me in everything I have done. When I packed up my car and moved to Washington, I received nothing but blind encouragement. Looking back, I probably should have received *some* questions, but it all worked out in the end. Thank you for only asking me a handful of times when I was going to graduate, and never being disappointed with the answer.

Finally, thank you to my friends who made Seattle my home and who graciously listened to me complain about the same things repeatedly over the years. A special thank you to Connie, Vanessa, and Laura, for your friendship and enduring graduate school life with me.

Chapter 1

Introduction

1.1 – Paraoxonase Gene Family

The paraoxonase gene family consists of three closely related genes, PON1, PON2 and PON3, aligned in tandem on mouse chromosome 6 and the long arm of human chromosome 7q21-22 (Primo-Parmo et al., 1996). These genes share nearly 70% sequence homology and phylogenic analysis suggests PON2 to be the oldest of the PON enzymes, from which PON1 and 3 evolved (Sorenson et al., 1995; Draganov & La Du 2004). While the gene family is named for the phosphotriesterase activity of PON1 to hydrolyze paraoxon, the active metabolite of the organophosphate pesticide parathion, PON2 does not hydrolyze paraoxon and functions minimally as a secondary esterase (Draganov et al., 2005). However, PON2, in addition to PON1 and 3, has been observed to hydrolyze methyl-paraoxon, the metabolite of methyl-parathion (Bar-Rogovsky et al., 2013). All three PONs possess lactonase activity, exhibiting both distinct and overlapping substrates for lactone hydrolysis. Endogenous substrates have been identified for PON1 and 3 as various esters, but the exact physiological purpose of their hydrolyzation and function is not fully understood (Furlong et al., 2016).

Further differentiating the paraoxonases are their localization and expression profiles. PON1 is primarily synthesized in the liver and circulates through the body in plasma attached to high-density lipoproteins (HDLs), depositing into tissues as needed (Deakin et al., 2002; Marsillach et al., 2008). PON3 functions in a similar manner, being produced in the liver and circulating in plasma bound to HDL, but differs from PON1 in that it is also directly synthesized in tissues such as the kidneys and intestine and found intracellularly in the mitochondria (Reddy

et al., 2000; Rothem et al., 2007; Marsillach et al., 2008). PON2 provides the most unique expression profile of the PONs, as it does not circulate and instead is an intracellular enzyme that is ubiquitously expressed in most tissues examined (Mochizuki et al., 1998; Ng et al., 2001; Marsillach et al., 2008). While the PONs exhibit different expression profiles and functions, most research into this gene family has focused on PON1 for its ability to hydrolyze organophosphates. PON2 and PON3, possessing minimal phosphotriesterase activity, have received modest attention in the literature.

1.2 – Paraoxonase 2 (PON2)

As discussed previously, PON2 is ubiquitously expressed and found in most tissues examined, with transcript and/or protein expression measured in heart, lung, kidney, brain, liver, intestine, pancreas, muscle, placenta, stomach, testis, endothelial cells, and macrophages (Ng et al., 2001; Levy et al., 2007; Marsillach et al., 2008; Giordano et al., 2011). In mice, PON2 levels are highest in the lung, small intestine, liver and heart, with lower levels found in the kidney, testis, and brain (Giordano et al., 2011). Subcellular localization studies suggest PON2 exhibits tissue-specific localization patterns, associating with the nuclear membrane and endoplasmic reticulum in vascular cells (Horke et al., 2007), microsomes and lysosomes in the jejunum (Levy et al., 2007), the cell membrane and mitochondria in neurons and astrocytes (Giordano et al., 2011), and the mitochondria in liver and heart tissue (Devarajan et al., 2011). In addition to tissue-specific localization, cellular state may also impact the localization of PON2, as oxidative stress has been shown to translocate PON2 to the plasma membrane *in-vitro* (Hagmann et al., 2014). In the mitochondria, PON2 associates with the inner mitochondrial membrane and interacts with Coenzyme Q10 and Complex III of the electron transport chain (Devarajan et al.,

2011). Mitochondria are a significant source of oxidative stress for the cell and generate superoxide ($O2^-$), a reactive oxygen anion, as a by-product of oxidative phosphorylation within the electron transport chain (Higgins et al., 2010). This leads to the production of hydrogen peroxide (H_2O_2), another reactive oxygen species (ROS), which can further produce hydroxyl radicals and damage cellular components (Kehrer & Klotz 2015). Given the mitochondrial localization and its interaction with Complex III, PON2 is proposed prevent the formation of these radicals produced during oxidative phosphorylation to mitigate oxidative stress in the mitochondria, but it is unable to scavenge the radicals once they are formed (Altenhöfer et al., 2010). Experimental evidence supporting this role shows PON2 deficiency leads to mitochondrial dysfunction (Devarajan et al., 2011), with deficient cells displaying higher susceptibility to oxidative damage upon exposure to hydrogen peroxide (H_2O_2) and 2,3-dimethoxy-1,4-naphthoquinone (DMNQ) (Giordano et al., 2011). Two single-nucleotide variants (SNVs) in PON2 have been identified in humans, an alanine-to-glycine substitution at position 147, and a serine-to-cysteine substitution at position 311 (Mochizuki et al., 1998). The S311C variant is associated with multiple diseases in epidemiological studies, such as cardiovascular disease (CVD) (Chen et al., 2013), diabetes (Mackness et al., 2005), stroke (Li et al., 2012), Alzheimer's disease (Shi et al., 2004), and higher mortality after myocardial infarction (Marchegiani et al., 2009). Although the full impact of these SNVs on PON2 functionality has yet to be understood, the S311C variant has been shown to impair lactonase activity (Stoltz et al., 2009).

As PON2 functions as a cellular protectant in the mitochondria, this exerts an anti-apoptotic effect and provides a protective function that can be exploited by cancerous cells (Witte et al., 2011). PON2 has been found upregulated in tumors from a variety of tissues, such

as bladder (Bacchetti et al., 2017), pancreatic (Nagarajan et al., 2017), gastric (Wang et al., 2019) and skin (Bacchetti et al., 2020) tumors, as well as a host of other investigated solid tumors (Shakhparonov et al., 2018). Higher PON2 expression in tumors generally correlates with a poorer patient prognosis (Witte et al., 2012), with PON2 experimentally found to protect cancerous cells from radio- and chemotherapy treatments (Krüger et al., 2015, Krüger et al., 2016, Shakhparonov et al., 2018). However, in ovarian cancer, PON2 overexpression has been found to impede tumor growth by inhibiting insulin like growth factor-1 (IGF-1) expression and signaling (Devarajan et al., 2018), suggesting PON2 may act as a tumor suppressor or promoter in a tissue-dependent manner. Given the current work examining the role of PON2 in cancer development and progression, concerns have been raised for pharmaceutical interventions aimed at increasing PON2 expression for cellular protection, as they may have unintended oncological consequences. Conversely, this work also points to PON2 as a possible target for novel cancer therapeutics in specific tumor types. To this end, further study to understand the underlying mechanisms of PON2 and its role in different organ systems will be critical to inform its potential use for therapeutic targeting.

Of the PON family, PON2 has the highest hydrolytic activity for acyl-homoserine lactones (acyl-HCL), molecules which function as bacterial quorum-sensing factors for *Pseudomonas aeruginosa* bacteria (Draganov et al., 2005). Quorum-sensing is a cell-to-cell communication system utilized by a variety of bacteria to regulate biofilm formation, virulence factor production, and population growth (Juhas et al., 2005). PON2 hydrolyzes and degrades these signaling factors, reducing the virulence of *P. aeruginosa* infection (Teiber et al., 2008) and affecting the host inflammatory response (Horke et al., 2010). PON2 deficiency significantly increases the amount of quorum-sensing molecules in airway epithelial cells (Stoltz et al., 2007)

and reduces *P. aeruginosa* bacterial clearance in the lungs and spleen (Devarajan et al., 2013), supporting an important role for PON2 in the lungs to prevent bacterial infection. This role for PON2 is owed in-part to its ability as an antioxidant, as PON2 deficient macrophages have increased oxidative stress and reduced phagocytic function, both of which are reversible by antioxidant treatment (Devarajan et al., 2013). Looking beyond quorum-sensing, the lactonase activity of PON2 has received minimal attention in the literature and the importance of its lactonase role in other systems beyond the lung is not fully understood.

Pathological consequences of PON2 deficiency have been investigated in the cardiovascular system, with PON2 mRNA and protein expression being found lower in plaques compared to adjacent non-plaque regions in the atherosclerotic lesions of patients (Fortunato et al., 2008). Supporting these findings, PON2 deficient mice develop exacerbated atherosclerotic lesions compared to wildtype (Devarajan et al., 2011). A proposed mechanism for this exacerbation is uncontrolled lipid accumulation in macrophages, leading to foam cell formation. PON2 has been found to inhibit lipid accumulation by modulating the activity, but not expression levels, of microsomal acyl-CoA:diacylglycerol acyltransferase 1 (DGAT1). In a PON2 deficient state, DGAT1 activity is increased and the rate of triglyceride synthesis increases. This activity modulation of DGAT1 is thought to be dependent on the antioxidant functionality of PON2, as incubation of PON2 deficient macrophages with another antioxidant, superoxide dismutase (SOD), can rescue the cells and reduce triglyceride synthesis (Shih & Lusis 2009, Rosenblat et al., 2009). The antioxidant capacity of PON2 is also important in the renal system, where it regulates oxidative stress in the renal proximal tubules (RPTs) and helps to maintain hemostatic blood pressure levels—further discussion of PON2 in the renal system can be found in chapter 4.

Investigation of PON2 in the brain has further supported its role as an important antioxidant. PON2 deficient neurons and astrocytes exhibit significantly higher levels of ROS when exposed to oxidative compounds H_2O_2 and DMNQ. Deficient striatal neurons and astrocytes also displayed higher levels of oxidative stress compared to those derived from the cerebellum, suggesting the striatum may be at a higher risk with PON2 deficiency (Giordano et al., 2011). PON2 has also been found to have sex-specific expression differences, with females expressing significantly more PON2 than males. This is thought to occur through estrogen receptor signaling, as ovariectomized females have similar levels of PON2 as males and exposure to estradiol increases PON2 protein levels. Furthermore, mechanistic work supports that signaling through estrogen receptor alpha, but not estrogen receptor beta, is responsible for the increase in PON2 expression (Giordano et al., 2013). The phytoestrogen quercetin has also been found to increase PON2 expression in neuronal cells and protect them from ROS when exposed to oxidants, providing evidence for exogenous compounds to modulate PON2 expression (Costa et al., 2013). Looking at binding partners, DJ-1 (PARK7) has been identified as interacting with PON2 in the brain. DJ-1 is noted as a Parkinson's disease (PD)-related gene and demonstrated to protect cells in oxidative stress models of PD *in-vitro* and *in-vivo,* with DJ-1 deficiency causing significant oxidative stress (Gu et al., 2009; Inden et al., 2006). Interestingly, PON2 can rescue oxidative hypersensitivity caused by DJ-1 deficiency *in-vitro,* and interaction with PON2 appears to be one of the ways DJ-1 exerts its antioxidant function (Parsanejad et al., 2014). While these studies have provided exciting evidence for an important role of PON2 in the brain, many questions remain on the function of PON2 and the consequences of its deficiency in this system.

1.3 – Redox Homeostasis and Oxidative Stress

Reactive oxygen species (ROS) are produced through endogenous processes within the body and received exogenously, exposing cells constantly to potential oxidative damage. To combat this damage, oxidative compounds are counteracted by the action of antioxidants. Redox homeostasis refers to the balance of these two systems, the pro-oxidant and anti-oxidant, within the cell. When imbalance within this system occurs, cellular function is impacted. An increase in pro-oxidants overwhelming the antioxidant capacity of a cell leads to oxidative stress, which in turn can have a significant impact on the cells function and cause cellular death (Pizzino et al., 2017). Conversely, too much antioxidant activity can create a reductive environment and negatively impact the cell by impairing signaling pathways, differentiation, and programmed apoptosis (D'Autréaux & Toledano 2007; Pizzino et al., 2017). The threshold for dysfunction is different for each cell type and organ system, with some organs able to recover from damage (e.g., regeneration of damaged hepatocytes) and others particularly vulnerable (e.g., permanent neuron loss in the CNS). Increased oxidative stress is associated with numerous disease states, such as cardiovascular disease (Madamanchi et al., 2005; Panth et al., 2016), inflammatory autoimmune disorders (Quiñonez-Flores et al., 2016; Dalmazi et al., 2016), neurodegenerative diseases (Aliev et al., 2014; Gaki & Papavassiliou 2014), cancer (Landriscina et al., 2009), diabetes (Maritim et al., 2003; Asmat et al., 2016), and hypertension (Harrison & Gongora 2009), demonstrating the importance of oxidative stress mitigation and redox balance. As discussed earlier in this chapter, PON2 functions as an antioxidant enzyme and is thought to be crucial to the redox balance of multiple systems, including the heart and brain. Accordingly, understanding the mechanisms and modulation of PON2 are important to further understanding

oxidative pathologies in these systems.

1.4 – Rationale and Objectives of Dissertation Research

PON2 deficiency in the brain has been associated with increased oxidative stress and cellular death *in-vitro* (Giordano et al., 2011; Giordano et al., 2013). As the brain has a limited capacity for the renewal of neurons once they die, PON2 deficiency has the potential for broad deleterious consequences on the nervous system. However, there is limited knowledge on the specifics of these consequences, such as how they impact behavior, global transcription changes, or impacts to critical signaling systems. To address this significant knowledge gap, I proposed to investigate PON2 deficiency in the brain, focusing on three areas: 1) developmental expression, 2) phenotype, and 3) the dopaminergic system.

The hypothesis was that **PON2 is developmentally regulated and PON2 deficiency will have significant impacts to the CNS, specifically in dopaminergic pathways.** The aims of this dissertation were to: **1) Examine PON2 expression over development and investigate PON2 deficiency in the aging nervous system, 2) characterize the behavioral phenotype of PON2 deficiency and investigate global transcriptional changes in the brain, and 3) investigate PON2 deficiency in the dopaminergic system of the CNS.**

In this dissertation, chapter 2 addresses the expression of PON2 in mice over early life development, while chapter 3 describes the behavioral phenotype and regional transcription profile in the brain of PON2 deficient mice. Chapter 4 examines the role of PON2 in the dopaminergic system by measurement of dopaminergic genes in PON2 deficient mice, as well as modulation of PON2 through dopamine receptor signaling. Chapter 5 discusses the effects of

PON2 deficiency in aged mice. Finally, chapter 6 summarizes the conclusions from these studies and provides insight on future directions.

Chapter 2

Developmental Expression of Paraoxonase 2

This chapter contains the research article:

Garrick, J. M., Dao, K., de Laat, R., Elsworth, J., Cole, T. B., Marsillach, J., Furlong, C. E., & Costa, L. G. (2016). Developmental expression of paraoxonase 2. *Chemico-Biological Interactions*, *259*(Pt B), 168–174.

2.1 – Introduction

As reviewed in chapter 1, paraoxonase 2 (PON2) is an intracellular enzyme expressed in most tissues examined and has been shown to exert an antioxidant effect (Ng et al., 2001; Horke et al., 2007; Levy et al., 2007; Horke et al., 2010; Giordano et al., 2010; Giordano et al., 2013), with subcellular localization studies suggesting it localizes primarily to the mitochondrial membrane (Devarajan et al., 2011; Giordano et al., 2011). Mitochondria are a considerable source of oxidative stress (Higgins et al., 2010), and the predominant localization of PON2 in mitochondria supports a role for it to prevent oxidative damage at the mitochondrial level. Increased levels of ROS are associated with numerous disorders such as cancer (Landriscina et al., 2009), cardiovascular disease (Madamanchi et al., 2005; Panth et al., 2016), diabetes (Maritim et al., 2003) and neurodegenerative diseases (Aliev et al., 2014; Gaki &Papavassiliou 2014), highlighting the importance of proper antioxidant control of ROS for mitigating disease.

PON2 is necessary for properly functioning mitochondria, as PON2-deficient mice display mitochondrial dysfunction (Devarajan et al., 2011). In the brain, the loss of PON2 in both neurons and astrocytes impairs their ability to recover from toxic levels of oxidative stress generated by oxidants hydrogen peroxide (H_2O_2) or 2,3-dimethoxy-1,4-naphthoquinone (DMNQ). Glutathione levels are identical in cells from wildtype and PON2 knockout mice,

suggesting that the difference in susceptibility to oxidative stress toxicity is due to PON2 and is not the consequence of other affected pathways (Giordano et al., 2011). Accordingly, PON2 appears to be a critical antioxidant in the CNS, with the loss of PON2 predisposing cells to increased ROS and subsequently death.

In addition to regional differences in the brain, gender differences have been described in PON2 expression (Giordano et al., 2013). Female mice are observed as having higher levels of PON2 than male mice, most likely owing to the differences in estradiol between sexes, as PON2 expression appears to be modulated by estrogens (Giordano et al., 2011). The polyphenolic compound quercetin, a phytoestrogen, also modulates PON2 expression and may utilize similar signaling pathways as estrogen to influence PON2 transcription (Costa et al., 2013). Of further relevance is that, in addition to differential susceptibility to oxidative stress between wild-type and PON2-null mice, significant differences in oxidant susceptibility have been associated with different levels of PON2 expression, exemplified by male and female differences in PON2 levels, or after positive modulation of PON2 by estradiol or quercetin (Giordano et al., 2013; Costa et al., 2013).

Development provides a unique and dynamic cellular environment, with specific implications for toxicant exposure. Young animals are known to be more sensitive to a variety of toxicities, and these exposures can have permanent effects that persist into adulthood. The differential expression of genes during development, as well as the anatomy and functional state of organ systems, are generally responsible for these differences and the creation of windows of susceptibility to toxicants (Bruckner 2000; Scheuplein et al., 2002). Antioxidants have been shown to be developmentally regulated and play an important role in susceptibility to oxidants (Khan & Black 2003), supporting the study of PON2 over development. Feasibly, if specific age

groups demonstrate lower levels of PON2, these ages may be at higher risk for cellular damage via oxidative stress. Further, PON2 has been shown to be hormonally regulated by estradiol (Giordano et al., 2013), which may support a role for PON2 in sexual maturation. The aim of this study was to determine PON2 expression during development in brain and liver and, in the latter, to compare it with that of PON1 and PON3.

2.2 – Results

PON2 Developmental Expression in Brain

PON2 in mouse brain

In a first experiment, we determined whether PON2 sex differences would be observed in whole brain. Fig. 2.1 shows that levels of PON2 protein in whole of brain of female mice (PND 21) were significantly higher than in males. Using a polyclonal antibody from Abcam (ab409969), more than one band is detected (Fig. 2.1B). PON2 is seen at its expected MW of 43 kDa, and this band was quantified in this and all other experiments. Western blot analysis using PON2 knockout brain tissue has shown the 43kDa band to be specific to PON2 with the polyclonal antibody used in this study.

Based on the observed sex difference at PND 21, female mice were utilized for the purposes of this study, due to their higher levels of PON2. Figures 2.2A and 2.2B show PON2 protein and mRNA expression levels, respectively, in whole mouse brain over the course of postnatal development (PND 1, 7, 14, 21, 30 and 60) capturing the developmental scale of neonatal to young adulthood. PON2 protein appears to be lowest directly after birth, steadily increasing with age up

until PND 21. A significant decrease in both protein and mRNA is noted from PND 21 to 30 and continuing to PND 60.

PON2 in the brain of non-human primates

We also measured PON2 protein levels in the ventral caudate region of the brain from African green monkeys across development. The investigated developmental time points were mid-gestation (gestational day 89), late-gestation (gestational day 148), infant (PND 27), juvenile (1.9 years), young adult (5–7 years), and aged (21–30 years). PON2 protein levels were lower at mid-gestation and gradually increased up to infant age (Fig. 2.3A). This was followed by a decrease in the juvenile stage and a stabilization, in which similar levels were found in young adult and in aged monkey brains (Fig. 2.3A). We also investigated sex differences in PON2 expression in brains from non-human primates, with Figs. 2.3B and 2.3C showing a significant difference in PON2 protein level between male and female young adult monkeys, with female expression being higher.

PON2 Developmental Expression in Liver

In addition to the brain, we measured PON2 protein and mRNA levels in liver of female mice of different ages. As shown in Fig. 2.4, PON2 levels increased with age from PND 1 to PND 60. In contrast with the brain, PON2 protein significantly increased with age, but did not exhibit a decrease after PND 21 (Fig. 2.4A). PON2 mRNA levels followed a similar trend of increasing with age, although the sample variability makes interpretation of the mRNA level trend between PND 21 and PND 60 uncertain (Fig. 2.4B).

PON1 and PON3 Developmental Expression in the Liver

For comparison with PON2 developmental expression, PON1 and PON3 protein and mRNA levels were also investigated in this study. PON1 and PON3 are not expressed at significant levels in brain tissue and were therefore only examined in the liver. Figs. 2.5 and 2.6 show PON1 and PON3 expression, respectively, in liver of female mice of different ages. Protein levels of PON1 (Fig. 2.5A) and PON3 (Fig. 2.6A) increased with age from PND 1 to PND 60. Levels of mRNA for PON1 (Fig. 2.5B) and PON3 (Fig. 2.6B) also increased with age from PND 1 to PND 21, but then appeared to stabilize from PND 21 to PND 60.

2.3 – Figures

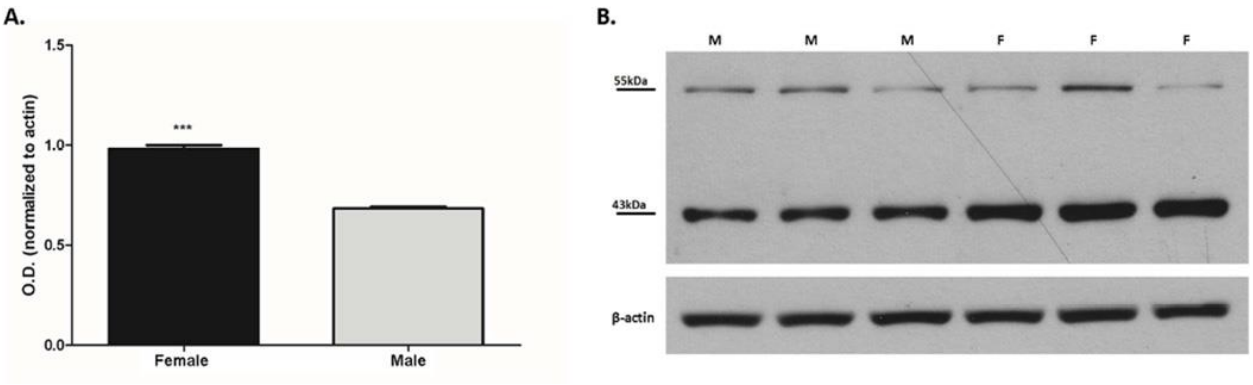

Figure 2.1 - PON2 protein levels in whole brain of mice. A. Quantification of PON2 protein in whole brain of female and male PND 21 mice after normalization to β-actin. Results show the means (± SE) of 3 animals/sex. Significantly different from male, *** $p < 0.001$. (Student's t-test). **B**. Western blots of the same brain samples. PON2 is seen at ~43kDa.

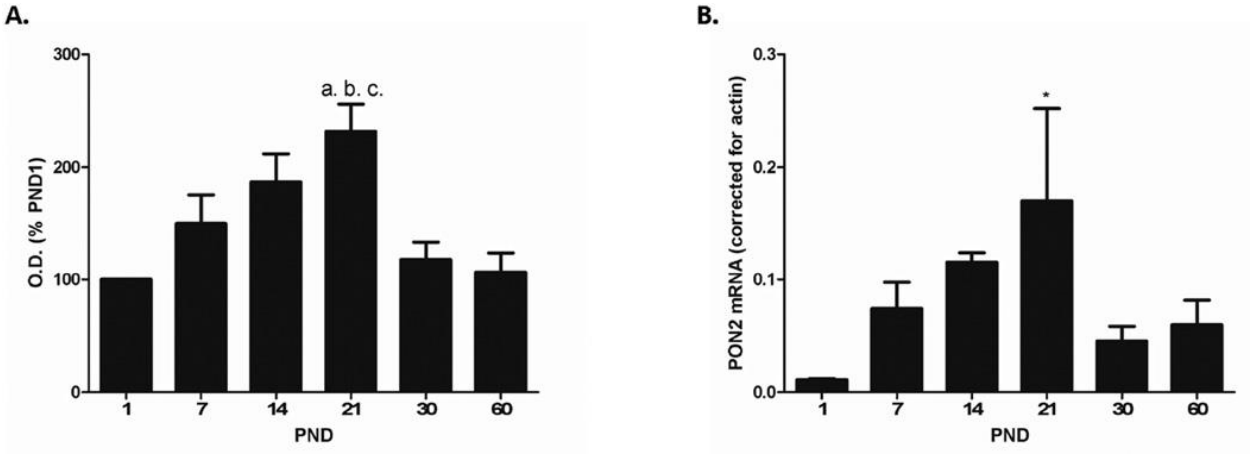

Figure 2.2 - PON2 protein and mRNA levels in brain of female mice during postnatal development. A. Quantification of PON2 protein after normalization to total protein. Results are expressed as percentage of PND 1 optical density (mean ± SE, with n = 4). a, b, c: significantly different from PND 1, PND 30, and PND 60, respectively (all $p < 0.01$). **B**. Levels of PON2 mRNA normalized for β-actin. Results represent the mean (± SE) of 3–4 mice. Significantly different from PND 1, * $p < 0.05$.

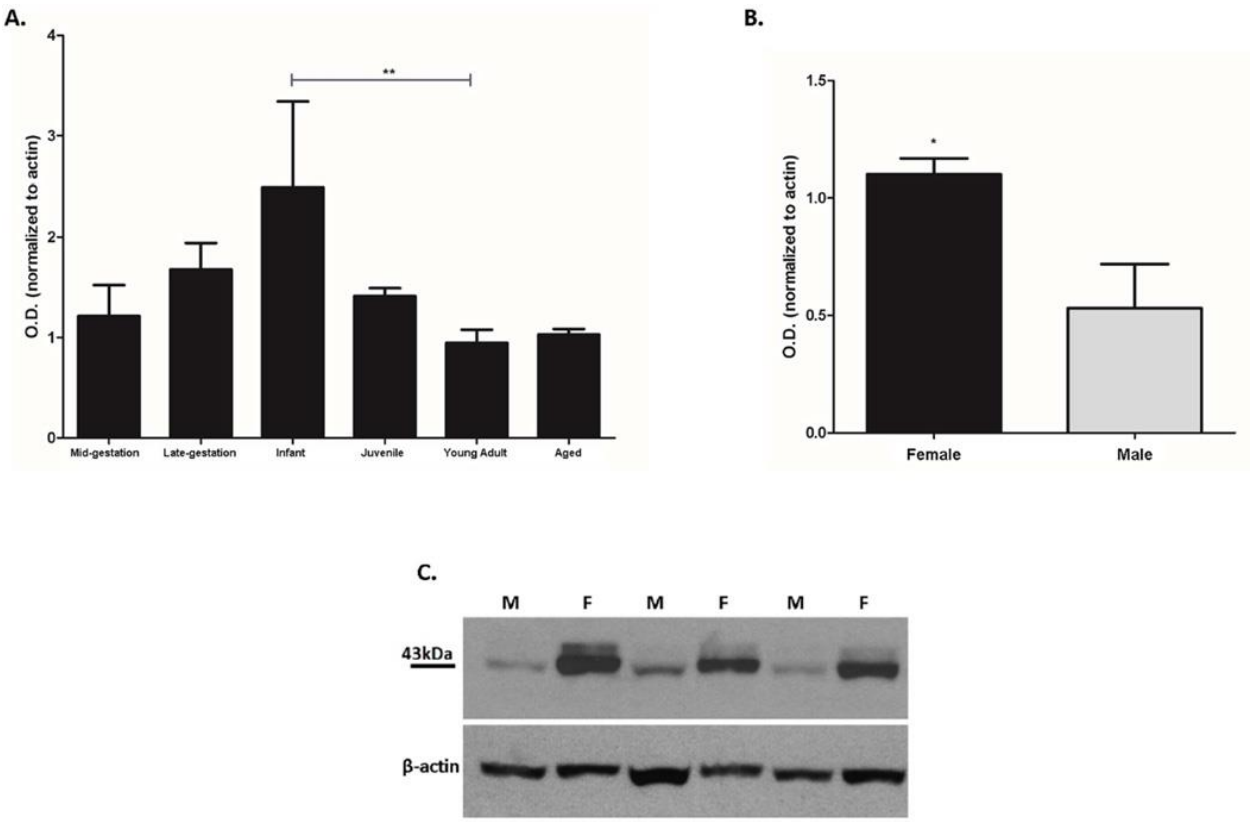

Figure 2.3 - PON2 protein levels in brain of non-human primates. **A**. Quantification of PON2 protein in brain (ventral caudate) of African green monkeys, after normalization to β-actin. Results represent the mean (± SE) with n = 5 (midgestation, late-gestation, infant and aged) 8 (juvenile) and 11 (young adult). Samples are mixed gender. Infant and juvenile stage significantly different, ** $p < 0.01$ **B**. Quantification of PON2 protein in brain (ventral caudate) of male and female young-adult monkeys after normalization to β-actin. Results show the mean (± SE) of 4–6 samples for each group. Significantly different from male, * $p < 0.05$ (Student t-test). **C**. Representative Western blot of monkey brain samples. PON2 is seen at ~43kDa.

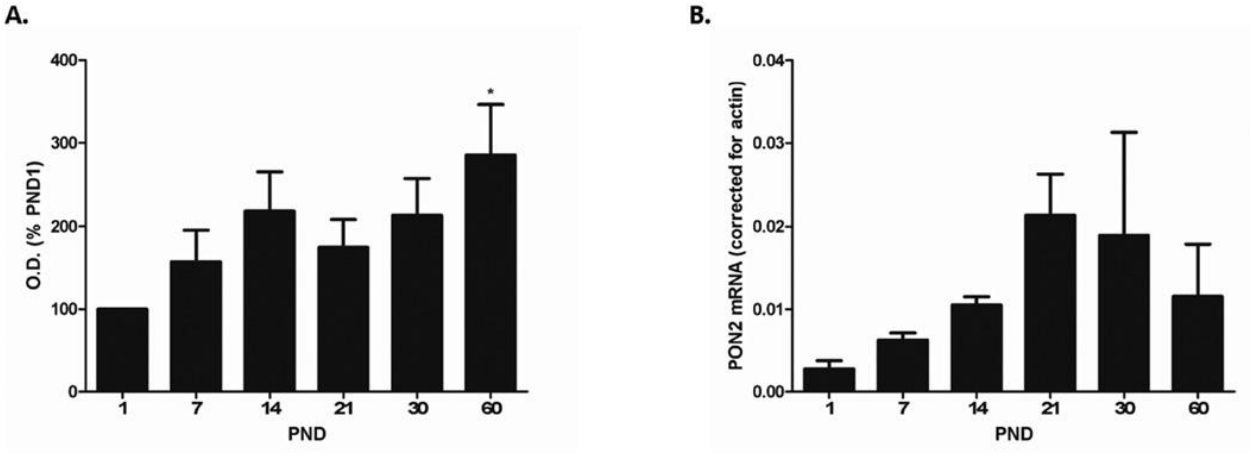

Figure 2.4 - Developmental expression of PON2 protein and mRNA levels in female mouse liver. **A**. Quantification of PON2 protein after normalization to β-actin. Results are expressed as percentage of PND 1 optical density and represent the mean (± SE) of 5 mice/group. Significantly different from PND 1, * $p < 0.05$. **B**. Levels of PON2 mRNA in liver from female mice of different ages, corrected for β-actin. Results are the mean (± SE) of 3 animals/group.

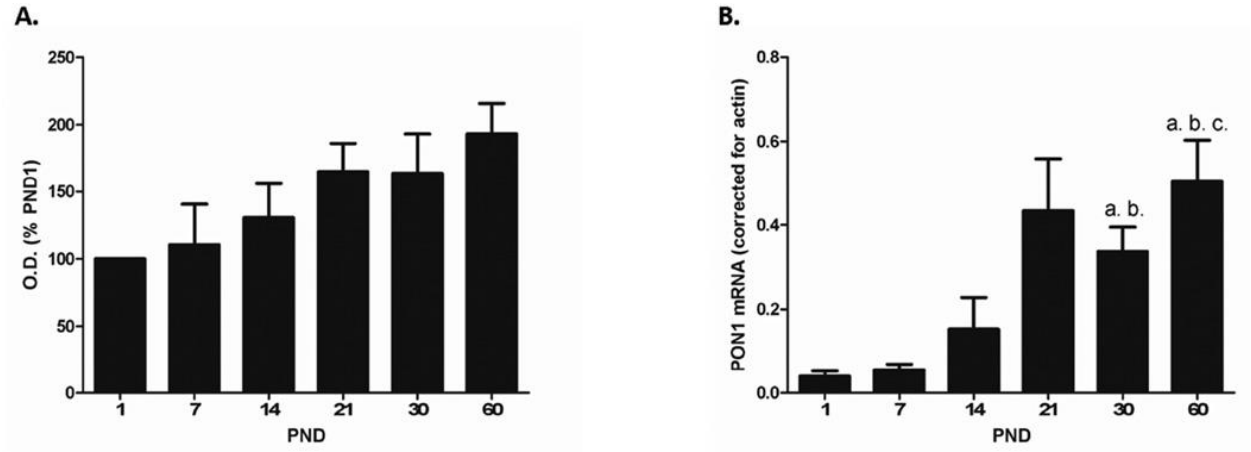

Figure 2.5 - Developmental expression of PON1 protein and mRNA levels in female mouse liver. **A**. Quantification of PON1 protein after normalization to β-actin. Results are expressed as percentage of PND 1 optical density and represent the mean (± SE) of 5 mice/group. **B**. Levels of PON1 mRNA in liver from female mice of different ages, corrected for β-actin. Results are the mean (± SE) of 3–4 animals/group except for PND 21 in which n = 2 and error bar denotes range. a, b, c: significantly different from PND 1, PND 7, and PND 14 (all, $p < 0.05$).

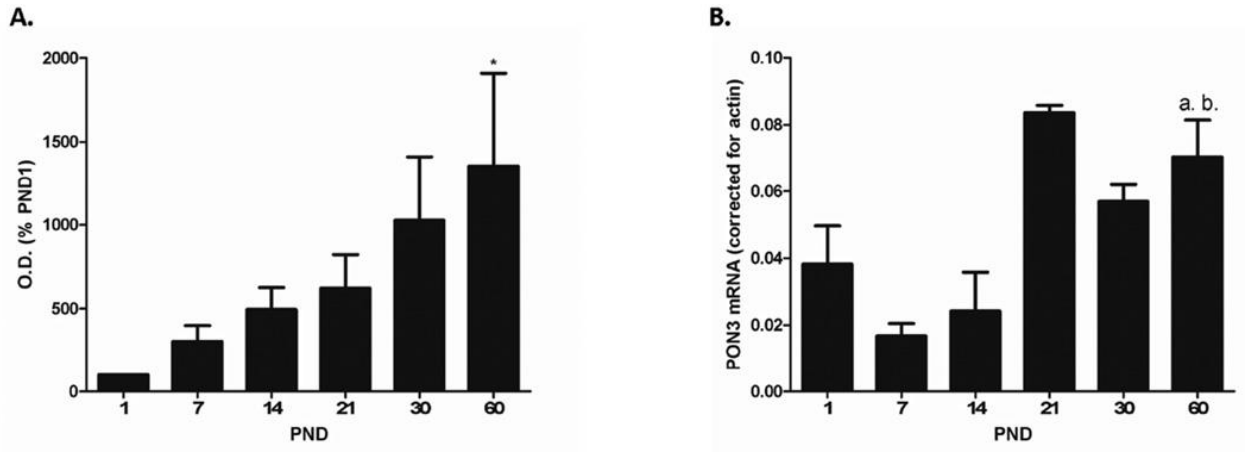

Figure 2.6 - Developmental expression of PON3 protein and mRNA levels in female mouse liver. **A**. Quantification of PON3 protein after normalization to β-actin. Results are expressed as percentage of PND 1 optical density and represent the mean (± SE) of 4 mice/group. Significantly different from PND 1,* $p < 0.05$. **B**. Levels of PON3 mRNA in liver from female mice of different ages, corrected for β-actin. Results are the mean (± SE) of 4 animals/group except for PND 21 in which n = 2 and error bar denotes range. a, b: significantly different from PND 7 ($p < 0.01$), and PND 14 ($p < 0.05$), respectively.

2.4 – Discussion

Results from this study are the first to describe the developmental expression of PON2 in the brain and to examine PON2 developmental expression in liver with respect to both protein and mRNA levels. We confirmed that PON2 protein levels were higher in whole brain homogenates from female mice compared with brain homogenates from male mice (Fig. 2.1), supporting previously published findings (Giordano et al., 2013). In addition, we found that in African green monkey brain, female animals had about twice the level of PON2 protein than males in the ventral caudate (Fig. 2.3B). Although the mouse and monkey sample sets were of different brain region (whole brain versus ventral caudate), it appears sex differences generally exist across species, which may be explained by the ability of estrogens to positively modulate PON2 expression. The functional consequences of higher expression of PON2 in females may have several ramifications, as multiple neurodegenerative diseases involve oxidative stress and neuroinflammation in their etiopathology and are divided on sex. For example, the incidence of Parkinson's disease (PD) is 90% higher in males (Wirdefeldt et al., 2011), pointing to a protective mechanism in females that may involve PON2. In brain, the PON2 polyclonal antibody recognized more than one band, the lower at MW ~43 kDa, which corresponds to the reported MW of PON2 (Fig. 2.1) and has been determined to be specific for PON2 in this study. Higher MW bands (e.g., 55 kDa) have been reported by some investigators (Ng et al., 2006; Horke et al., 2007; Horke et al., 2010; Witte et al., 2011), but not by others (Ng et al., 2001; Levy at al. 2007), and may represent PON2 alloforms, though their exact nature has not been defined yet.

Overall, analysis of PON2 protein and mRNA in brain of female mice showed an increase in PON2 levels during early development followed by a decrease (Fig. 2.2). A similar developmental pattern was observed in brain of non-human primates (Fig. 2.3A), although species

differences in rates of brain development and differences in time points used due to sample availability limit direct comparison of PON2 levels between species. However, the overall trend observed in both species reveals a possible window of susceptibility to oxidative stress in young adult mice and monkeys which may point to a change in cellular environment driving a decrease in PON2 expression. Of interest is that the developmental profile of PON2 in monkey brain seen in this study agrees with previous findings on susceptibility to MPTP- and methamphetamine-induced dopaminergic toxicity, with infant brain observed as the most resistant (Morrow et al., 2011; Morrow et al., 2012). Further study will be required to determine what biological changes are mediating the decrease in PON2, and whether these persist into later ages in mice as observed in monkeys. One avenue of research could be the estrus cycle, which was not accounted for in this study. As indicated earlier, estradiol has been demonstrated to increase PON2 expression in-vitro by increasing PON2 transcription (Giordano et al., 2013). In the estrus cycle of the female mouse, estrogen levels vary during different points in the cycle, peaking during pro-estrus (Caligioni 2009), and could lead to variable levels of PON2 corresponding to circulating levels of estrogen.

While whole brain was utilized for the present study, brain region analysis of PON2 protein levels shows regional differences, with the highest levels of PON2 observed in the dopaminergic areas of the brain such as the nucleus accumbens, substantia nigra and striatum (Giordano et al., 2011). These three regions are known to sustain high levels of oxidative stress due to dopamine metabolism (Miyazaki & Asanuma 2008) and may have higher levels of PON2 to address the increased ROS. Further research into the regional developmental expression of PON2 should be of interest to determine if there are differences, either at the expression level or temporal level, in the various regions of the brain and potentially identify regions which may be at increased risk for ROS toxicity due to lower PON2 levels. In addition, genetic variation could contribute to inter-

individual differences in PON2 expression, and would be a valuable avenue of study to determine potential susceptible populations with regards to ROS toxicity. Although not thought to influence antioxidant capacity, the Cys(311)Ser polymorphism of PON2 has been shown to impair lactonase activity (Altenhöfer et al., 2010) and could prove to be an additionally valuable avenue of study along with genetic expression differences.

As previously indicated, the lower levels of PON2 during early development and young adulthood may represent windows of susceptibility to oxidative stress in the brains of mice and monkeys, particularly when considering data from our laboratory showing that PON2 is critical for mitigating oxidative stress in the central nervous system (Giordano et al., 2011). Compensatory antioxidant mechanisms, such as ROS scavenging by glutathione, do not appear to correct the elevated oxidative stress levels in situations of decreased PON2, highlighting the potential pathological significance of lower PON2 levels (Giordano et al., 2011). These windows of susceptibility are of interest for neurodegenerative diseases, as evidence mounts for mitochondrial dysfunction and elevated oxidative stress as key mediators of diseases such as Alzheimer's and Parkinson's disease (Aliev et al., 2014; Gaki & Papavassiliou 2014; Thanan et al., 2014). Recent data suggest that PON2 interacts directly with DJ-1 (PARK7), allowing DJ-1 to exert antioxidant properties through the regulation of PON2 (Parsanejad et al., 2014). Loss of function mutations in DJ-1 are associated with some familial forms of Parkinson's disease (Bonifati et al., 2003), offering a potential link between PON2 and neurodegenerative disease pathogenesis. Furthermore, PON2 is known to associate with dopamine receptors in the kidney (Yang et al., 2012; Yang et al., 2015), acting as an important antioxidant in the renal dopamine system, and whether this same relationship exists in brain dopaminergic regions needs to be investigated.

In mouse liver, PON2 protein and mRNA increased with age from PND 1 to PND 60 (Fig. 2.4). The findings were in accordance with the developmental profiles of other paraoxonases, PON1 and PON3, which also generally increased with age (Figs. 2.5 and 2.6). Unfortunately, non-human primate liver samples were not available for analysis, and the persistence of expression patterns between species for PON2 in the liver is unclear. Previous studies had examined the developmental expression of PON1 mRNA in liver and of paraoxonase activity in plasma of mice, and found PON1 levels to increase with age (Li et al., 1997; Cole et al., 2003; Cheng & Klaassen 2012), in agreement with the present findings. PON3 temporal expression has received less attention, with limited studies showing a decrease or an increase with age (Belteki et al., 2010; Shih et al., 2010; Cheng & Klaassen 2012). Belteki et al., found a time dependent increase of PON3 mRNA levels prenatally in rat and sheep in various tissues, including the liver. Shih et al., reported lower levels of PON3 mRNA in various tissues of newborn mice compared to adult mice, while Cheng and Klaassen found high levels of PON3 mRNA in prenatal mouse liver, followed by a decline at PND5 then a gradual increase in levels.

In summary, results of the present study confirm that sex is an important determinant of PON2 expression, and provides novel information indicating that age also modulates the levels of PON2. Because of the role of PON2 as a potent intracellular antioxidant and anti-inflammatory factor, strategies attempting to modulate its level of expression should also consider sex and age as additional variables.

2.5 – Materials and Methods

Materials

Anti-PON1, PON2, and PON3 antibodies were from Abcam (Cambridge, MA, USA). Anti β-actin antibody was from Sigma-Aldrich (St. Louis, MO, USA), while 10x Tris-buffered saline, Tween-20, Coomassie Brilliant Blue R-250 were from Bio-Rad Laboratories (Hercules, CA, USA). XCell II™ Blot Module, XCell SureLock™ Electrophoresis Cell, NuPAGE® MOPS SDS Running Buffer 20x, NuPAGE® LDS Sample Buffer 4x, NuPAGE® Antioxidant, NuPAGE® Sample Reducing Agent 10x and NuPAGE® 10% Bis-Tris Protein Gels were from Life Technologies (Carlsbad, CA, USA). Immobilon®-P Transfer Membrane was from Millipore Corporation (Billerica, MA, USA). Restore™ Western Blot Stripping Buffer, PageRuler™ Prestained Protein Ladder, SuperSignal® West Pico Chemiluminescent Substrate, SuperScript® III Reverse Transcriptase and TaqMan® Gene Expression Assays were from Thermo-Fisher Scientific (Waltham, MA, USA). Anti-rabbit IgG HRP-linked antibody and Cell Lysis Buffer 10x were from Cell Signaling Technology (Danvers, MA, USA). HRP Goat Anti-Mouse Ig was from BD Biosciences (San Jose, CA, USA). RNeasy® Mini Kit was purchased from Qiagen (Hilden, Germany). TaqMan® Gene Expression Master Mix was from Applied Biosystems (Foster City, CA, USA).

Mice

Wild-type C57BL/6J mice were used for this study. Mice were sacrificed at postnatal day (PND) 1, 7, 14, 21, 30 or 60 and brain and livers were removed and flash-frozen in liquid nitrogen. Whole brains were pulverized with a pre-chilled mortar and pestle into a fine powder, stored at -80°C and aliquoted into appropriate lysis buffers for protein and RNA extraction as needed,

utilizing sonication for homogenization. Liver tissue was mechanically homogenized in appropriate lysis buffer using a Wheaton Potter-Elvehjem tissue grinder followed by sonication. Mice were housed in a specific pathogen-free facility on a 12-hour light/dark cycle with *ad libitum* access to food and water. All procedures were conducted in accordance with the National Institute of Health Guide for the Use and Care of Laboratory Animals and were approved by the University of Washington Institutional Animal Care and Use Committee.

Non-human primate samples

Flash frozen ventral caudate samples from brains of African green or vervet monkeys (*Chlorocebus sabaeus*) were provided by Dr. John Elsworth from Yale University School of Medicine. Animals were housed in the St. Kitts Biomedical Research Foundation, an AAALAC accredited facility. All tissue samples were from animals that were controls for other studies each with their own protocol approved by the Yale University Institutional Animal Care and Use Committee. Tissue samples were shipped on dry ice and processed as the mouse samples.

Immunoblotting

Immunoblots were carried out as previously described [21]. Briefly, 25 μg of protein was mixed with SDS running buffer and sample reducing agent and subjected to sodium dodecyl sulfate-polyacrylamide gel electrophoresis (SDS-PAGE). Following electrophoresis, proteins were transferred to polyvinylidene difluoride membranes and the membrane blocked for 1 hour with 5% nonfat milk. Membranes were then probed with the following diluted primary antibodies: 1:750 for brain PON2, 1:1000 for liver PON1, PON2 and PON3. Following primary antibody

incubation, membranes were washed with Tris-buffered saline with 0.1% Tween-20 (pH = 7.5) and incubated with horseradish peroxidase-conjugated anti-rabbit secondary antibody at a dilution of 1:1500 (brain PON2) or 1:1000 (liver PON2), or with horseradish peroxidase-conjugated anti-mouse secondary antibody at a dilution of 1:1000 (liver PON1 and PON3). Membranes were stripped with Restore™ Western Blot Stripping Buffer and re-probed for β-actin using a dilution of 1:1000 for the β-actin primary antibody and 1:2500 for the horseradish peroxidase-conjugated anti-mouse secondary antibody. Total protein was measured using Coomassie Brilliant Blue R-250 at a concentration of 0.025% weight/volume. Intensity of bands was measured by densitometry using ImageJ software (NIH), with the band intensity normalized to β-actin expression or total protein as noted. Monkey brain tissue was homogenized in CLB buffer (10 mM HEPES, 150 mM NaCl, 1 mM CaCl2, 0.5 mM MgCl2, 1 mM PMSF,50 mM NaF, 1 mM sodium orthovanadate) and whole homogenates were subjected to SDS-PAGE and immunoblotting using rabbit anti-PON2 (1:500), or mouse anti-β-actin (1:1000) antibodies. After electrophoresis, proteins were transferred to polyvinylidene difluoride membranes and incubated with the above antibodies. Membranes were rinsed in Tris-buffered saline with 0.1% Tween-20 and incubated with horseradish peroxidase–conjugated anti-rabbit IgG or with horseradish peroxidase–conjugated anti-mouse IgG (for actin) at the appropriate dilutions (1:2000, 1:5000, respectively).

RT-PCR

PONs mRNA levels were measured by RT-PCR. Reverse transcription was performed according to the manufacturer's established protocol using total RNA and the SuperScript® III First-Strand Synthesis System. For gene expression measurements, 4 μL of cDNA were included in a PCR reaction (20 μL final volume) that also consisted of 1 μL of appropriate TaqMan® Gene

Expression Assay mixture and 10 μL TaqMan® Gene Expression Master Mix. Amplification and detection of PCR amplicons were performed with the ABI PRISM 7900 system (Applied Biosystems, Foster City, CA) with the following PCR reaction profile: 1 cycle of 95°C for 10 min, 40 cycles of 95°C for 30 sec and 62°C for 1 min. β-actin amplification plots taken from serial dilutions of an established reference sample were used to create a linear regression formula in order to calculate expression levels, and β-actin gene expression levels were utilized as an internal control to normalize the data.

Statistical Analysis

Data are expressed as the mean ± SEM of at least three independent experiments. One-way ANOVA followed by the Tukey test for multiple comparisons was utilized for statistical analysis, while Student's t-test was utilized for comparing two groups as noted.

2.6 – Acknowledgements

This study was supported in part by grants P42ES004696 and P30ES07033 from the National Institute of Environmental Health Sciences. Primate research at Yale University was supported by grant AG048918 from the National Institute on Aging. We thank Zahra Afsharinejad from the Functional Genomics and Proteomics Facility in the Department of Environmental and Occupational Health Sciences at the University of Washington for measuring mRNA levels.

Chapter 3

Paraoxonase 2 Deficiency in Mice Alters Motor Behavior and Causes Regional and Sex-Specific Transcript Changes in the Brain

This chapter contains the research article:

Garrick, J. M., Cole, T. B., Bammler T.K., MacDonald J.W., Marsillach J., Furlong C.E., & Costa, L. G. (2021). Paraoxonase 2 Deficiency in Mice Alters Motor Behavior and Causes Region-Specific Transcript Changes in the Brain. Under review in *Neurotoxicology and Teratology*.

3.1 – Introduction

As discussed in chapter 1, PON2 has been demonstrated to exert an antioxidant effect (Ng et al., 2001; Horke et al., 2007; Levy et al., 2007; Giordano et al., 2011; Giordano et al., 2013) and is necessary for mitochondrial homeostasis, as PON2 deficient mice display mitochondrial dysfunction (Devarajan et al., 2011). Superoxide (O_2^-) is an incidental by-product of the electron transport chain at the mitochondrial membrane and leads to the production of hydrogen peroxide (H_2O_2), another reactive oxygen species (ROS), which can further produce hydroxyl radicals (Kehrer & Klotz 2015). This lends the mitochondria to be an important site for antioxidant action to mitigate cellular damage caused by these radicals. Oxidative stress is a principle mechanism by which endogenous and exogenous neurotoxicants exert toxicity (Sayre et al., 2008; Deavall et al., 2012) and higher levels of ROS are associated with numerous morbidities.

In the brain, PON2 expression has been found highest in dopaminergic regions such as the striatum, nucleus accumbens and substantia nigra (Giordano et al., 2011). Differential expression among cell types has also been observed, with astrocytes expressing significantly more PON2 than neurons (Giordano et al., 2011). However, PON2 deficiency in both cell types

impairs their ability to recover from oxidative stress generated by *in-vitro* exposure to oxidants hydrogen peroxide (H_2O_2) and 2,3-dimethoxy-1,4-naphthoquinone (DMNQ) (Giordano et al., 2011). Glutathione, a principle antioxidant in the body, does not appear to be altered by PON2 deficiency, supporting that the observed sensitivity to oxidant challenge in PON2 deficient cells is due to the loss of PON2 and not the loss of additional antioxidant function (Giordano et al., 2011). As such, PON2 appears to be a critical antioxidant enzyme in the brain and warrants additional investigation.

To further characterize the effects of PON2 deficiency in the brain, we sought to determine if PON2 deficient mice display a behavioral phenotype, with particular emphasis on motor behavior, as PON2 is expressed highest in dopaminergic regions and motor deficits are hallmarks of dopaminergic neuron loss (Grosch et al., 2016). Additionally, we conducted an RNA-Seq experiment comparing brain tissue from PON2 deficient and wildtype mice to evaluate regional mRNA expression changes to further understand the pathways and processes in which PON2 is involved. Taken together with existing literature, the results of this study begin to provide a more robust understanding of the role of PON2 in the brain and offers compelling evidence for further toxicological study of PON2.

3.2 – Results

PhenoTyper

Home-cage behavior was analyzed for 67 hours using the Noldus PhenoTyper system and EthoVision tracking software (Figure 3.1A). The arena zones marked in the cage are noted in Figure 3.1B. Mice could freely roam the cage and were not disturbed for the duration of the experiment. When evaluating movement, PON2 deficient (PON2-def) mice were recorded as

having spent more time moving around the cage during the dark cycle than WT mice (Figure 3.2A) as well as moving longer distances during this time (Figure 3.2B). Movement during the light cycle was unchanged. When evaluating time spent in various zones of the arena, PON2-def mice spent significantly more time in the center of the arena during the dark cycle than WT mice, while no difference was noted during the light cycle (Figure 3.2C). Conversely, PON2-def mice spent significantly less time in the hidden shelter during the dark cycle, while no difference was noted during the light cycle (Figure 3.2D). No differences were observed for time spent in the perimeter of the arena during either light or dark cycle (Figure 3.2E). A sex interaction was noted for time spent at the food hopper, with female PON2-def mice spending significantly more time at the hopper than WT during the dark cycle, with no difference observed during the light cycle (Figure 3.2F). Time spent at the food hopper was not significantly different for males during either cycle (Figure 3.2G). Time spent at the water bottle was not significantly different between PON2-def and WT mice at either light or dark cycle (Figure 3.2H)

Rotarod

Mice were placed on a spinning rod which increases speed at regular intervals, beginning at 4 RPM and ramping up to 40 RPM over a 5-minute span. PON2-def mice had a significantly shorter latency to fall than WT mice (Figure 3.3), suggesting PON2 deficiency causes motor coordination deficits.

CatWalk

Gait was assessed using the Noldus CatWalk system, with evaluated metrics falling into four general domains: temporal parameters, coordination, spatial patterns of individual paws and

spatial pattern relationships between paws. No differences were observed in PON2-def mice compared to WT for the temporal parameters of average speed of the mouse (Figure 3.4A), cadence (Figure 3.4B), swing (Figure 3.4C) and swing speed (Figure 3.4D). Likewise, no differences were observed in the coordination metrics of the sequence regularity index (Figure 3.34E) and percentage measurement of the step sequences (Figure 3.4F). Metrics of spatial relationships between paws were also largely unaffected, with no observed differences in base of support (Figure 3.4G) and most postural positions examined (Figure 3.4H and 3.4I). However, PON2-def mice spent significantly less time in a girdle support posture compared to WT (Figure 3.4H), where they place their weight on either their two front or two hind limbs simultaneously. Individual paw metrics of stride length, print intensity, print area, print length and print width were similarly unaffected by PON2 deficiency (data not shown).

RNA-Seq Overview

RNA-Seq was conducted using three brain regions (cerebral cortex, striatum, and cerebellum) from WT and PON2-def mice, previously tested for behavioral endpoints. PON2-def mice were confirmed to be deficient in all regions examined, with the cerebellum showing the least amount of PON2 expression in both sexes (Figure 3.35A). When comparing female and male expression profiles, WT mice displayed hundreds of differentially expressed genes (FDR<0.1) between female and males outside of anticipated sex-chromosome specific genes (Figures 3.5B – E), with gene totals varying depending on region. However, these sex differences appear to be lost in the cortex and striatum of PON2-def mice, where female and male mice only differ in a handful of sex-chromosome specific genes (Figures 3.5B – D). In the cerebellum, minor gene differences were observed for both groups, although the population of

differentially expressed genes differed (Figures 3.5B and 3.5E). When comparing PON2-def and WT mice on a regional level, differential expression was highly sex- and region-dependent. While PON2-def female mice exhibited significant differences from WT in the striatum, there were no appreciable differences in the cortex and cerebellum (Figure 3.6A). Complimentarily, PON2-def male mice exhibited the opposite pattern, with significant differences from WT in the cortex and cerebellum, but no differences in the striatum (Figure 3.6A). There was minimal overlap of the differentially expressed genes between regions, supporting discrete regional impacts due to PON2 deficiency (Figure 3.6B – E).

PON2 Deficiency in the Cerebral Cortex

Comparing PON2-def and WT gene expression in the cerebral cortex of males, 287 genes were differentially expressed. Utilizing iPathwayGuide analysis, no significant KEGG pathways were identified after controlling for multiple comparisons. The top 5 significant Biological Processes Gene Ontology (GO) categories altered from PON2 deficiency were found to be glutamate reuptake, positive regulation of nuclear-transcribed mRNA poly(A) tail shortening, transcription by RNA polymerase II, meiotic spindle organization, and peptidyl-lysine dimethylation (Figures 3.7A and 3.7B).). The top 5 significant Molecular Functions GO categories perturbed by PON2 deficiency were cyclo-ligase activity, methylated histone binding, RNA polymerase binding, core promoter sequence-specific DNA binding, and chromatin binding (Figures 3.7C and 3.7D). Based on the differentially expressed genes, iPathwayGuide predicts upstream regulators which may be activated or inactivated. In the cerebral cortex, transcription factors MLX interacting protein like (Mlxipl), neuronal PAS domain protein 2 (Npas2), and circadian locomotor output cycles kaput (Clock) were all predicted to be activated

in PON2-def mice (Figure 3.8G) based on the gene expression changes noted in figures 3.8E and 3.8F. Chemical, drug and toxicant exposure was also predicted based on gene expression profiles. This prediction tool compared the expression profile of our samples to various compounds in the iPathwayGuide database to identify exposures which PON2 deficiency may mimic on a transcriptional level. PON2 deficiency leads to gene expression changes like those observed after aflatoxin B1 (Figure 3.8A) and dibutyl phthalate (Figure 3.8B) exposure, which are both predicted to be present (Figure 3.8D). Conversely, PON2 deficiency leads to gene expression changes suggesting the absence of troglitazone (Figure 3.8C and 3.8D), an anti-diabetic and anti-inflammatory drug. These data indicate that PON2-def mice display a transcriptional profile like that of an untreated diabetic and/or an animal experiencing inflammation.

PON2 Deficiency in the Striatum

Comparing PON2-def and WT gene expression in the striatum of females, 64 genes were differentially expressed. iPathwayGuide analysis identified the top 5 significantly altered KEGG pathways due to PON2 deficiency as basal cell carcinoma, melanogenesis, hippo signaling pathway, breast cancer and Cushing syndrome (Figure 3.9A). All pathways were linked to changes in the same gene set (Figure 3.9B). The top 5 significant Biological Processes GO categories altered from PON2 deficiency were found to be regulation of asymmetric cell division, Wnt signaling pathway involved in midbrain dopaminergic neuron differentiation, forebrain neuroblast division, cerebellar granule cell differentiation, and negative regulation of signaling receptor activity (Figures 3.9C and 3.9D). The top 5 significant molecular functions affected by PON2 deficiency were steroid hormone receptor activity, formaldehyde

dehydrogenase activity, fatty acid peroxidase activity, S-(hydroxymethyl) glutathione dehydrogenase activity and proteasome regulatory particle binding (Figures 3.9E and 3.9F). No significant upstream regulators were identified in the striatum.

PON2 Deficiency in the Cerebellum

Comparing PON2-def and WT gene expression in the cerebellum of males, 260 genes were differentially expressed. iPathwayGuide analysis identified no significant altered KEGG pathways after controlling for multiple comparisons. The top 5 significant Biological Processes GO categories affected by PON2 deficiency were found to be negative regulation of transcription by RNA polymerase II, inactivation of MAPK activity, ADP biosynthetic process, glutamate reuptake, and histone H3 deacetylation (Figures 3.10A and 3.10B). The top 5 Molecular Functions GO categories altered with PON2 deficiency were identified as protein tyrosine/serine/threonine phosphatase activity, transcription cofactor binding, pre-mRNA binding, RNA polymerase II regulatory region sequence-specific DNA binding, and protein kinase B binding (Figures 3.10C and 3.10D). Based on the differentially expressed genes noted in Figure 11A, predicted upstream regulators in the cerebellum were transcription neuronal PAS domain protein 2 (Npas2), circadian locomotor output cycles kaput (Clock) and aryl hydrocarbon receptor nuclear translocator like (Arntl) (Figure 3.11B).

3.3 – Figures

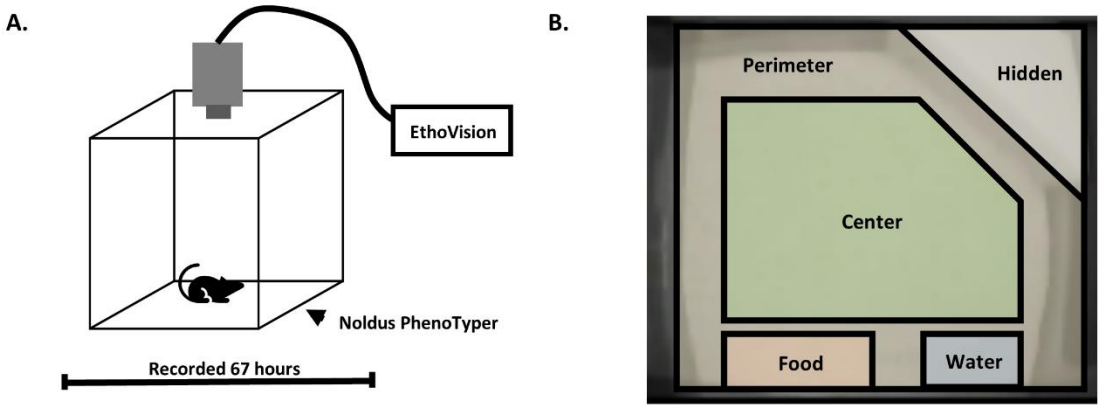

Figure 3.1 – PhenoTyper Setup. A. Schematic demonstrating setup of PhenoTyper cage and camera location. **B.** Arena zones defined during PhenoTyper experiment.

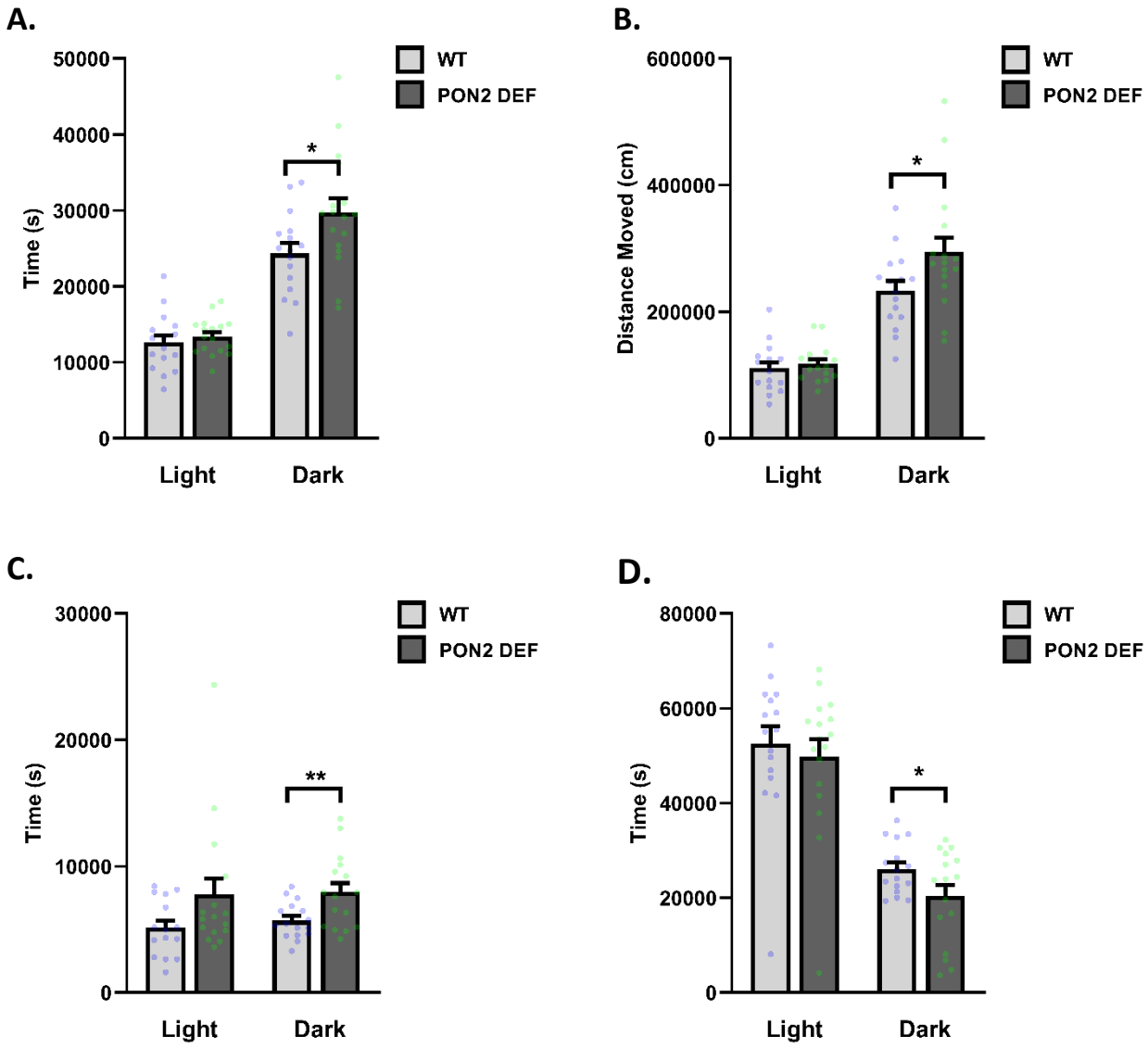

Figure 3.2 – Home-cage Metrics Assessed by PhenoTyper. A. Time spent moving in cage during the light and dark cycles (male and female mice combined), measured in seconds (s), n = 16 – 17 per group, * $p < 0.05$. **B.** Distance moved in cage during the light and dark cycles (male and female mice combined), measured in centimeters (cm), n = 16 – 17 per group, * $p < 0.05$. **C.** Time spent in center of arena during light and dark cycles (male and female mice combined), measured in seconds (s), n = 16 – 17 per group, * $p < 0.05$. **D.** Time spent in the hidden shelter during light and dark cycles (male and female mice combined), measured in seconds (s), n = 16 – 17 per group, * $p < 0.05$.

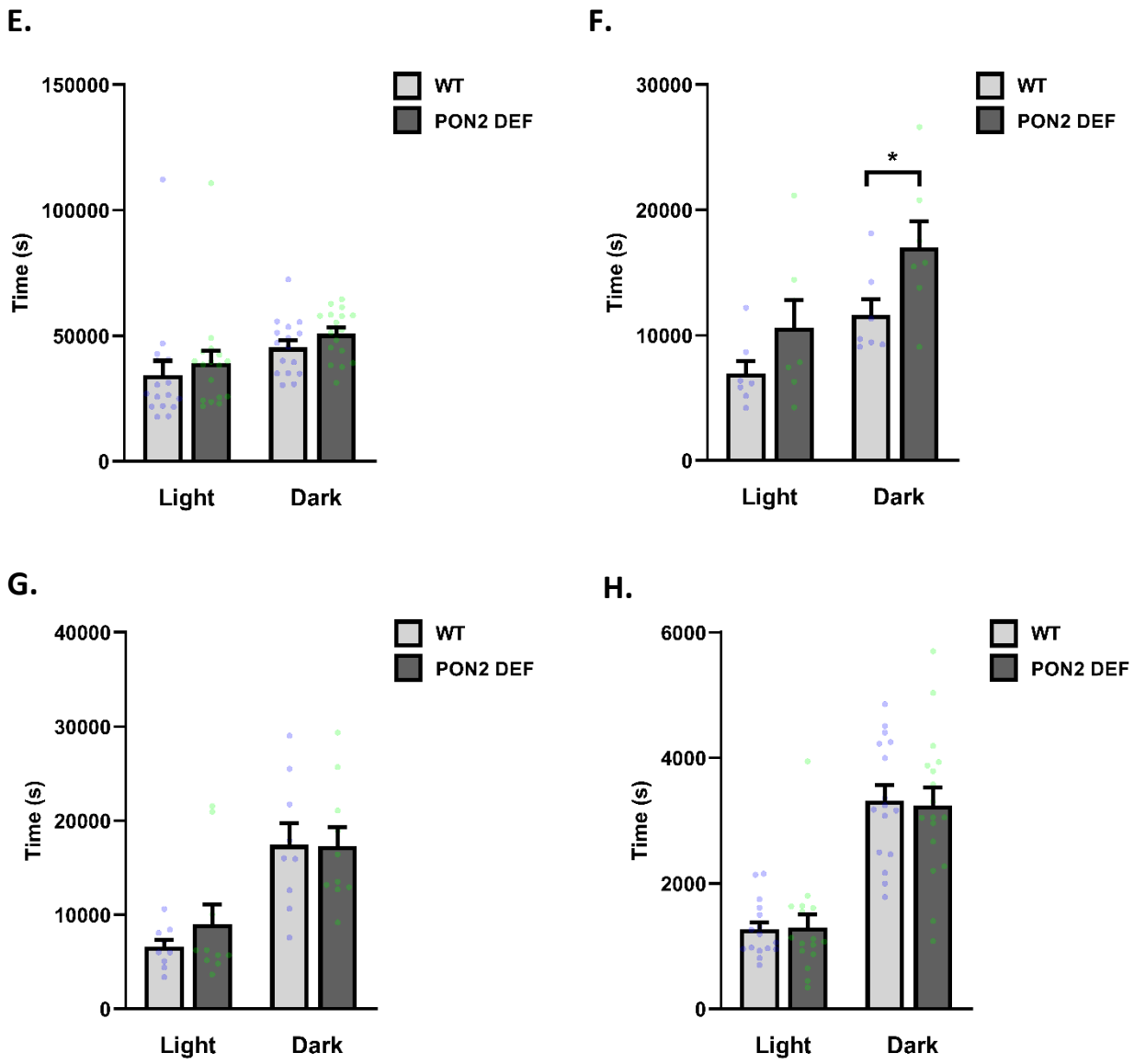

Figure 3.2 – Home-cage Metrics Assessed by PhenoTyper *(continued)*. E. Time spent in the perimeter of the arena during light and dark cycles (male and female mice combined), measured in seconds (s), n = 16 – 17 per group. **F.** Time spent at the food hopper by female mice during the light and dark cycles, measured in seconds (s), n = 7 per group, * $p < 0.05$. **G.** Time spent at the food hopper by male mice during the light and dark cycles, measured in seconds (s), n = 9 – 10 per group. **H.** Time spent at the water bottle during the light and dark cycles (male and female mice combined), measured in seconds (s), n = 16 – 17 per group.

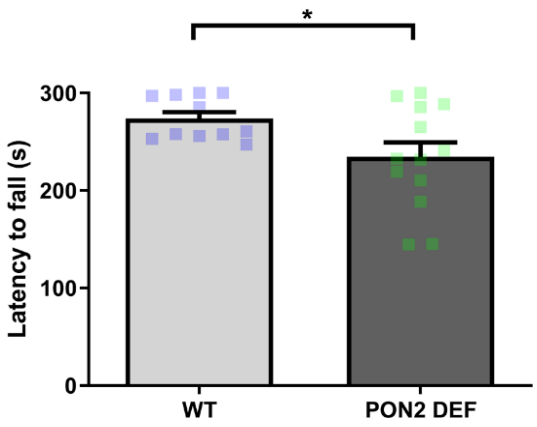

Figure 3.3 – Latency to Fall from Rotarod. Latency in seconds (s) for mice to fall from rotating rod, starting at 4 RPM and ramping continuously to 40 RPM over a 5-minute period. N = 11 – 13 per group, * $p < 0.05$.

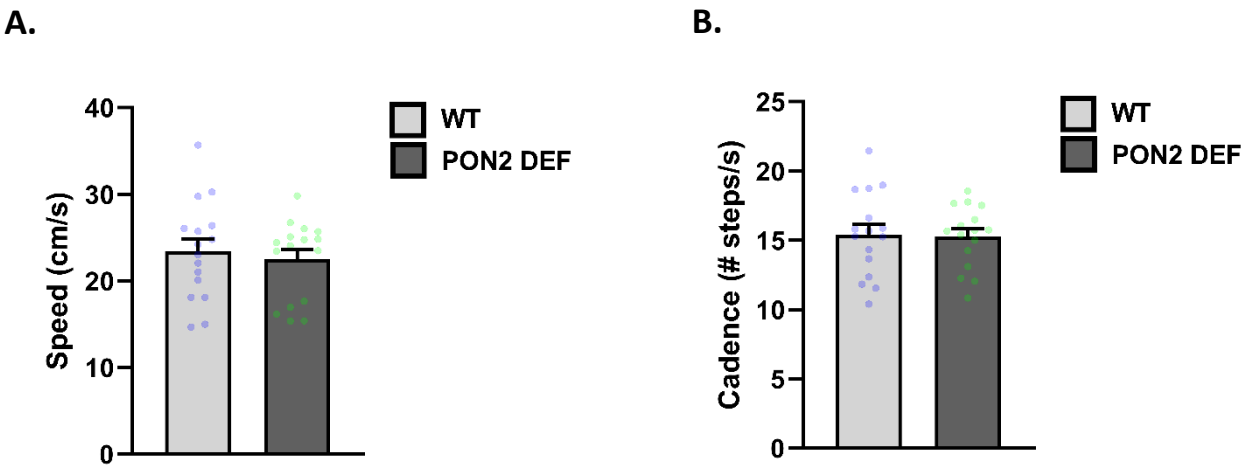

Figure 3.4 – Gait Metrics Measured by CatWalk. A. Average speed of mice, measured in centimeters/second (cm/s), n = 16 – 17 per group. **B.** Cadence of mice, measured as number of steps/second (steps/s), n = 16 – 17 per group. All figures combine male and female mice.

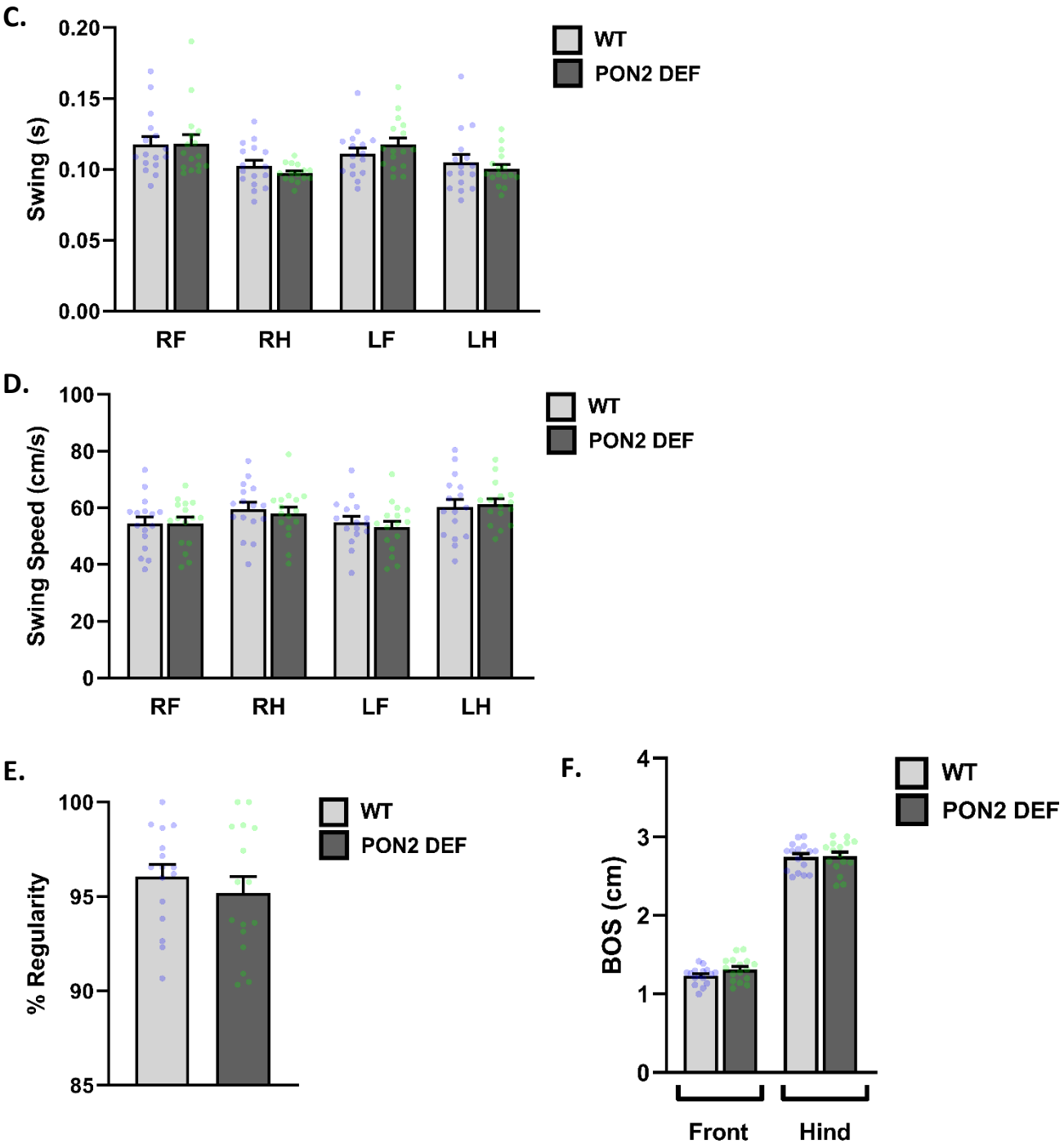

Figure 3.4 – Gait Metrics Measured by CatWalk (*continued*) C. Swing of mice, measured in centimeters (cm), n = 16 – 17 per group. **D.** Average swing speed of mice, measured in centimeters/second (cm/s), n = 16 – 17 per group. **E.** Sequence Regularity Index of gait, measured as percent, n = 16 – 17 per group. **F.** Base of support for front and hind limbs, measured in centimeters (cm), n = 16 – 17 per group

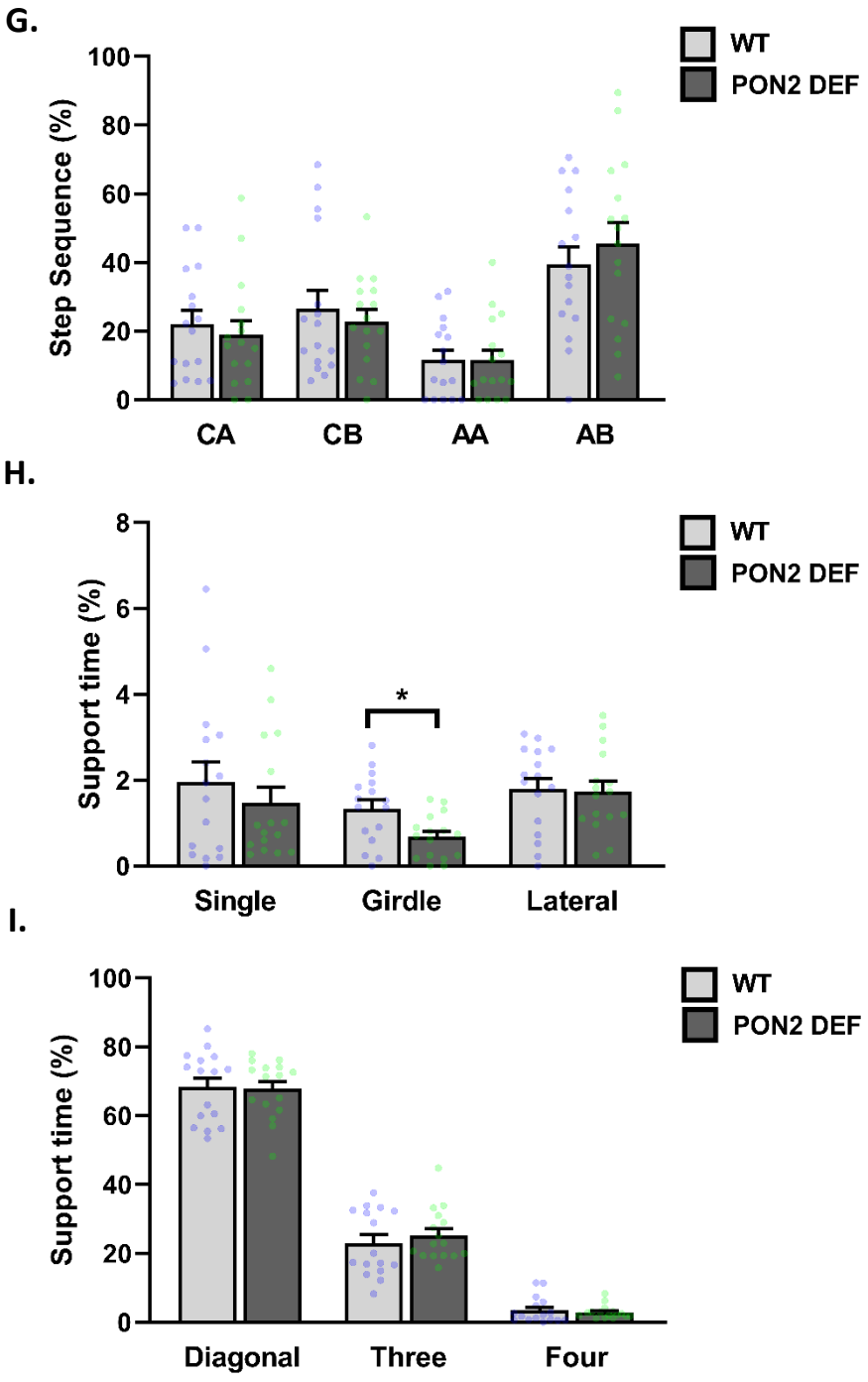

Figure 3.4 – Gait Metrics Measured by CatWalk (*continued*). G. Percentage of steps falling into outlined rodent step sequences, n = 16 – 17 per group. **H.** Percentage of time spent supporting in single, girdle and lateral positions, n = 16 – 17 per group, * $p < 0.05$. **I.** Percentage of time spent supporting in diagonal, three and four positions, n = 16 – 17 per group. All figures combine male and female mice.

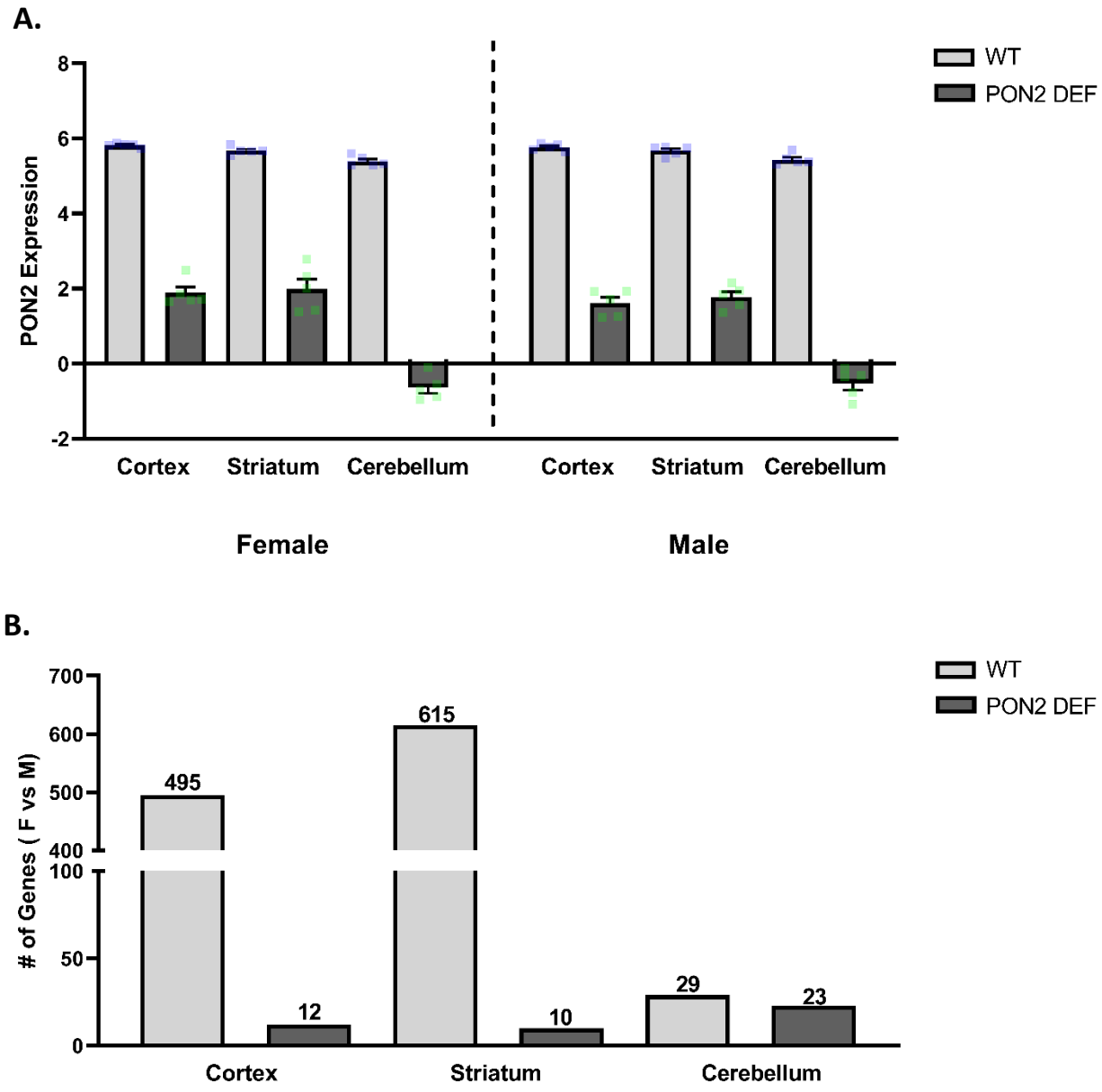

Figure 3.5 – RNA-Seq Overview: PON2 deficiency Removes Sex Differences. A. Expression of PON2 by region (cortex, striatum, cerebellum) and sex (female and male) in WT and PON2 deficient mice. **B.** Differentially expressed genes in WT and PON2 deficient mice per region, comparing female to male expression, filtered by FDR<0.1.

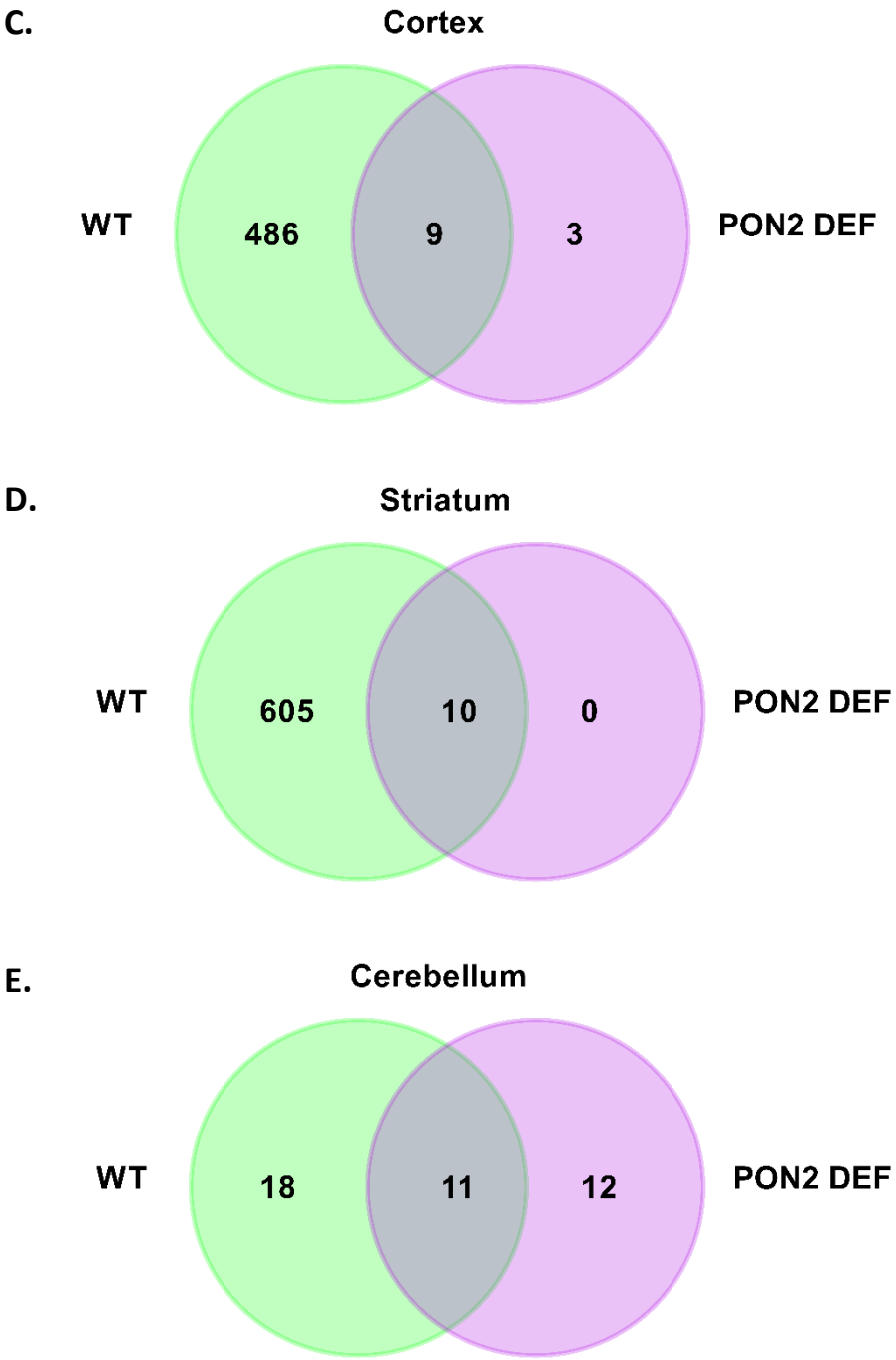

Figure 3.5 – RNA-Seq Overview: PON2 deficiency Removes Sex Differences (*continued*). C. Venn diagram comparing sex differences (female vs male expression) between WT (green) and PON2 deficient (purple) mice in cortex. **D.** Venn diagram comparing sex differences (female vs male expression) between WT (green) and PON2 deficient (purple) mice in striatum. **E.** Venn diagram comparing sex differences (female vs male expression) between WT (green) and PON2 deficient (purple) mice in cerebellum.

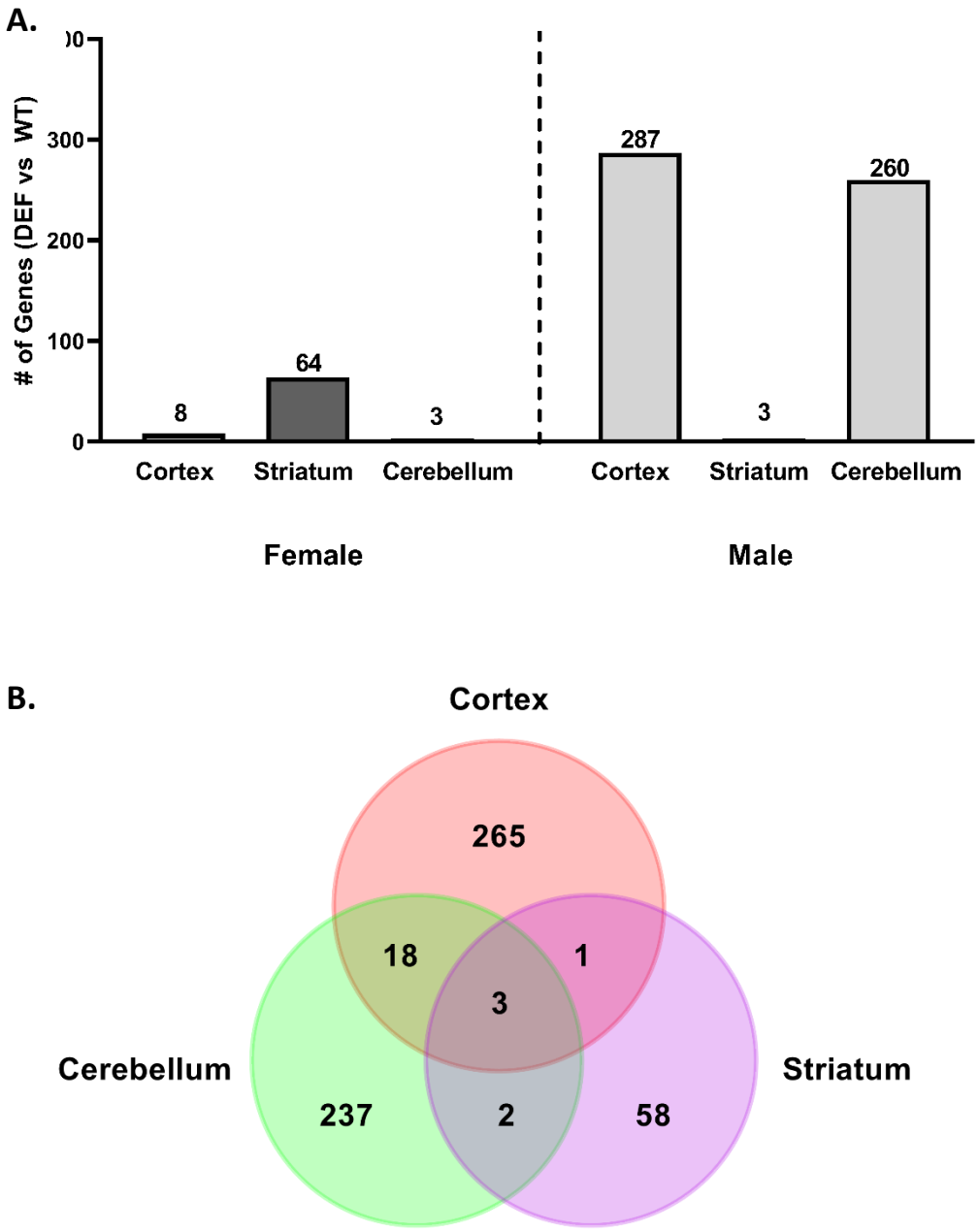

Figure 3.6 – RNA-Seq Overview: Comparing PON2 deficient and WT Brain Regions. A. Overview of differentially expressed genes by region (cerebral cortex, striatum, cerebellum) and sex (female and male), comparing PON2 deficient to WT, filtered by FDR<0.1. **B.** Venn diagram of three regions (male cerebral cortex, female striatum, male cerebellum) with significant amount of differentially expressed genes comparing PON2 deficient to WT.

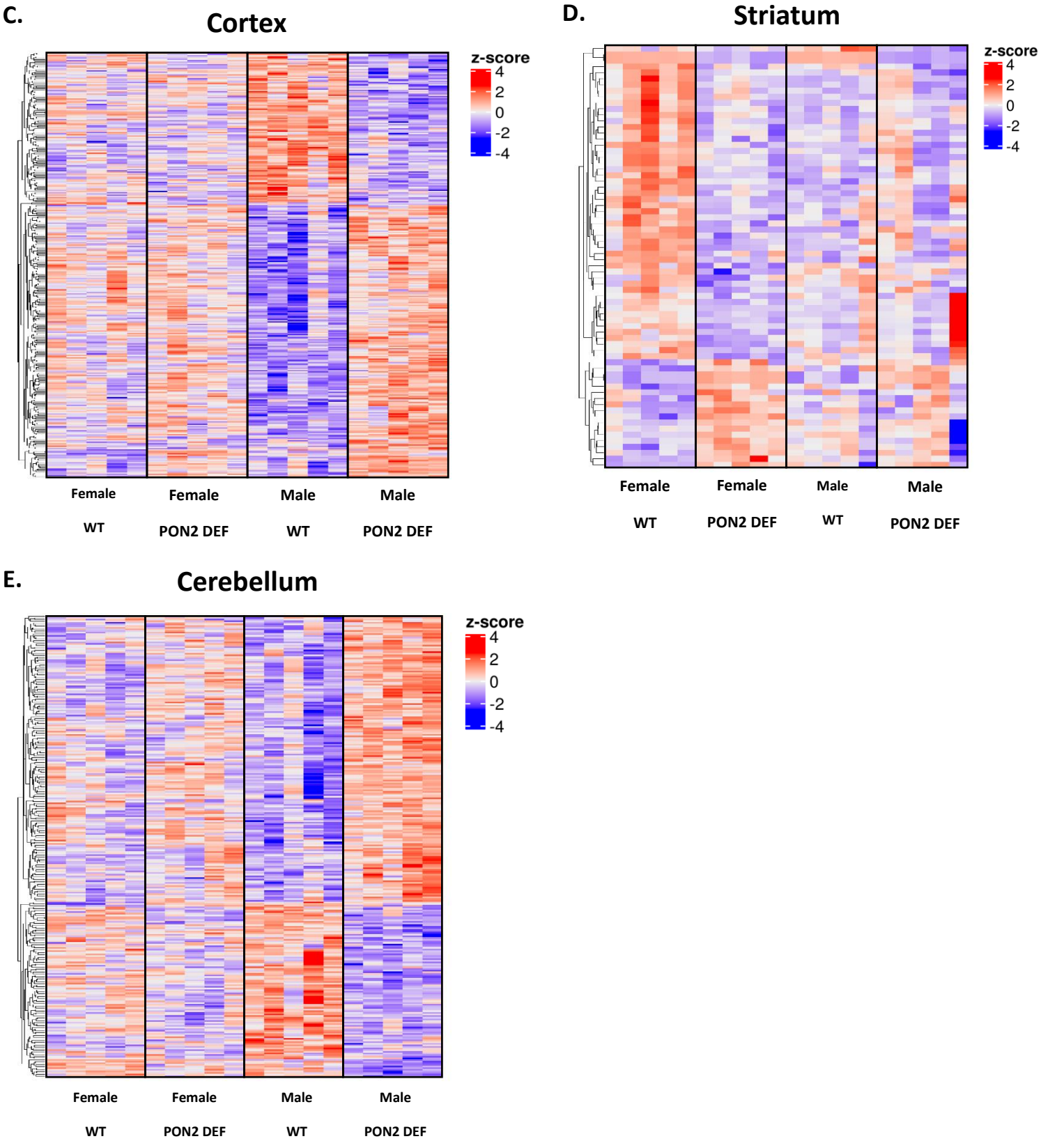

Figure 3.6 – RNA-Seq Overview: Comparing PON2 deficient and WT Brain Regions (*continued*). C. Heatmap of gene expression in the cerebral cortex for PON2 deficient and WT mice. **D.** Heatmap of gene expression in the striatum for PON2 deficient and WT mice. **E.** Heatmap of gene expression in the cerebellum for PON2 deficient and WT mice. Colors in the heatmaps represent row-wise z-scores.

A.

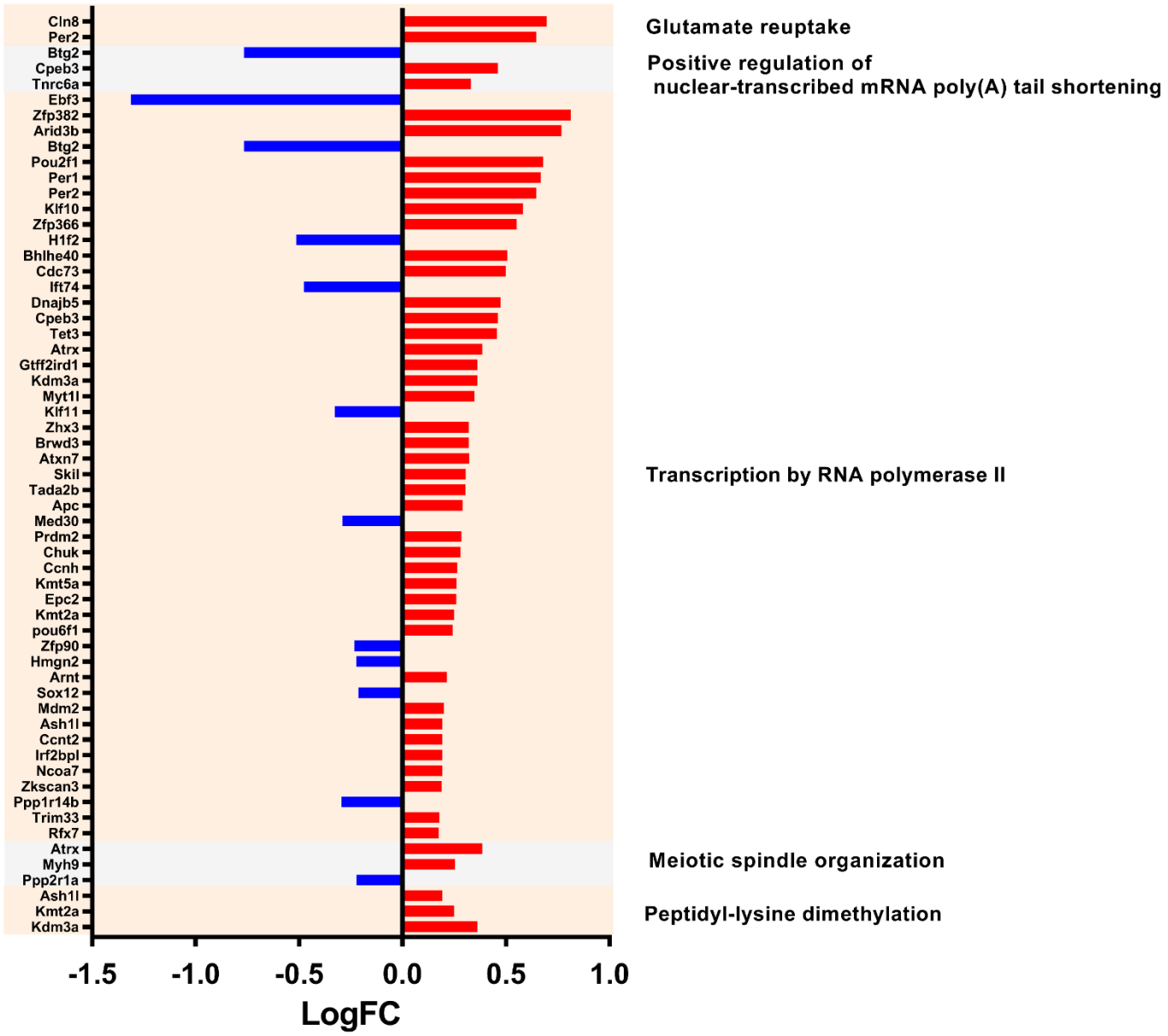

Figure 3.7 – RNA-Seq: PON2-deficient Cortex Pathway Analysis. A. Differentially expressed genes (PON2 deficient vs WT) and associated Biological Processes GO categories in the male cerebral cortex, upregulated genes are shown in red and downregulated genes are shown in blue.

B.

GO Term – Biological Processes	# DE Genes	P-Value
Glutamate reuptake	2/3	7.900e-4
Positive regulation of nuclear-transcribed mRNA poly(A) tail shortening	3/12	8.500e-4
Transcription by RNA polymerase II	48/1748	8.800e-4
Meiotic spindle organization	3/14	0.001
Peptidyl-lysine dimethylation	3/15	0.002

Figure 3.7 – RNA-Seq: PON2-deficient Cortex Pathway Analysis (*continued*). B. Top 5 Biological Processes GO categories significantly impacted by PON2 deficiency in the male cerebral cortex, corrected for multiple comparisons using false discovery rate (FDR).

C.

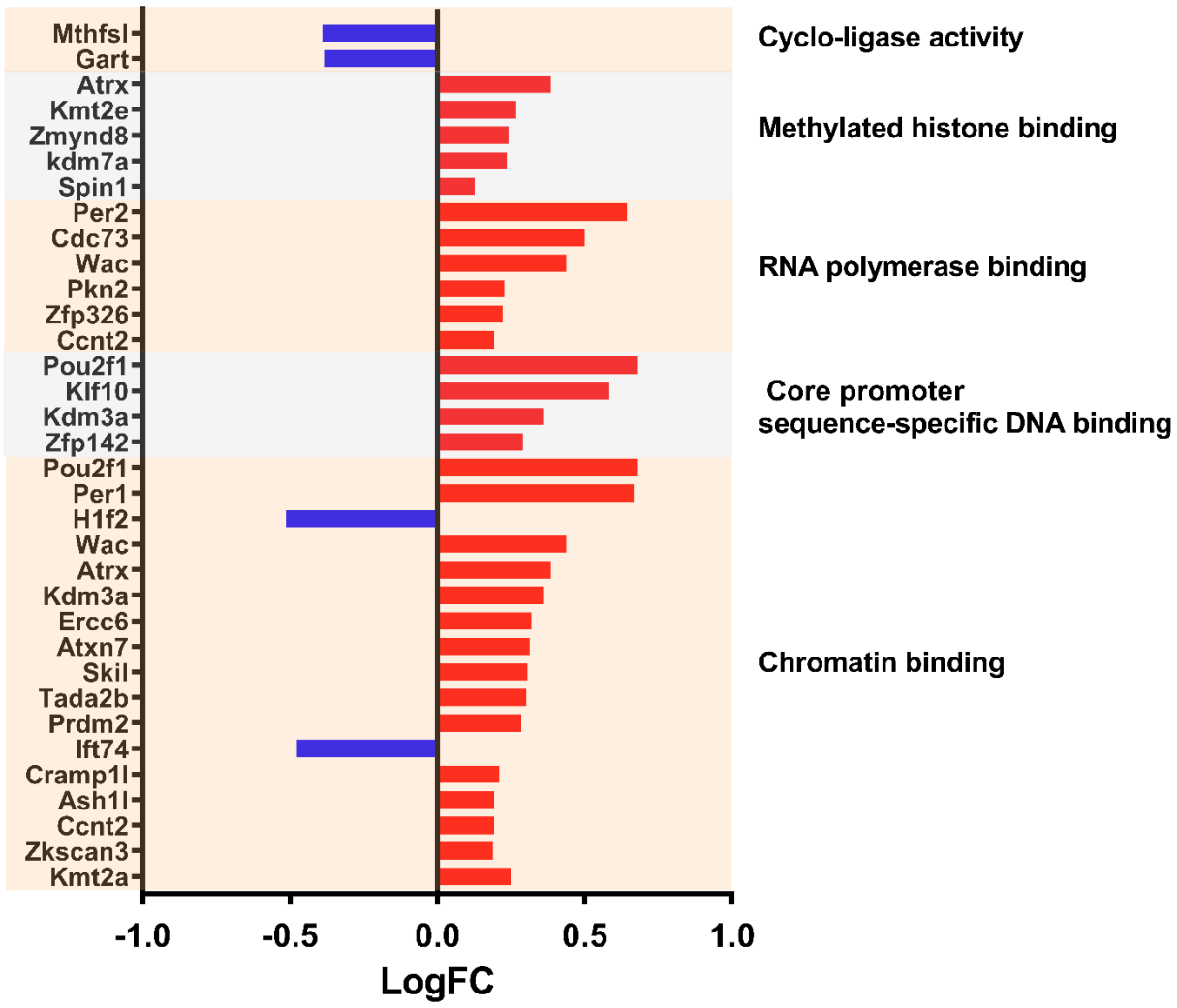

Figure 3.7 – RNA-Seq: PON2-deficient Cortex Pathway Analysis (*continued*). C. Differentially expressed genes (PON2-deficient vs WT) and associated molecular functions in the male cortex, upregulated genes are shown in red and downregulated genes are shown in blue.

D.

GO Term – Molecular Functions	# DE Genes	P-Value
Cyclo-ligase activity	2/3	8.300e-4
Methylated histone binding	5/57	0.003
RNA polymerase binding	6/55	0.007
Core promoter sequence-specific DNA binding	4/46	0.007
Chromatin binding	17/527	0.013

Figure 3.7 – RNA-Seq: PON2-deficient Cortex Pathway Analysis (*continued*). D. Top 5 molecular functions significantly impacted by PON2 deficiency in the male cortex, corrected for multiple comparisons using false discovery rate (FDR).

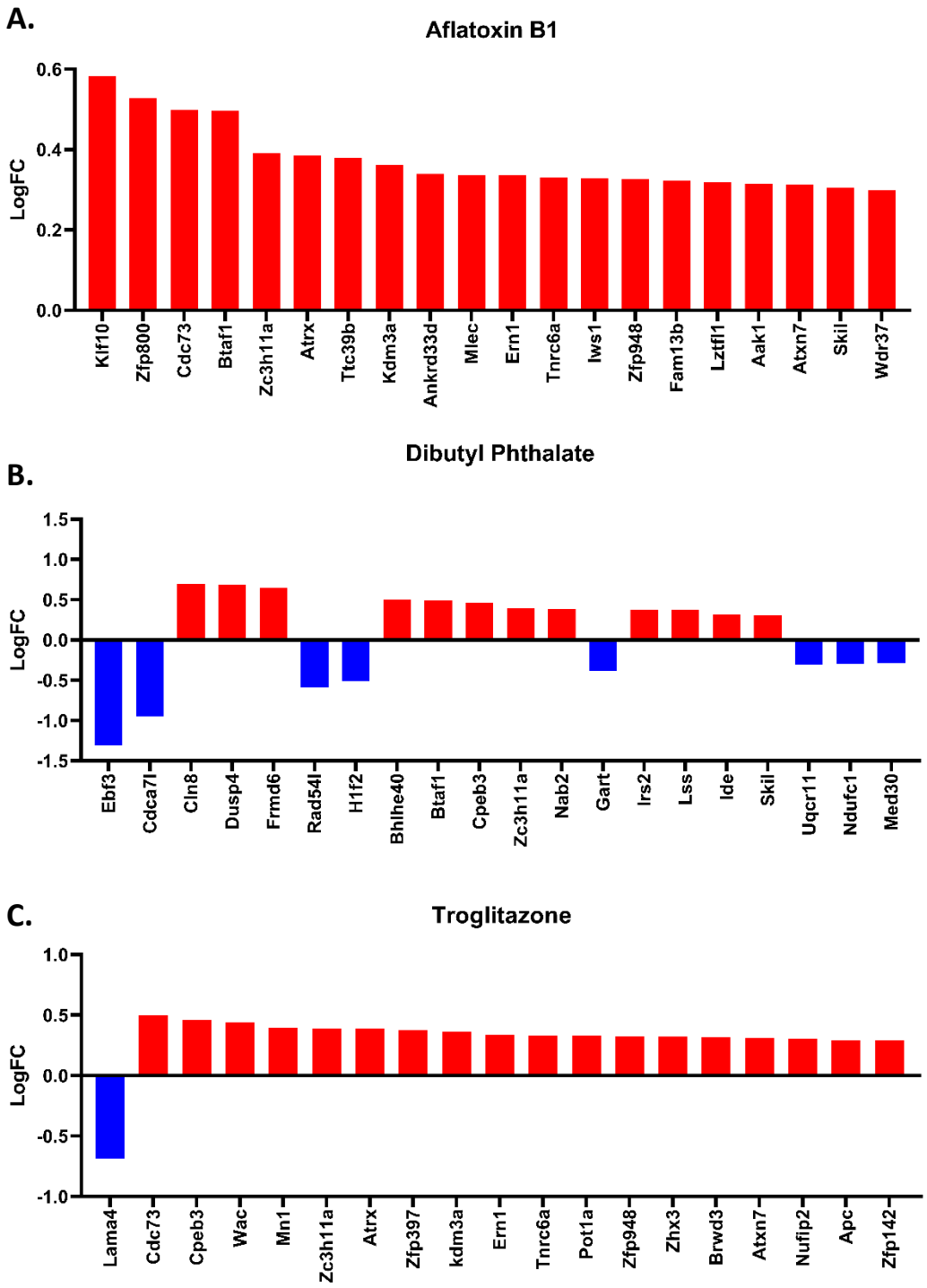

Figure 3.8 – RNA-Seq: Predicted Upstream Regulators in the PON2-deficient Cortex. A. Differentially expressed genes in PON2-deficient male cortex related to aflatoxin B1 exposure. **B.** Differentially expressed genes in PON2-deficient male cortex related to dibutyl phthalate exposure. **C.** Differentially expressed genes in PON2-deficient male cortex related to troglitazone exposure.

D.

Predicted Upstream Regulator Analysis – Chemicals, Drugs, Toxicants (CDTs)	Prediction	P-Value
Aflatoxin B1	Present	1.048e-7
Dibutyl Phthalate	Present	0.007
Troglitazone	Absent	3.914e-10

Figure 3.8 – RNA-Seq: Predicted Upstream Regulators in the PON2-deficient Cortex (*continued*). D. Predicted Upstream Regulator Analysis of Chemicals, Drugs and Toxicants predicted to be present or absent based on gene expression, corrected for multiple comparisons using false discovery rate (FDR).

E.

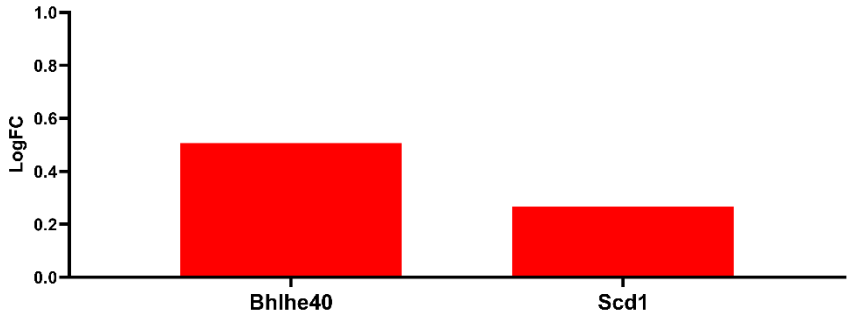

F.

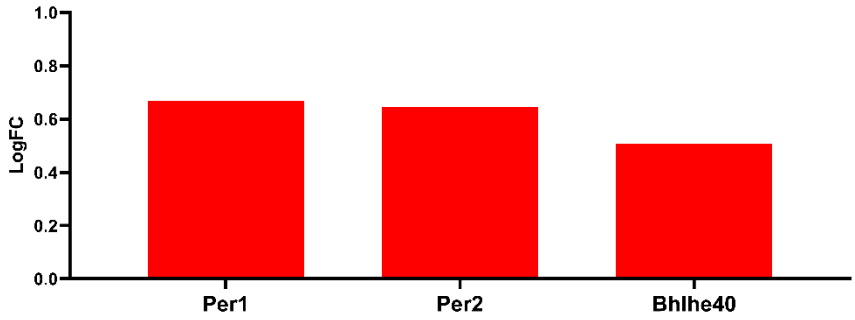

G.

Predicted Upstream Regulators	Prediction	P-Value
Mlxipl	Activated	0.030
Npas2	Activated	0.032
Clock	Activated	0.043

Figure 3. 8 – RNA-Seq: Predicted Upstream Regulators in the PON2-deficient Cortex (*continued*).). E. Differentially expressed genes targeted by Mlxipl (MLX interacting protein-like) **F.** Differentially expressed genes targeted by Npas2 (neuronal PAS domain protein 2) and Clock (circadian locomotor output cycles kaput). **G.** Predicted Upstream Regulators and their predicted activation status, corrected for multiple comparisons using false discovery rate (FDR).

A.

Pathway Analysis	P-Value
Basal cell carcinoma	2.700e-4
Melanogenesis	7.900e-4
Hippo signaling pathway	8.500e-4
Breast cancer	8.800e-4
Cushing syndrome	0.001

B.

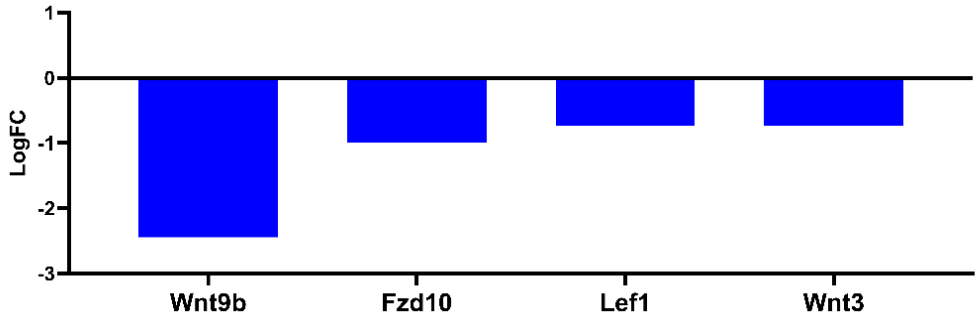

Figure 3.9 – RNA-Seq: PON2-deficient Striatum Pathway Analysis. A. Top 5 predicted KEGG pathways affected by PON2 deficiency in the female striatum, corrected for multiple comparisons using false discovery rate (FDR)**. B.** Differentially expressed genes (PON2 deficient vs WT) linked to predicted affected KEGG pathways.

C.

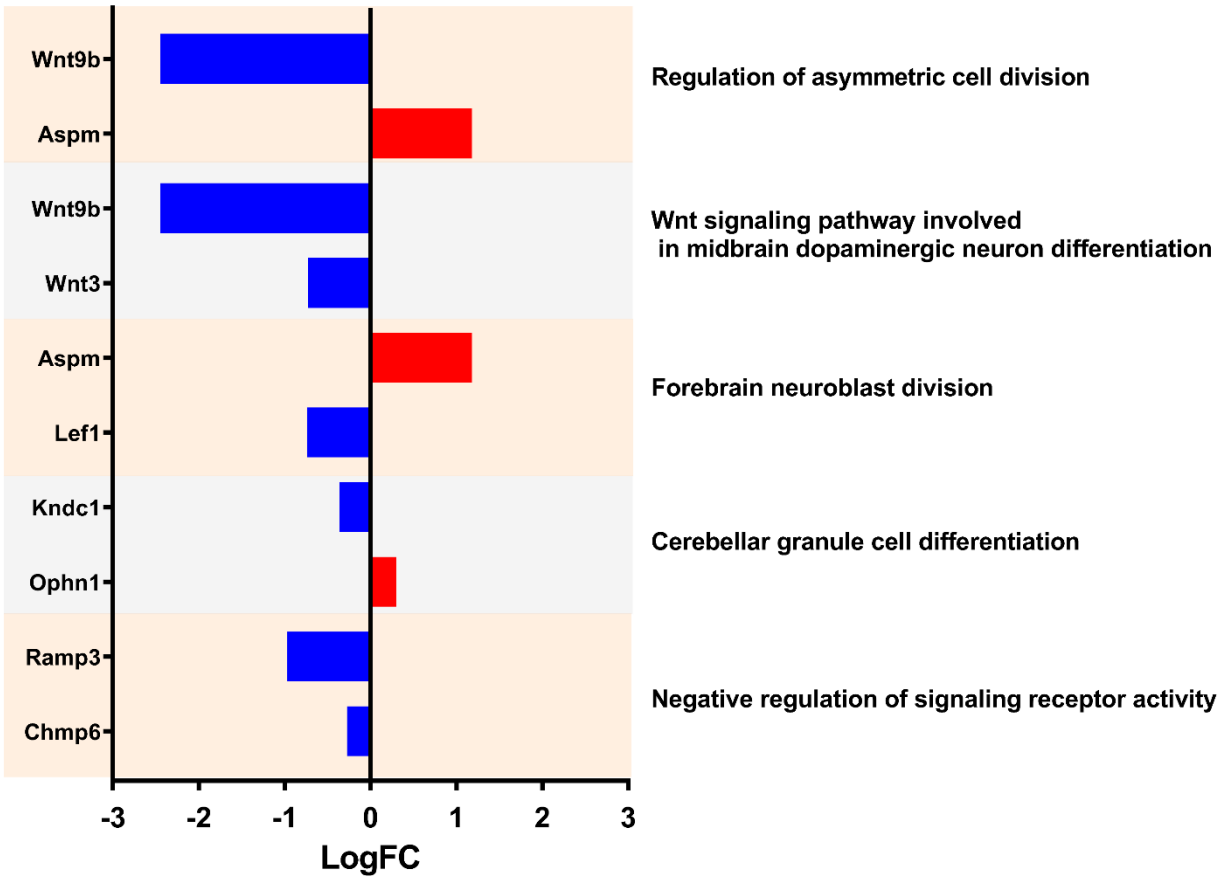

D.

GO Term – Biological Processes	# DE Genes	P-Value
Regulation of asymmetric cell division	2/3	4.200e-5
Wnt signaling pathway involved in midbrain dopaminergic neuron differentiation	2/7	2.900e-4
Forebrain neuroblast division	2/9	4.900e-4
Cerebellar granule cell differentiation	2/10	6.200e-4
Negative regulation of signaling receptor activity	2/25	0.004

Figure 3.9 – RNA-Seq: PON2-deficient Striatum Pathway Analysis (*continued*). C. Differentially expressed genes (PON2 deficient vs WT) and associated Biological Processes GO categories in the female striatum, upregulated genes are shown in red and downregulated genes are shown in blue**. D.** Top 5 Biological Processes GO categories significantly impacted by PON2 deficiency in the female striatum, corrected for multiple comparisons using false discovery rate (FDR).

E.

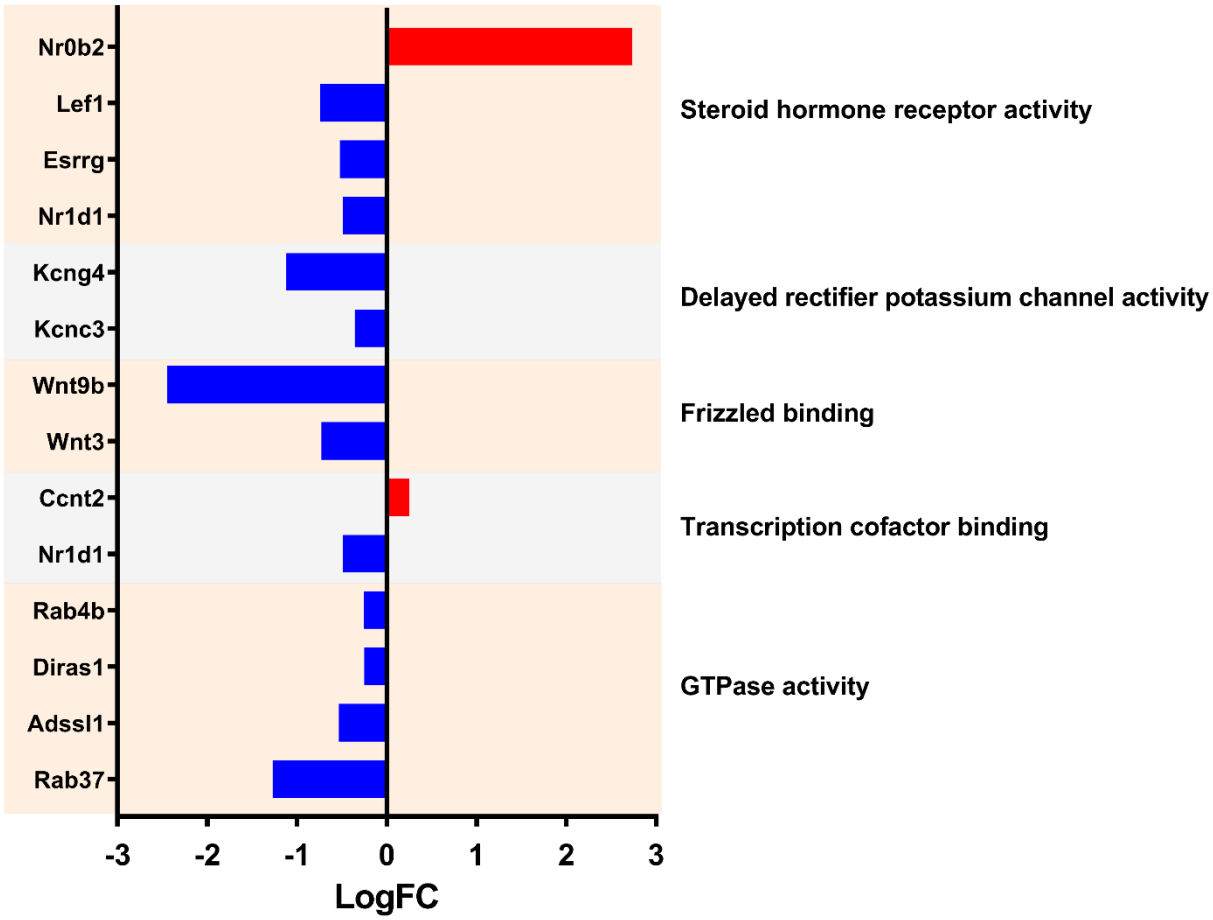

F.

GO Term – Molecular Functions	# DE Genes	P-Value
Steroid hormone receptor activity	4/46	2.700e-5
Delayed rectifier potassium channel activity	2/26	0.004
Frizzled binding	2/40	0.010
Transcription cofactor binding	2/49	0.015
GTPase activity	4/271	0.019

Figure 3.9 – RNA-Seq: PON2-deficient Striatum Pathway Analysis (*continued*). E. Differentially expressed genes (PON2 deficient vs WT) and associated Molecular Functions GO categories in the female striatum, upregulated genes are shown in red and downregulated genes are shown in blue. **F.** Top 5 Molecular Functions GO categories significantly impacted by PON2 deficiency in the female striatum, corrected for multiple comparisons using false discovery rate (FDR).

A.

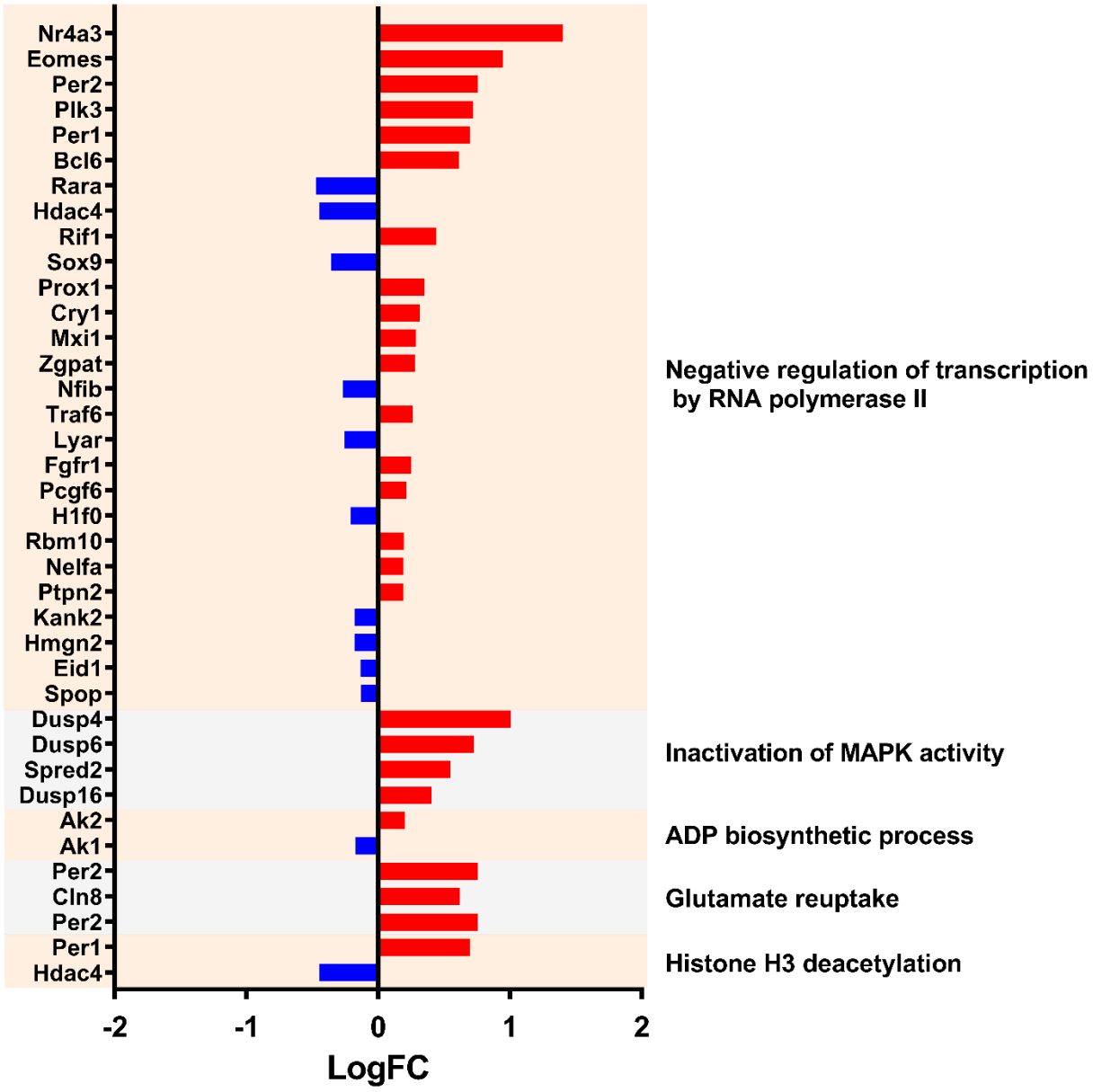

Figure 3.10 – RNA-Seq: PON2 deficient Cerebellum Pathway Analysis. A. Differentially expressed genes (PON2 deficient vs WT) and associated Biological Processes GO categories in the male cerebellum, upregulated genes are shown in red and downregulated genes are shown in blue.

B.

GO Term – Biological Processes	# DE Genes	P-Value
Negative regulation of transcription by RNA polymerase II	27/747	1.900e-5
Inactivation of MAPK activity	4/17	9.800e-5
ADP biosynthetic process	2/3	6.600e-4
Glutamate reuptake	2/3	6.200e-4
Histone H3 deacetylation	3/14	0.001

Figure 3.10 – RNA-Seq: PON2-deficient Cerebellum Pathway Analysis (*continued*). **B.** Top 5 Biological Processes GO categories significantly impacted by PON2 deficiency in the male cerebellum, corrected for multiple comparisons using false discovery rate (FDR).

C.

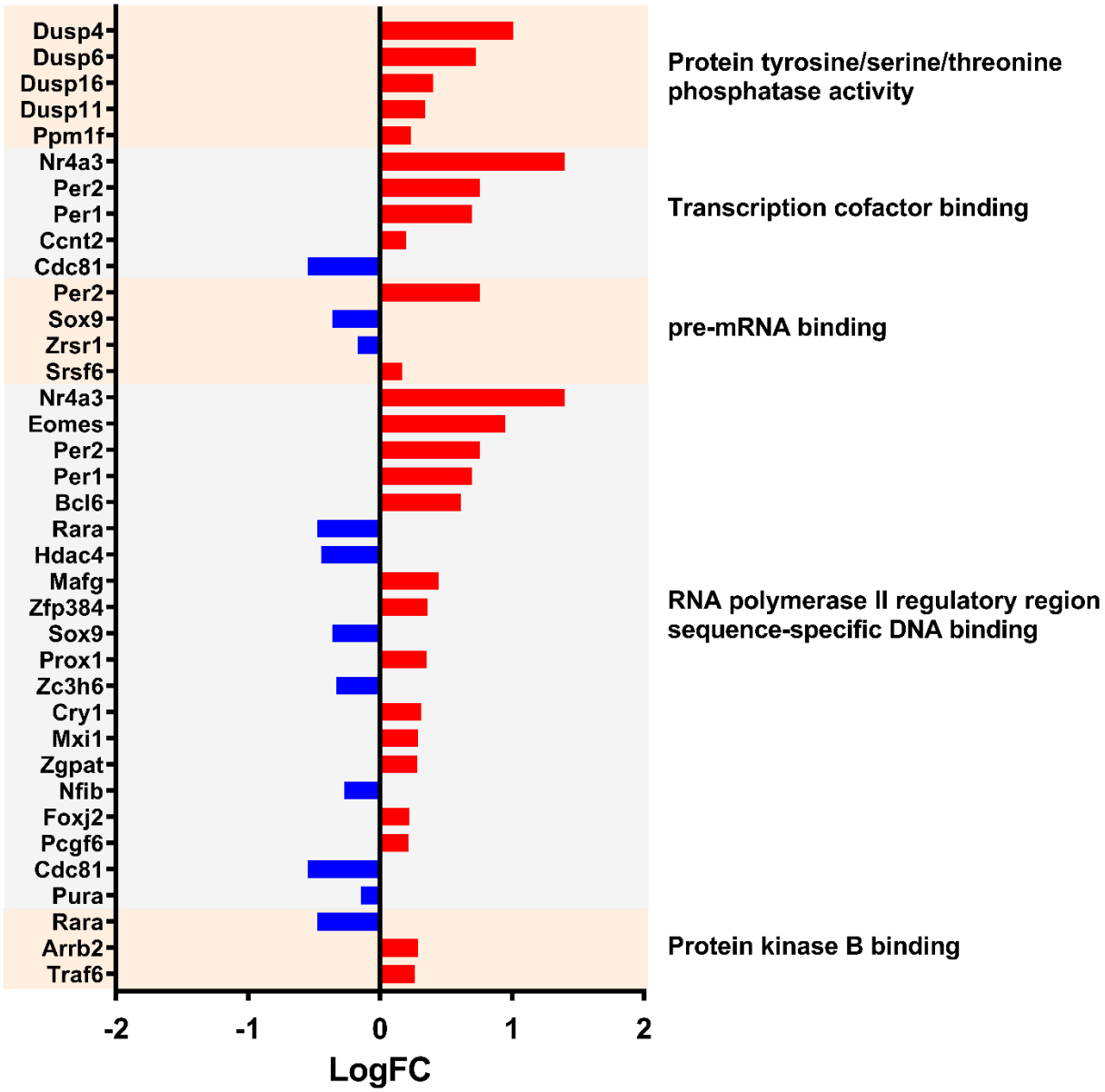

Figure 3.10 – RNA-Seq: PON2-deficient Cerebellum Pathway Analysis (*continued*). C. Differentially expressed genes (PON2 deficient vs WT) and associated Molecular Functions GO categories in the male cerebellum, upregulated genes are shown in red and downregulated genes are shown in blue.

D.

GO Term – Molecular Functions	# DE Genes	P-Value
Protein tyrosine/serine/threonine phosphatase activity	5/35	1.600e-4
Transcription cofactor binding	5/49	7.700e-4
pre-mRNA binding	4/32	0.001
RNA polymerase II regulatory region sequence-specific DNA binding	20/654	0.002
Protein kinase B binding	3/17	0.002

Figure 3.10 – RNA-Seq: PON2-deficient Cerebellum Pathway Analysis (*continued*). D. Top 5 Molecular Functions GO categories significantly impacted by PON2 deficiency in the male cerebellum, corrected for multiple comparisons using false discovery rate (FDR).

A.

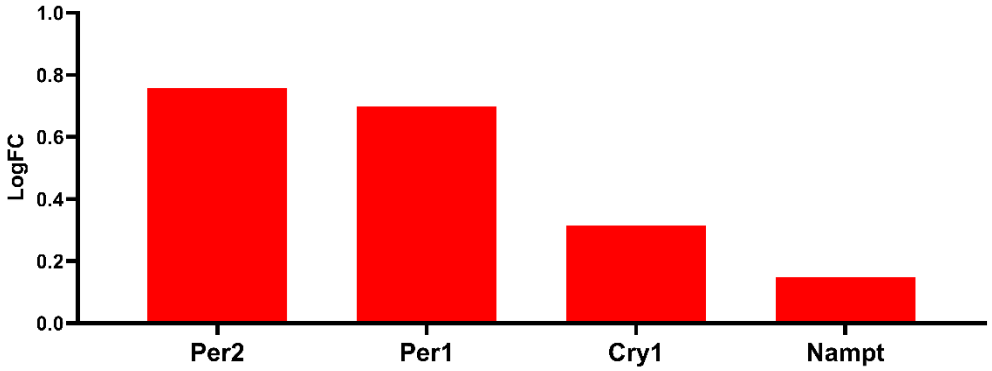

B.

Upstream regulators	Prediction	P-Value
Npas2	Activated	0.002
Clock	Activated	0.003
Arntl	Activated	0.005

Figure 3.11 - RNA-Seq: Predicted Upstream Regulators in the PON2 deficient Cerebellum. **A.** Differentially expressed genes targeted by Npas2 (neuronal PAS domain protein 2), Clock (circadian locomotor output cycles kaput) and Arntl (aryl hydrocarbon receptor nuclear translocator like). **B.** Predicted Upstream Regulators and their predicted activation status, corrected for multiple comparisons using false discovery rate (FDR).

3.4 – Discussion

Limited attention has been given to the role of PON2 in the central nervous system (CNS). As oxidative stress is increasingly implicated in multiple disease etiologies and known as a common mechanism by which neurotoxicants exert toxicity, further characterization of antioxidant genes, like PON2, in the CNS is warranted to inform gene-environment interaction studies. Single nucleotide polymorphisms (SNPs) affecting PON2 activity, potentially mimicking a 'deficient' state, are known to exist in the population (Dasgupta et al., 2011), underscoring a translational benefit to thoroughly understanding the effects of PON2 deficiency.

When evaluating behavior, PON2 deficiency in our study significantly impacted multiple home-cage metrics. Changes were only observed during the dark cycle, when mice are at peak wake activity (Ripperger et al., 2011). PON2-def mice spent more time moving and moved longer distances than WT, suggesting a mild hyperactivity phenotype. PON2-def mice also spent significantly more time in the center of the arena and less time in the hidden shelter. As prey animals, mice possess a defensive instinct and naturally prefer the safety of the hidden shelter, as open areas lend them to predation in the wild. More time spent in the center could support an anxiolytic phenotype, where PON2-def mice are less anxious in the home-cage environment and feel comfortable exploring the center more frequently. Additionally, this behavior could point to a reduction in fear response, where the PON2-def mice are unable to respond to environmental conditions which would usually induce fear behavior. Further exploration of this behavior using targeted tests, such as the elevated plus maze, would be beneficial, as would assessing impacts to their conditioned fear response. The only metric with an observed sex-interaction was time spent at the food hopper, where PON2-def females spent significantly more time at the hopper than WT. PON2 deficiency has recently been investigated in relation to obesity, with PON2-def mice

exhibiting diet-prone obesity when fed a high-fat diet (Shih et al., 2019). No differences in body mass were noted between PON2-def and WT mice in our study, nor were there recorded differences in food consumption by hopper kibble weight (data not shown). As such, the additional time spent by female PON2-def mice at the food hopper may be unrelated to food consumption and due to the location of the food hopper within the cage. Alternatively, these mice may be playing with the food for additional enrichment. Mice are singly housed for the duration of this experiment and lack the usual social interaction provided by their cage mates. Feasibly, PON2-def female mice may be more sensitive to disruptions to social interaction and require more enrichment. Further evaluation to measure social and play behavior with PON2 deficiency would be of interest.

PON2-def mice had significantly shorter latency to fall during the rotarod experiment, suggesting impaired motor coordination (Figure 3.3). When evaluated for gait metrics on the CatWalk system, PON2-def mice also spent significantly less time using girdle postural support (Figure 3.4H). This posture is when the mice support their weight on either their two front or two hind limbs simultaneously. Given the nature of the rotarod test, this reduction in girdle postural support may influence their success on the rotarod, particularly if their ability to balance on their two front limbs is impaired. A reduction in front limb balancing could reduce their ability to recover from a slip on the rod, as a slip usually begins with the loss of hind limb rod contact and forces the mouse to balance on their two front limbs until they reestablish hind limb contact or fall off the rod completely. Additional targeted testing of cerebellar function, both motor and autonomic, would be of interest as the cerebellum was found to be the tissue most deficient in PON2.

Transcript changes were noted in a highly region- and sex-specific manner in our study, with the full list of differentially expressed genes available in Appendix B Tables 1 - 3. Although sex differences have been reported in the literature relative to PON2 expression, with females showing higher expression than males (Giordano et al., 2011; Giordano et al., 2013), this was not observed in the present study where PON2 expression in WT females and males was comparable. However, PON2 deficiency appears to significantly change the differences between female and male expression patterns on a global transcription scale as noted in Figures 3.5C – E. While WT females had hundreds of differentially expressed genes in the cerebral cortex and striatum compared to males, these differences were not observed in PON2-def females, with only the expected sex chromosome genes notably different. The differential gene expression was less dramatic in the cerebellum, where WT females had a smaller number of differentially expressed genes compared to WT males, and PON2-def females had a similar value. However, the composition of these genes differed between the WT and PON2-def populations, suggesting significant alterations. Taken together, these results support that PON2 deficiency significantly affects sex-specific expression patterns and removes sex differences in the brain at the transcript level, which may have potential consequences on morbidities with sex interactions. These results have specific implications for toxicological studies, as exposure and response to toxicants is noted to be sexually dimorphic (Gochfeld 2017). Understanding genes which may drastically alter the transcriptome and cause biologically female animals to present transcriptionally as male, or vise-versa, is critical when assessing gene-environment interactions to toxicants. Furthermore, these results also have impacts for assessing individual toxicant susceptibility based on genotype. PON2 is known to be polymorphic in the population, with SNPs affecting general PON activity (Dasgupta et al., 2011). This could be of particular importance if

individuals with PON2 polymorphisms which reduce PON2 activity are exposed to a toxicant or prescribed a medication with sexually dimorphic outcomes, as they may have an idiosyncratic response. Although limited work has addressed the functional impact of PON2 polymorphisms, variability of PON1 levels or activity vary by at least 15-fold among individuals (Furlong et al., 2006; Furlong 2007), and it is possible that a similar observation may be seen with PON2. No other PONs (PON1, PON3) were differentially expressed in our dataset, suggesting that no compensatory upregulation within the PON family occurs from PON2 deficiency. However, PON3, also located at the mitochondria, may be able to function in a similar manner to PON2 and compensate without an increase in transcript, but by increasing its activity. Enzymatic activity of the PONs was not investigated in our study but would be of interest to evaluate for future studies of PON2 deficiency.

Our study focused on assessing the effect of PON2 deficiency on the baseline transcriptome of specific brain regions. At odds with our hypothesis, oxidative stress pathways were not the predominant pathways perturbed by PON2 deficiency when looking at the iPathwayGuide analysis. These findings were surprising, as PON2 deficiency has been reported to increase oxidative stress in multiple systems by numerous investigators (Devarajan et al., 2011; Giordano et al., 2013; Yang et al., 2015; Sulaiman et al., 2019). Feasibly, impacted oxidative stress pathways may be more apparent if the mice were challenged with an oxidant, an aspect that was not addressed in this study. While no direct pathways were picked up by this analysis, supporting evidence for increased oxidative stress was noted in the male cerebral cortex with the chemical, drug, and toxicant exposure prediction tool. When comparing the expression profile of our samples to various compounds in the iPathwayGuide database, PON2 deficiency leads to gene expression changes like those observed after aflatoxin B1 exposure (Figure 3.8A).

While aflatoxin B1 exhibits well-documented hepatotoxicity and is a known carcinogen, it also has neurotoxic effects, largely mediated through increased oxidative stress (Bbosa et al., 2013). Recent work has additionally identified that aflatoxin B1 alters calcium homeostasis and causes mitochondrial dysfunction in human astrocytes *in-vitro* (Park et al., 2020) and increases ROS in the brain of mice *in-vivo* (Huang et al., 2020). As such, the predicted presence of aflatoxin B1 exposure by iPathwayGuide may be related to the reported mitochondrial dysfunction and oxidative stress noted with PON2 deficiency. Furthermore, this finding suggests PON2 deficiency may confer increased sensitivity to aflatoxin B1 exposure, if the expression of similar genes targeted by the toxin are already altered. This may point to individuals with lower PON2 levels as a previously unidentified sensitive population to aflatoxin B1 exposure. Considering the wide global distribution of aflatoxin contaminated food commodities, this could pose a significant public health concern and warrants further investigation regarding the relationship of PON2 deficiency and aflatoxin exposure. Similarly, iPathwayGuide predicted PON2 deficiency to mimic dibutyl phthalate exposure (Figure 3.8B). Dibutyl phthalate is one of the most used phthalate esters in plastics manufacturing and is a ubiquitous environmental contaminant, with demonstrated neurotoxic effects attributed to an increase in ROS (Wójtowicz et al., 2017). In a similar manner to aflatoxin B1, PON2 deficiency may confer sensitivity to dibutyl phthalate exposure and further investigation of this would be of interest. Finally, PON2 deficiency leads to gene expression changes suggesting the absence of troglitazone (Figure 3.8C), an anti-diabetic and anti-inflammatory drug, supporting an increase in inflammation and/or dysregulation of insulin pathways. Insulin degrading enzyme (Ide) was found significantly upregulated in PON2-def cerebral cortex (Appendix B Table AB.1), further linking PON2 deficiency and insulin dysregulation.

Neurological disorders, ranging from neurodevelopment to aging, are often sex dependent. In early life, males are four times as likely to develop autism spectrum disorder (ASD) than females, with the underlying mechanism for this difference currently unknown but speculated to be a complex combination of genetic and environmental factors (Park et al., 2016). In contrast, females are twice as likely to experience affective disorders such as anxiety, post-traumatic stress disorder, and major depression, with evidence supporting sex hormone interactions as a possible culprit (Bangasser & Valentino 2014). In our study, female PON2-def mice had significantly higher expression of the small heterodimer partner Nr0b2 (nuclear receptor subfamily 0, group B, member 2) in the striatum. Nr0b2 has been shown to interact with estrogen receptors and inhibit their function (Seol et al., 1996), as well as function as a mediator of endocrine homeostasis in male mice (Vega et al., 2015). Indeed, iPathwayGuide analysis showed steroid hormone receptor activity as the highest impacted molecular functions pathway from PON2 deficiency in the striatum (Figure 3.9F). This alteration of Nr0b2 and steroid hormone receptor activity may inhibit estrogen signaling in the striatum of female mice and contribute to the male-presenting transcriptome observed in this study. Perturbations in estrogen response *in-vitro* are noted in the literature with PON2 deficiency, where estradiol protects primary WT astrocytes from oxidative damage, but does not protect primary astrocytes from PON2-def mice (Giordano et al., 2013). These results are consistent with those of our study and support the concept that PON2 deficiency may inhibit estrogen signaling, although targeted study of this should be addressed. Behaviorally, PON2-def mice displayed a mild anxiolytic phenotype, as noted by their increased time spent in the center of the arena and decreased time in the hidden shelter during the PhenoTyper assessment. Feasibly, this may also be related to the

inhibitory effects on the hypothalamic-pituitary axis (HPA) by Nr0b2 and sex steroid hormone pathways which affect mood and behavior (Bangasser & Valentino 2014).

Neurodegenerative diseases also differ between sexes, with Parkinson's disease affecting males more than females, and Alzheimer's disease affecting females at a higher prevalence compared to age-matched males (Ullah et al., 2019). Alzheimer's disease is marked by aggregation of amyloid beta (Aβ) and progressive neuron loss, with multiple hypotheses as to how these aggregates destroy neurons. One line of evidence suggest Aβ plaques inhibit glutamate uptake, leading to excitotoxic levels of glutamate to bind to postsynaptic glutamate receptors (Danysz &Parsons 2012). In our study, glutamate reuptake related genes Cln8 (ceroid-lipofuscinosis, neuronal 8) and Per2 (period 2) were upregulated in the cerebral cortex and cerebellum of PON2-def male mice. While this would support a potential protective effect against excitotoxicity for neurons, over-clearance of glutamate from the synaptic cleft may have its own deleterious effects, reducing sensitivity to reward and contributing to symptoms of depression. The increase in reuptake may also point to increases in glutamate output, requiring increases in reuptake to prevent excitotoxicity. Additional investigation of reward seeking behavior and depression would be of interest in PON2-def mice, as well as further probing of the glutamatergic system.

In addition to sex differences, regional differences were highly specific, with iPathwayGuide analysis revealing few common GO terms shared among them. In the cerebral cortex and the cerebellum of PON2-def male mice, a variety of RNA processing and transcription-mediating pathway changes were noted (Figures 7 and 10). Changes in general transcription could have downstream implications on countless pathways and would require targeted hypothesis-testing to determine the precise impact of PON2 deficiency in a specific

pathway or disease state, which were not addressed in this study. Predicted upstream regulators in these regions were also identical, with the majority of these in the family of circadian regulators, namely Clock and its paralogue Npas2. Although circadian rhythm disruptions were not noted in PON2-def mice during home-cage assessment, the hyperactivity during the dark cycle may be related to activated circadian pathways. Additionally, Per1 and Per2, both upregulated in the cerebral cortex and cerebellum of PON2-def male mice and transcriptionally controlled by the CLOCK complex, have been shown to play an important role in cancer cell biology, where overexpression of PER1 sensitizes human cancer cells to DNA-damage induced apoptosis (Gery et al., 2006). Indeed, multiple cellular division pathways are under circadian control and the involvement of circadian genes in cancer biology is emerging as an important area of study (Masri & Sassone-Corsi 2018). The role of PON2 in cancer biology has also been examined, with PON2 often found upregulated in cancer cells, likely providing apoptotic protection through the management of ROS at the mitochondrial level (Kruger et al., 2015). Whether PER1 expression plays a role in the ability for PON2 to protect cells against apoptosis has not been addressed in the literature but would be of interest for further evaluation. PON2 deficiency in the striatum of female mice in our study had significant decreases in expression of Wnt9b (wingless-type 9b), Fzd10 (frizzled-10), Lef1 (lymphoid enhancer-binding factor 1) and Wnt3 (wingless-type 3) (Figure 9B). These decreases in gene expression are anticipated to impact multiple cancer-related pathways, as noted in Figure 9A. Given the role of WNT signaling in cancer development, decreased expression of WNT may have a protective effect for cancer promotion but have deleterious effects on the brain in normal aspects of WNT signaling, such as cellular differentiation. The protective effects on cancer development and/or progression from PON2 deficiency have not been studied in detail, although targeted PON2 knockdown has

been shown to make human cancer cells more susceptible to irradiation damage (Kruger et al., 2015) and the modulation of PON2 in this arena may be of further interest.

Looking further at the predicted circadian regulators, Arntl was predicted to be activated in the male cerebellum in our dataset (Figure 3.11B). ARNTL1 (also known as BMAL1) is part of the CLOCK complex, forming a heterodimer with CLOCK and binding to the E-box response element of circadian-controlled genes to control their expression (Aryal et al., 2017). ARNTL1 is also known to interact with the aryl hydrocarbon receptor (AhR), a transcription factor that plays a major role in responding to exogenous chemical exposure by regulating the expression of detoxifying enzymes in the cytochrome P450 family. Ligand-bound AhR forms a complex with hydrocarbon nuclear translocator (ARNT), which is required for AhR to bind to DNA regulatory elements and modulate transcription (Neavin et al., 2018). In the cortex and cerebellum of male PON2-def mice, Arnt was found to be significantly upregulated in our study (Tables AB.1 and AB.3), although AhR transcript levels were not altered. Further investigation of AhR function in PON2-def mice would be of interest, to determine if xenobiotic metabolism is affected by PON2 deficiency.

While PON2 has been identified as an important modulator of oxidative stress in the CNS, limited work has been done to address the effects of PON2 deficiency in the brain on a global level. Our study begins to address key gaps in the literature regarding the impact of PON2 deficiency in the CNS and what global changes, both biochemically and phenotypically, may be caused by the loss of PON2. We have shown that PON2 deficiency leads to behavioral changes, specifically related to locomotion, and significant biochemical alterations at the transcript level impacting a variety of molecular functions that have implications for affective disorders, cellular differentiation, and cancer biology. Highly specific sex and regional changes were observed

when looking at RNA expression, indicating that PON2 may play a variety of distinct roles in different regions of the brain in a sex-specific manner. Many of the differentially expressed genes identified in this study were previously unknown to be affected by PON2 deficiency and provide novel directions for future PON2 research. Further investigation looking at temporal elements, additional brain regions and behavioral domains would be of interest to further characterize the role of PON2 in the brain and the consequences of its deficiency.

3.5 – Materials and Methods

Mice

Male and female WT and PON2-def mice (Ng et al., 2006) on a C57BL/6J background were used for this study. Seven to ten animals were used per sex per group. Mice were bred from PON2 deficient heterozygous crosses with resulting WT and PON2-def homozygous littermates used in rolling cohorts. Behavioral testing began at 3 – 4 months of age. Mice were housed in a specific pathogen-free facility on a 14-hour light/ 10-hour dark cycle with *ad libitum* access to food and water. All procedures were conducted in accordance with the National Institute of Health Guide for the Use and Care of Laboratory Animals and were approved by the University of Washington Institutional Animal Care and Use Committee.

Tissue

Mice were sacrificed at 3 – 4 months of age upon conclusion of behavioral testing utilizing a carbon dioxide chamber. Cerebral cortex, striatum, and cerebellum were freshly dissected (Spijker 2011) and flash frozen in liquid nitrogen. Tissues were pulverized with a pre-chilled mortar and pestle into a fine powder, stored at −80°C and aliquoted into appropriate

buffers for later testing.

Noldus PhenoTyper

Home-cage behavior was evaluated as the first behavioral endpoint using the Noldus PhenoTyper system (Noldus Information Technology, Wageningen, The Netherlands). Mice were placed into plexiglass cages with cameras recording from the cage top downward. All cages were recorded simultaneously for 67 hours, beginning at 12PM and ending at 7AM. EthoVision XT software (Noldus Information Technology, Wageningen, The Netherlands) was used to track the movement of the mice for the duration of the experiment. Utilizing this software, the cage is divided into various zones (arena center, arena perimeter, food hopper, water bottle, hidden shelter) and the amount of time spent within each zone, as well as the travel between zones and the speed of their travel is recorded for each mouse.

Noldus CatWalk

Gait assessment took place 3-5 days after PhenoTyper analysis using the Noldus CatWalk XT system (Noldus Information Technology, Wageningen, The Netherlands). This system is comprised of an enclosed glass walkway 1.3 m long, with the walkway illuminated from the side in green fluorescent light and the top of the system in red fluorescent light which illuminates downward. The room is darkened to allow for a camera under the glass to read the green light measurements and detect when the mouse's paw contacts the glass. For a given trial, the mouse was placed at the left end of the apparatus and allowed to freely explore the enclosed system. The innate desire to explore new environments was utilized to drive the mouse to the other side of the system. Once the mouse had fully crossed the experimental field, the run was

determined to be compliant based on time to cross the experimental field (10 sec or less) and whether the mouse freely walked the length of the experimental field (no stops for investigatory behavior). Each mouse was tested until 3 compliant trials were acquired, with each mouse generally requiring 10 trials to achieve compliance. The compliant trials were analyzed and combined to output gait information for the mouse focusing on four domains: temporal parameters (average speed, cadence, swing, and swing speed), coordination (sequence regularity index and step pattern), spatial patterns of individual paws (stride length, print intensity, print area, print length, and print width) and spatial pattern relationships between paws (base of support and support time). Each parameter is briefly summarized as follows:

- Average speed: Walk speed measured as distance over time, expressed in centimeter/second (cm/s).
- Cadence: Frequency of steps during the trial, expressed as number of steps/second.
- Swing: Time of paw spent in the air between two consecutive steps, expressed in seconds (s).
- Swing speed: Parameter calculated using swing and stride length, expressed in centimeter/second (cm/s).
- Sequence Regularity Index: Percentage index measuring interlimb coordination, calculates based on the number of normal step sequence patterns (NSSP), number of paws and paw placements, SRI = 100% * (NSSP * # paws) / # of paw placements.
- Step sequence: Measures percentage spent in the six normal step sequence patterns (NSSP) noted in mice:

    - CA – RF – LF – RH – LH
    - CB – LF – RF – LH – RH
    - AA – RF – RH – LF – LH
    - AB – LF – RH – RF – LH
    - RA – RF – LF – LH – RH (not observed in our study)
    - RB – LF – RF – RH – LH (not observed in our study)
- Stride length – Distance between paw placement in two consecutive steps of the same paw, expressed in centimeters (cm).
- Print intensity: The average pressure exerted by a single paw on floor contact, expressed in arbitrary units (a.u.).
- Print area: Measurement of the complete paw print including all frames that makes up a stance, expressed in cm^2.
- Print length: Measured length of the print area, expressed in centimeters (cm).
- Print width: Measured width of the print area, expressed in centimeters (cm).
- Base of support: Describes the distance between either two hind paws or two front paws, expressed in centimeters (cm).
- Support time: Relative duration spent supporting weight on all combinations of paws. Combinations include zero paw (not observed in our study), single paw, girdle two paws (LF & RF or LH & RH), lateral two paws (LF & LH or RF & RH), diagonal two paws (LF & RH or RF & LH), three paws or four paws.

Rotarod

Mice were moved to the testing room 15 minutes prior to the start of the experiment for acclimation. A five lane Rota-Rod treadmill (Med Associates Inc., Vermont, USA) was utilized with adjacent lanes separated by a disk-wall. Mice were given a training trial at a constant speed of 4 RPM, 1 min on the rod and 1 min of rest for a total of 3 times. The testing consisted of a 5-min trial with rod speed ramping from 4 RPM to 40 RPM over the 5-min period. Time to fall (latency) was recorded when the mouse completely fell off the rod or rode around the rod for a full revolution. Each mouse was given ten 5-min test trials and the five highest latency trials, expected to reflect the maximum ability of the mouse for this test, were averaged to provide their latency score. Mice that repeatedly jumped from the apparatus were removed from the study and not included in further analysis.

RNA-Seq

RNA was extracted from 30 – 50 mg of pulverized brain tissue utilizing a Qiagen RNeasy kit (Qiagen, Hilden, Germany) according to the manufacturer's recommended protocol. The quantity of total RNA was determined by measuring the OD260 with a NanoDrop ND-1000 Spectrophotometer (Thermo Fisher Scientific, Waltham, MA). RNA purity was assessed by measuring OD260/280 and OD260/230 ratios. RNA integrity was determined using an Agilent 2100 Bioanalyzer (Agilent Technologies, Santa Clara, CA). Only total RNA samples with RNA Integrity Numbers (RIN) > 8, OD260/280 as well as OD260/230 ratios of 1.8 – 2.1 were used for RNA-Seq analysis. Samples were commercially sequenced by Beijing Genomics Inc. (BGI, Shenzen, China) using their proprietary sequencer which generates 150 nt paired-end sequences. The reads were aligned against the Genecode M23 trranscriptome using the Salmon aligner (Patro et al., 2015) to generate estimated counts for each transcript. Transcript counts were summarized to gene counts using the Bioconductor tximport package (Soneson et al., 2015).

Gene counts are proportional to the underlying transcript abundance and were utilized as raw data for all analyses. Differential gene expression was assessed using the Bioconductor limma package, using the 'limma-voom' pipeline, which fits a weighted analysis of variance (ANOVA) model to the log counts/million counts (Law et al., 2014). Univariate p-values were corrected using false discovery rate (FDR), and genes were selected at an FDR<0.1. The data were further analyzed at the pathway level using iPathwayGuide from Advaita Bioinformatics (https://www.advaitabio.com/ipathwayguide). This analysis tool utilizes the 'Impact Analysis' approach which takes into consideration the direction and type of signals on a pathway as well as the role and type of specific genes (Donato et al., 2013). Pathway and predicted upstream regulator analysis p-values were corrected for multiple comparisons utilizing FDR. Biochemical processes and molecular functions data were corrected utilizing a weighted pruning method which assigns weight to each gene annotated to a gene ontology (GO) term based on the scores of neighboring GO terms (Alexa et al., 2006). GO terms consisting of only one gene were excluded from the analysis regardless of p-value.

Statistical Analysis

Data are expressed as the mean ± SEM of at least five independent experiments. Male and female data were combined in behavioral analysis for increased power if no sex interaction was observed. One-way ANOVA followed by the Holm-Šídák test for multiple comparisons was utilized for statistical analysis of more than two groups, while Student's t-test was utilized for comparing two groups.

3.6 – Acknowledgements

This work was supported in part by the Superfund Research Program (SRP) grant P42ES004696 and the Environmental Pathology/Toxicology training grant T32 ES007032-37 from the National Institute of Environmental Health Sciences. We thank Khoi Dao for her assistance with animal husbandry and Zahra Afsharinejad from the Functional Genomics & Bioinformatics Core of the SRP at the University of Washington for processing of RNA samples.

Chapter 4

Effects of Paraoxonase 2 Deficiency on the Dopaminergic System in the Mouse Brain

This chapter contains the research article:

Garrick, J. M., Dao, K., & Costa, L. G. (2021). Effects of Paraoxonase 2 Deficiency on the Dopaminergic System in the Mouse Brain. Preparing to submit.

4.1 – Introduction

Inhibition of radical formation is of particular importance in the dopaminergic system of the CNS where dopamine (DA) metabolism generates free radicals and reactive quinones through DA oxidation (Meiser et al., 2013). This continuous oxidative burden from DA metabolism renders dopaminergic neurons more vulnerable to additional oxidative stressors and cellular death (Wang & Michaelis 2010). Indeed, a leading hypothesis on the etiology of Parkinson's disease (PD) suggests uncontrolled oxidative stress cascades leading to DA neuron death likely play a critical role in disease pathology (Blesa et al., 2015). This hypothesis is supported by compelling *in-vivo* evidence of higher oxidative stress markers in the brains of human PD patients (Khan & Ather Ali 2018) and genetic mouse models (Varçin et al., 2012). Neurotoxicant animal models mimic PD via exposure to 6-hydroxydopamine (6-OHDA), 1-methyl-4-phenyl-1,2,3,6-tetrahydropyridine (MPTP), or agropesticides which cause mitochondrial dysfunction and/or oxidative stress to destroy DA neurons (Blesa et al., 2015), highlighting the importance of both redox balance and mitochondrial function for survival and proper function of DA neurons.

PON2 has been shown to be differentially expressed in the brain, with mice having significantly higher PON2 in dopaminergic regions such as the striatum and substantia nigra (Giordano et al., 2011). *In-vitro* PON2 has been shown to interact with DJ-1 (PARK7) and the protective antioxidant effects of DJ-1 are mediated partly through PON2 expression (Parsanejad et al., 2014). DJ-1 is implicated in PD etiology and loss-of-function mutations of DJ-1 account for 1% of all familial PD cases; whether PON2 plays a role in PD etiology is currently unknown and no additional studies related to PON2 and PD exist in the literature. In the kidney, studies have shown PON2 plays an important antioxidant role in the renal dopaminergic system, a critical system for maintaining homeostatic blood pressure (Harris & Zhang 2013). Dopamine receptor (DRD2 and DRD5) activity upregulates PON2 which in turn inhibits renal NADPH oxidases, pro-oxidant enzymes that produce ROS (Yang et al., 2012; Yang et al., 2015). Unhampered ROS in the renal system can have detrimental effects to both electrolyte balance and systemic blood pressure, demonstrating the importance for antioxidants such as PON2 to maintain redox balance in this system.

Considering the expression pattern and antioxidant functionality of PON2, as well as evidence from other organ systems, it is feasible that PON2 may play an important role in the dopaminergic system of the CNS. Minimal studies have addressed the role of PON2 in the CNS, despite *in-vivo* and epidemiological evidence suggesting its importance. To address whether PON2 plays an important role in this system, we examined wildtype (WT) and PON2 deficient (PON2-def) striatum and compared the transcript and protein levels of key dopaminergic-related targets, to determine if PON2 deficiency leads to expression changes. Additionally, we conducted *in-vitro* experiments with cultured primary neurons to determine if PON2 expression

was modulated upon exposure to two dopamine receptor agonists, fenoldopam (DRD1/5) and quinpirole (DRD2).

4.2 – Results

PON2 Expression

Measuring PON2 expression in WT and PON2-def tissue, the PON2-def mice had nearly 30 times lower transcript expression of PON2 (Figure 4.1A), and 2 – 3 times lower protein expression (Figure 4.1B)—no sex difference was observed in expression. These results were consistent with previously reported expression levels of PON2 in the deficient mice as observed in chapters 3 and 5, but not in chapter 2.

Dopamine Receptors

In the striatum, PON2-def mice had significantly higher levels of dopamine receptor 1 (DRD1) (Figure 4.2A) and 5 (DRD5) (Figure 4.2G) transcript compared to WT mice, while dopamine receptor 2 (DRD2) (Figure 4.2D) levels were identical. To further investigate changes at the protein level, these targets were also measured using Western blot analysis. However, no differences were seen when comparing protein levels of any dopamine receptor 1, 2 and 5 respectively (Figures 4.2B, 4.2E, 4.2H).

Dopamine Metabolism and Transport

Various genes involved in dopamine metabolism and transport were measured at the transcript and protein level using RT-PCR and Western blot analysis. Transcript for tyrosine

hydroxylase (TH), the rate limiting enzyme in dopamine metabolism, was measured and found significantly higher in PON2-def striatum compared to WT (Figure 4.3A), with an opposite effect observed in the measured protein levels, where PON2-def striatum had decreased TH protein compared to WT (Figure 4.3C). Vesicular monoamine transporter 2 (VMAT2), the principle solute carrier which shuttles dopamine from the cytosol into synaptic vesicles for release at the presynaptic membrane, was found to have significantly higher transcript levels in PON2-def striatum compared to WT (Figure 4.3B), although there were no significant differences in the protein levels (Figure 4.3D). Dopamine transporter (DAT), the synaptic transmembrane transporter which recovers dopamine from the synaptic cleft back into the cytosol, was unchanged at both the transcript (Figure 4.3E) and protein level (Figure 4.3F). Similarly, when investigating the expression of monoamine oxidase B (MAOB), an enzyme in the catabolic pathway of dopamine, there were no differences in transcript (Figure 4.3G) or protein levels (Figure 4.3H) between WT and PON2-def tissue.

Antioxidant Enzymes

Oxidative balance is of particular importance in dopaminergic neurons and we sought to determine if PON2 deficiency affects the expression of specific antioxidant enzymes in the striatum. Transcript levels of heme-oxygenase 1 (HO-1) and 2 (HO-2) were significantly higher in PON2-def striatum compared to WT (Figures 4.4A and 4.4D), while no differences were observed at the protein level (Figures 4.4B and 4.4E). Similarly, NADPH oxidase 2 (NOX2) transcript levels were significantly increased in PON2-def mice (Figure 4.4G), while the protein levels of NOX2 were unchanged (Figure 4.4H).

Dopamine receptor 1 and 5 Signaling

To investigate whether PON2 may play a role in dopamine signaling, we exposed neurons to a DRD1/5 agonist, fenoldopam, and measured PON2 transcript and protein. 24-hour incubation with 3μM fenoldopam did not alter PON2 expression compared to untreated cells at the transcript (Figure 4.5A) or protein level (Figure 4.5B). Higher concentrations of up to 20μM did not affect PON2 expression (data not shown).

Dopamine receptor 2 Signaling

In addition to DRD1 signaling pathways, we evaluated whether PON2 is involved in DRD2 signaling by exposing neurons to DRD2 agonist quinpirole. 24-hour incubation with 3μM quinpirole significantly increased the expression of PON2 at both the transcript and protein level (Figures 4.6A and 4.6B). A 1-hour pre-treatment with a competitive DR2 antagonist, L-741,626, was able to abolish the increased PON2 expression (Figure 4.6A and 4.6B), supporting that the observed expression increase of PON2 was due to DRD2 binding.

4.3 – Figures

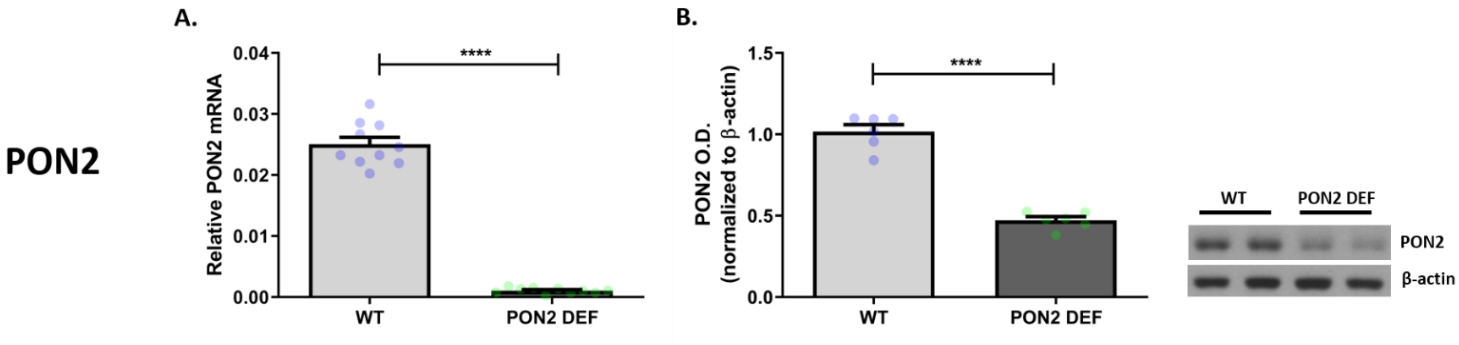

Figure 4.1 – mRNA and Protein Expression of Paraoxonase 2 (PON2) in PON2 deficient mouse striatum. A. Quantification of PON2 mRNA normalized to GAPDH, mean (± SEM), n = 10 per group, **** $p < 0.0001$. **B**. Quantification of PON2 protein normalized to β-actin, mean (± SEM), n = 5 per group, **** $p < 0.0001$.

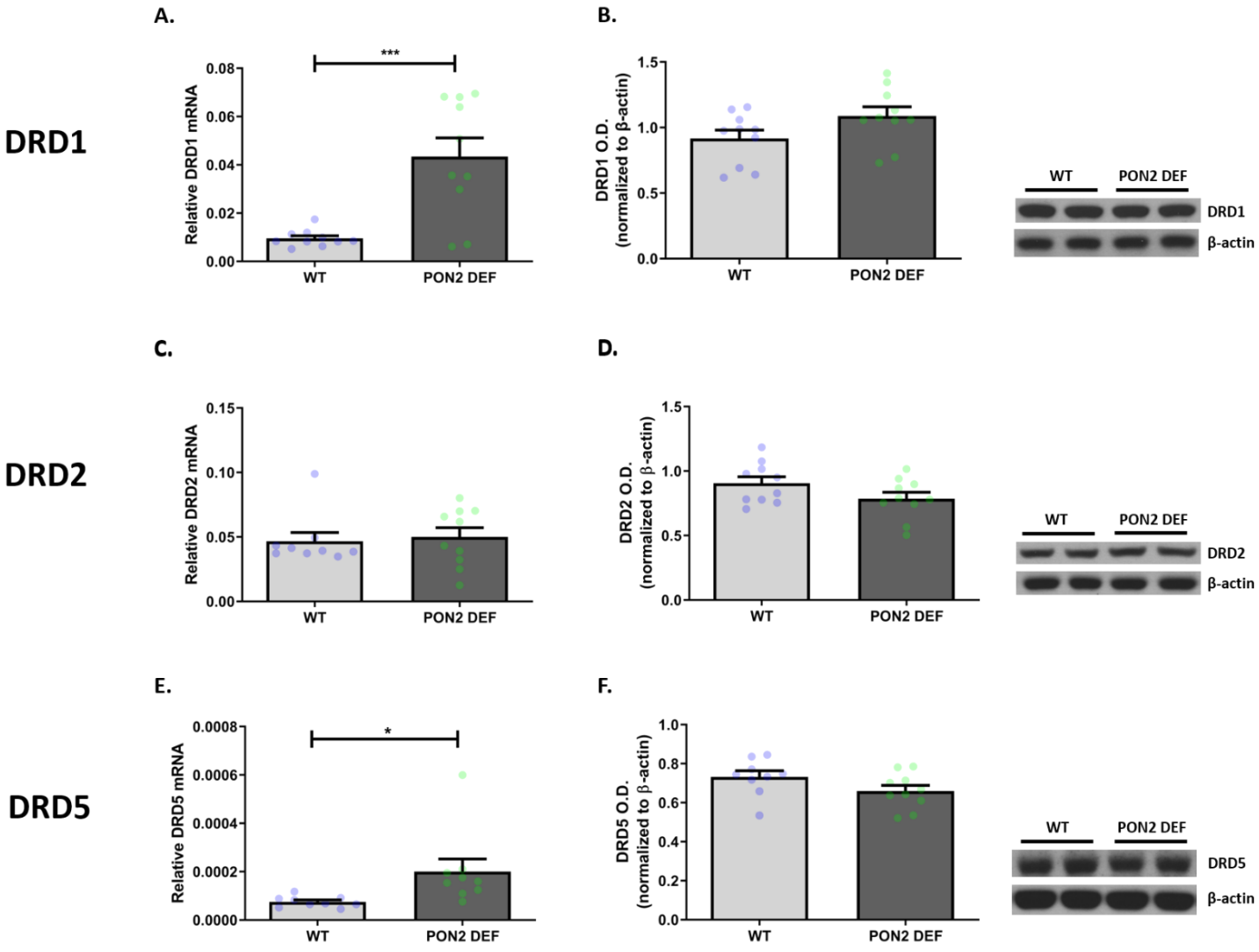

Figure 4.2 – mRNA and Protein Expression of Dopamine Receptors in PON2 deficient mouse striatum. A. Quantification of dopamine receptor 1 (DRD1) mRNA normalized to GAPDH, mean (± SEM), n = 9 - 10 per group, *** $p < 0.001$. **B**. Quantification of dopamine receptor 1 (DRD1) protein normalized to β-actin, mean (± SEM), n = 8 - 10 per group. **C.** Quantification of dopamine receptor 2 (DRD2) mRNA normalized to GAPDH, mean (± SEM), n = 9 - 10 per group. **D**. Quantification of dopamine receptor 2 (DRD2) protein normalized to β-actin, mean (± SEM), n = 9 - 10 per group. **E.** Quantification of dopamine receptor 5 (DRD5) mRNA normalized to GAPDH, mean (± SEM), n = 9 - 10 per group, * $p < 0.05$. **F**. Quantification of dopamine receptor 5 (DRD5) protein normalized to β-actin, mean (± SEM), n = 9 - 10 per group.

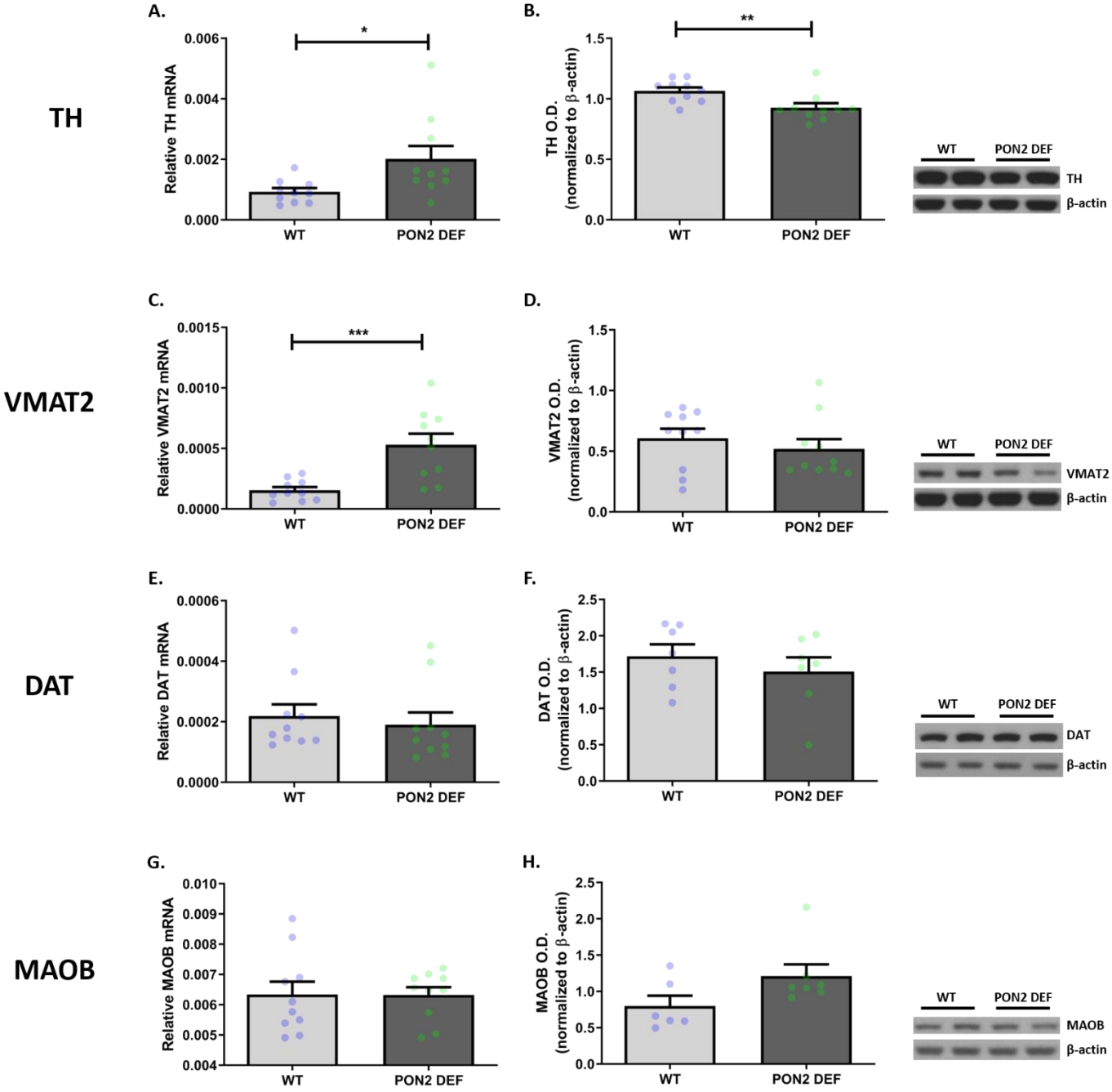

Figure 4.3 – mRNA and Protein Expression of Dopamine Metabolism Genes in PON2 deficient mouse striatum. A. Quantification of tyrosine hydroxylase (TH) mRNA normalized to GAPDH, mean (± SEM), n = 8 - 10 per group, * $p < 0.05$. **B**. Quantification of tyrosine hydroxylase (TH) protein normalized to β-actin, mean (± SEM), n = 8 - 10 per group. ** $p < 0.01$ **C.** Quantification of vesicular monoamine transporter 2 (VMAT2) mRNA normalized to GAPDH, mean (± SEM), n = 9 - 10 per group, *** $p < 0.001$ **D**. Quantification of vesicular monoamine transporter 2 (VMAT2) protein normalized to β-actin, mean (± SEM), n = 9 - 10 per group. **E.** Quantification of dopamine transporter (DAT) mRNA normalized to GAPDH, mean (± SEM), n = 10 per group. **F**. Quantification of dopamine transporter (DAT) protein normalized to β-actin, mean (± SEM), n = 7 - 10 per group. **G.** Quantification of monoamine oxidase B (MAOB) mRNA normalized to GAPDH, mean (± SEM), n = 8 – 10 per group. **H.** Quantification of monoamine oxidase B (MAOB) protein normalized to β-actin, mean (± SEM), n = 9 - 10 per group.

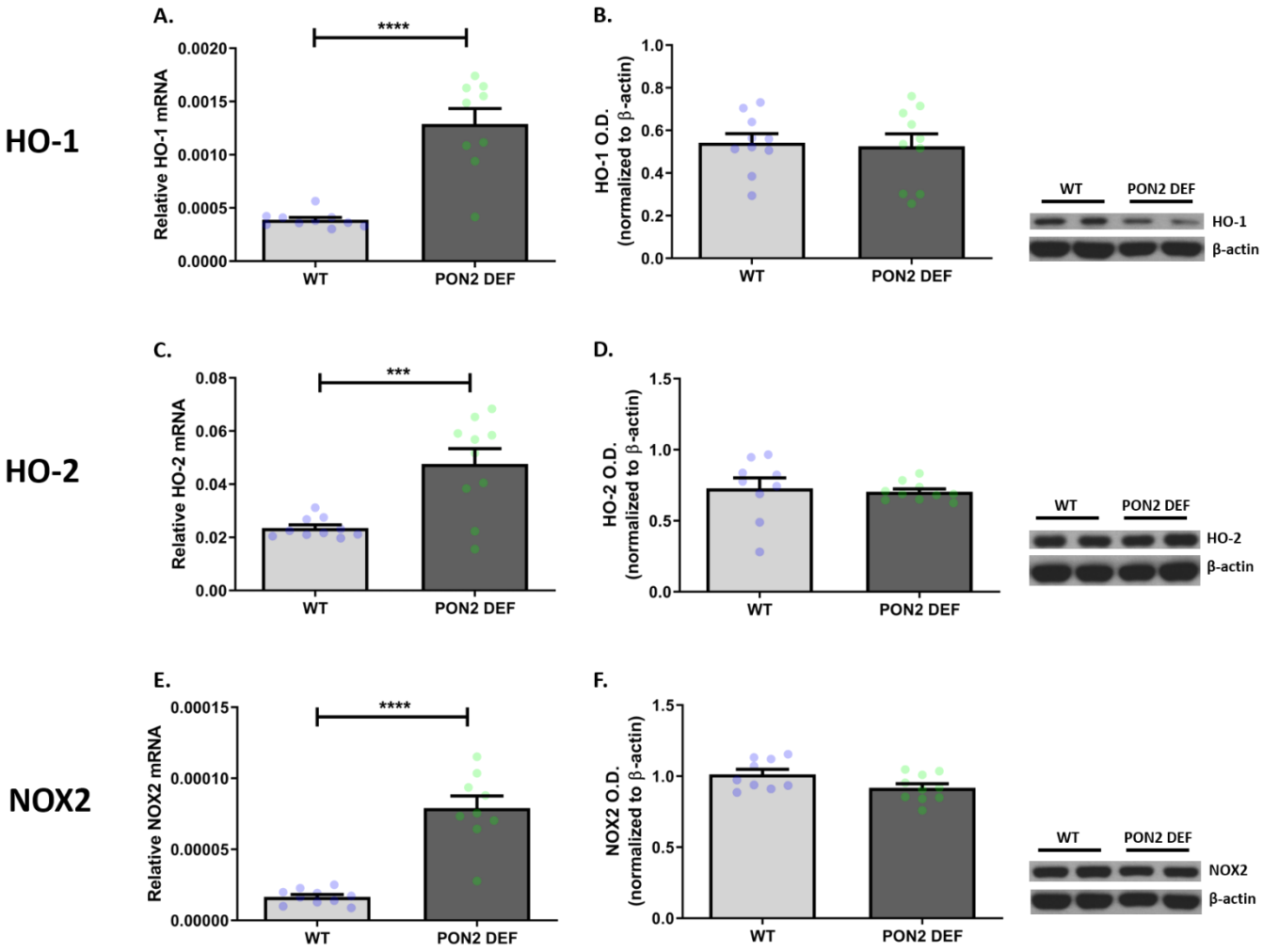

Figure 4.4 – mRNA and Protein Expression of Antioxidant Genes in PON2 deficient mouse striatum. A. Quantification of heme oxygenase 1 (HO-1) mRNA normalized to GAPDH, mean (± SEM), n = 9 - 10 per group, **** $p < 0.0001$. **B**. Quantification of heme oxygenase 1 (HO-1) protein normalized to β-actin, mean (± SEM), n = 8 - 10 per group. **C.** Quantification of heme oxygenase 2 (HO-2) mRNA normalized to GAPDH, mean (± SEM), n = 9 - 10 per group, *** $p < 0.001$. **D**. Quantification of heme oxygenase 2 (HO-2) normalized to β-actin, mean (± SEM), n = 9 - 10 per group. **E.** Quantification of NADPH oxidase 2 (NOX2) mRNA normalized to GAPDH, mean (± SEM), n = 8 - 10 per group, **** $p < 0.0001$. **F**. Quantification of NADPH oxidase 2 (NOX2) protein normalized to β-actin, mean (± SEM), n = 8 – 9 per group.

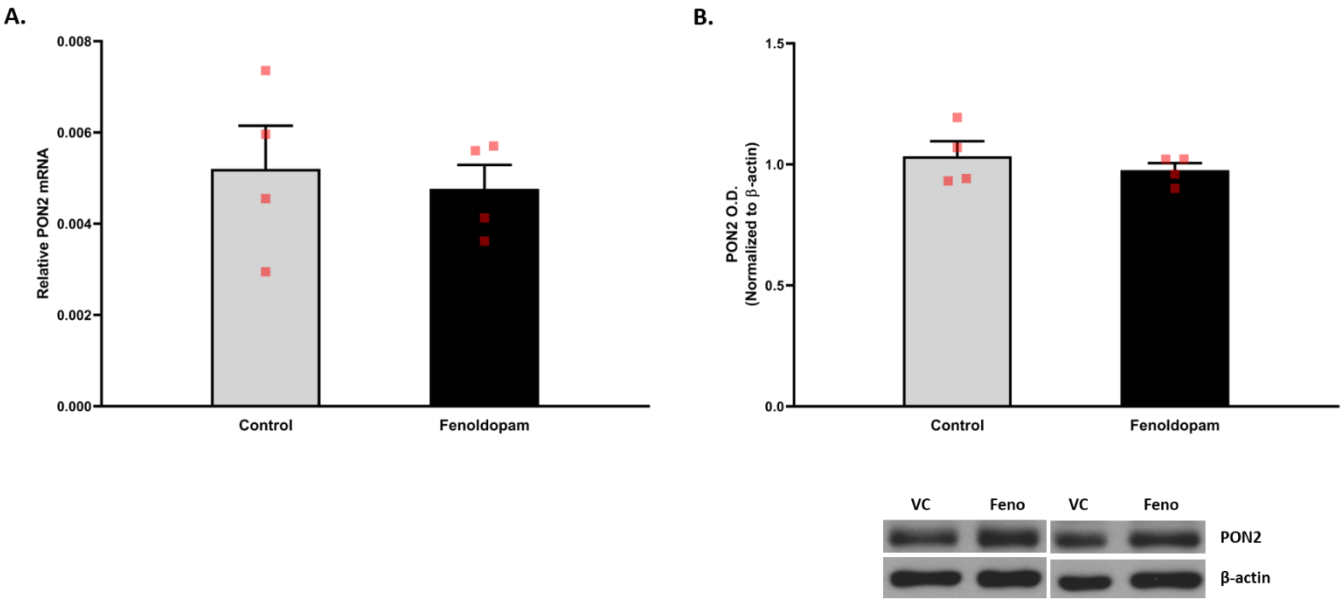

Figure 4.5 – mRNA and Protein Expression of PON2 after Exposure to Dopamine Receptor 1/5 Agonist Fenoldopam. A. Quantification of paraoxonase 2 (PON2) mRNA in cerebellar granule neurons after 24-hour exposure to 3μM fenoldopam, normalized to GAPDH, mean (± SEM), n = 4 per group **B**. Quantification of paraoxonase 2 (PON2) protein in cerebellar granule neurons after 24-hour exposure to 3μM fenoldopam, normalized to β-actin, mean (± SEM), n = 4 per group

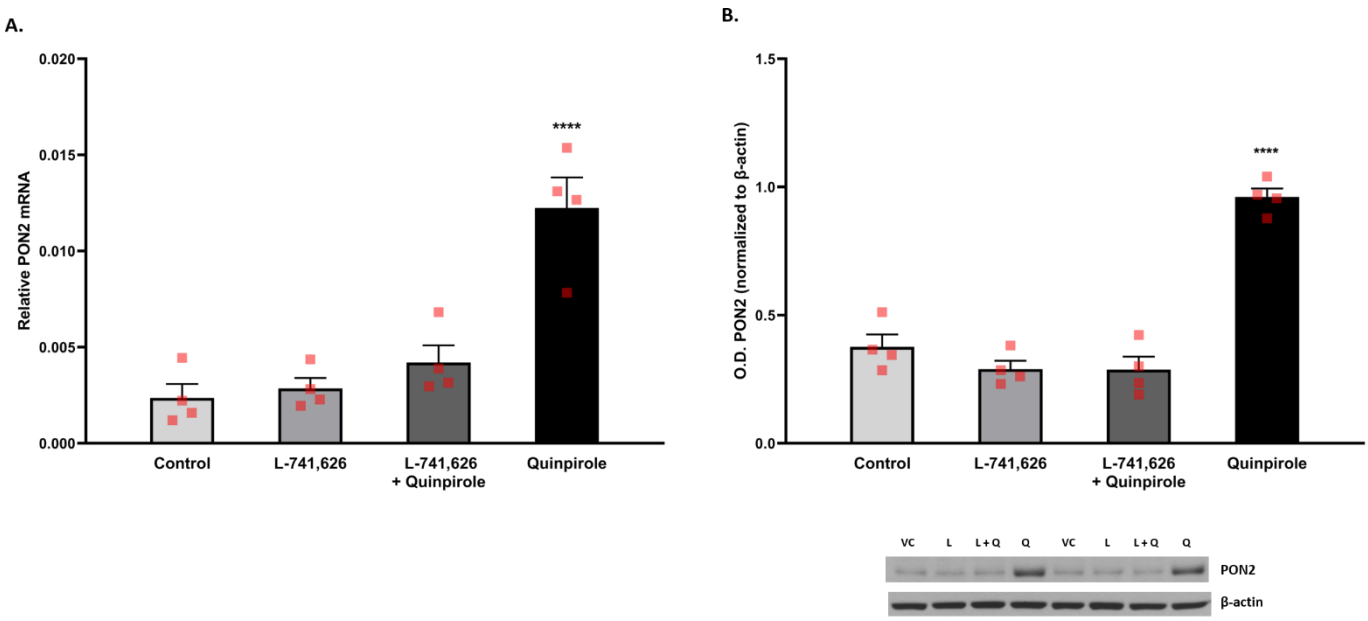

Figure 4.6 – mRNA and Protein Expression of PON2 after Exposure to Dopamine Receptor 2 Agonist Quinpirole. A. Quantification of paraoxonase 2 (PON2) mRNA in cerebellar granule neurons after 24-hour exposure to 3μM quinpirole or 3μM dopamine receptor 2 antagonist L-741,626 alone or combined with 3μM quinpirole, normalized to GAPDH, mean (± SEM), n = 4 per group **B**. Quantification of paraoxonase 2 (PON2) protein in cerebellar granule neurons after 24-hour exposure to 3μM quinpirole or 3μM dopamine receptor 2 antagonist L-741,626 alone or combined with 3μM quinpirole, normalized to β-actin, mean (± SEM), n = 4 per group.

4.4 – Discussion

While widely expressed in the brain, PON2 levels are highest in dopaminergic regions such as the striatum, suggesting a function in these areas (Giordano et al., 2011). Feasibly, PON2 expression is higher in these regions due to increased oxidative stress burden stemming from dopamine metabolism. Using a PON2 deficient mouse model, we have shown that PON2 deficiency in the striatum significantly impacts multiple dopaminergic-related genes at the transcript level, upregulating DRD1, DRD5, TH and VMAT2. Transcripts of antioxidant enzymes NOX2, HO-1 and HO-2 were also significantly increased in PON2 deficient mice, suggesting these animals may have higher burdens of oxidative stress in the striatum, or that a common upstream regulator is impacted by PON2 deficiency.

Despite significant increases in transcript, most targets were unchanged at the protein level. In the case of tyrosine hydroxylase (TH), the transcript and protein effects observed were opposite (Figure 4.3A and B). PON2 deficient mice may have a reduction in dopamine metabolism as a result of lower TH protein expression, although analysis of dopamine metabolites would be necessary to confirm this. These discrepancies in transcript and protein could be the result of multiple factors and are not uncommon, as correlation between transcript and protein is known to be poor, with Pearson correlation coefficients reported as low as $R = 0.36$ across multiple studies (Maier et al., 2009).

Looking further at these discrepancies, there may be a temporal element to changes in the dopaminergic system that our study was unable to capture. Increased transcript may be present for quick translation and rapid increase in protein levels under physiological conditions that were not present at the time our tissue was collected. While transcript is expected to predict steady-state protein levels, defining ‘steady-state’ presents a challenge as cells are constantly adapting to

their environment and can be in numerous states of change in a given period, such as during proliferation, differentiation, or apoptosis (Liu et al., 2016). Our study utilized striatal tissue comprised of multiple neural cell types, ranging from non-proliferating neurons to highly dynamic glial cells. Further investigation of specific cell types would be of interest to determine if there are differences in neural and glial populations, as well as additional time points after oxidative challenge to determine if these increases in transcript are primed for an adaptive response. Additionally, these discrepancies may point to a dysregulation in transcription mediation in PON2 deficient mice, where transcription is increased but translational controls maintain constant protein levels. This could be the result of increased activity of specific transcription factors to elicit transcription upregulation, while micro RNA (miRNA) activity and *trans*-acting proteins prevent increases of protein (Hershey et al., 2012). Indeed, as discussed in chapter 3, PON2 deficiency was identified to impact multiple transcription related pathways. While transcript controls may be compromised in PON2-def mice, excess protein can be further targeted for degradation through the ubiquitin-proteosome pathway to maintain proteostasis if previous translational controls are insufficient (Cooper 2000). Although increased transcript levels may not pose a risk when these controls are in place, loss of translational and chaperone control is noted in aged animals (Anisimova et al., 2018). If these higher transcript levels persist for the lifespan of the PON2 deficient animal, effects on the dopaminergic system may be more apparent in old age as these control systems break down and protein levels become aberrant. Increased expression of dopamine receptors may lead to signaling abnormalities and subsequent cognitive impairment (Kellendonk et al., 2006) if translational controls break down and allow for the increased DRD1 and 5 transcripts to produce more protein. Further study on the life stages of PON2 deficient mice, as well as proteostasis controls, would be of additional interest.

Previous studies utilizing kidney cells have shown PON2 to be involved in dopamine receptor signaling, with dopamine receptor agonists increasing PON2 expression (Yang et al., 2012, Yang et al., 2015). Our study in neurons shows that, like the kidney, PON2 expression was increased upon exposure to DRD2 agonist quinpirole. However, unlike the kidney, no expression increase was observed upon exposure to DRD1/5 agonist fenoldopam. These data suggest there could be cell- and organ-specific differences in the role of PON2 in dopamine signaling. Furthermore, no differences in DRD2 transcript or protein were observed in PON2 deficient mice compared to WT, supporting that PON2 is downstream of DRD2 and PON2 deficiency alone is not enough to alter DRD2 expression. This supports the existing literature examining PON2 levels in the kidney of DRD2 KO mice, where renal PON2 levels were 33% lower in DRD2 KO tissue compared to WT (Yang et al., 2012).

PON2 is primarily located to the mitochondrial membrane in the brain, although it has been additionally detected at the plasma membrane of neurons and astrocytes (Giordano et al., 2011). While the function at the plasma membrane is largely unknown, work in HEK 293T cells has shown PON2 translocates to the plasma membrane under oxidative stress conditions to mitigate lipid peroxidation (Hagmann et al., 2014). Although currently untested, PON2 may also translocate in neurons and astrocytes to interact with DRD2 at the synaptic membrane. Indeed, DRD2 and PON2 co-localize at the brush border of mouse renal proximal tubules (Yang et al., 2012), supporting extra-mitochondrial localization and direct DRD2 interaction in some cell types. Alternatively, PON2 may be upregulated in the mitochondria through DRD2 signaling cascades. In astrocytes, DRD2 has been found to modulate neuroinflammation by increased expression of αB-crystallin (CRYAB) (Shao et al., 2013). DRD2 null mice are reported to have an increased inflammatory response and dopaminergic neuron sensitivity to the neurotoxic

compound 1-methyl-4-phenyl-1,2,3,6-tetrahydropyridine (MPTP) (Shao et al., 2013), potentially owing to a decrease in CRYAB expression. CRYAB, a member of the heat shock protein family, primarily locates to the mitochondria where it exerts anti-inflammatory and anti-apoptotic action (Ousman et al., 2007). While no direct interactions between PON2 and CRYAB have been reported in the literature, this may be a further avenue of study going forward to determine if astrocytic modulation of neuroinflammation through the DRD2-CRYAB pathway involves PON2. Of additional interest would be examination of PON2 expression in subcellular fractions upon DRD2 agonist exposure to determine if the upregulation of PON2 is at the plasma membrane or at the mitochondria level, something that was not addressed in our current study.

Evidence supports PON2 as a critical antioxidant enzyme in the brain, however studies on its role in the CNS have been limited to date. Our study addresses key gaps in the literature regarding the effects of PON2 deficiency in the dopaminergic system of the CNS and demonstrates that PON2 deficiency significantly upregulates the transcript of multiple dopaminergic related genes in the striatum of mice. As well, this study identified potential organ-specific upregulation of PON2 through selective dopamine receptor signaling. Given the findings of this study, further investigation into the role of PON2 in the dopaminergic system would be warranted as well as the examination of the downstream consequences of these observed transcript changes with further examination into the role of PON2 in dopamine receptor signaling in the brain.

4.5 – Materials and Methods

Materials

Anti-DRD1, DRD2, DRD5, DAT, HO-1, HO-2, MAOB, NOX2, TH and VMAT2 antibodies were purchased from Abcam (Cambridge, MA, USA). Anti-PON2 antibody was purchased from Genscript (Piscataway, NJ, USA). Anti β-actin antibody, papain, poly-D-lysine, quinpirole hydrochloride, fenoldopam mesylate and L-741,626 were purchased from MilliporeSigma (Burlington, MA, USA). Anti-rabbit IgG HRP-linked antibody and Cell Lysis Buffer 10x were purchased from Cell Signaling Technology (Danvers, MA, USA). HRP Goat Anti-Mouse IgG was purchased from BD Biosciences (San Jose, CA, USA). XCell II Blot Module, XCell SureLock Electrophoresis Cell, NuPAGE MOPS SDS Running Buffer 20x, NuPAGE LDS Sample Buffer 4x, NuPAGE Antioxidant, NuPAGE Sample Reducing Agent 10x, NuPAGE 10% Bis-Tris Protein Gels, Neurobasal-A medium, B-27 supplement with and without antioxidant, fungizone, HBSS medium (No Ca2+) and 10 mM HEPES were purchased from Life Technologies (Carlsbad, CA, USA). Immobilon-P Transfer Membrane was purchased from Millipore Corporation (Billerica, MA, USA). Restore Western Blot Stripping Buffer, PageRuler Prestained Protein Ladder, SuperSignal West Pico Chemiluminescent Substrate and Costar 6-well TC plates were purchased from Thermo Fisher Scientific (Waltham, MA, USA). RNeasy Mini Kit was purchased from Qiagen (Hilden, Germany). iScript cDNA Synthesis Kit, iTaq Universal SYBR Green Supermix and CFX384 Real-Time Detection System were purchases from Bio-Rad Laboratories (Hercules, CA, USA). All qPCR primers were purchased from Integrated DNA Technologies (Newark, NJ, USA).

Mice

Wild-type and PON2 deficient (PON2-def) mice (Ng et al., 2006) on a C57BL/6J background were used for this study. Mice were sacrificed at postnatal day (PND) 60 and striatal

tissue was dissected, and flash frozen in liquid nitrogen. Tissue was pulverized with a pre-chilled mortar and pestle into a fine powder, stored at −80°C and aliquoted into appropriate lysis buffers for protein and RNA extraction as needed, utilizing sonication for homogenization when indicated. Mice were housed in a specific pathogen-free facility on a 14-hour light/ 10-hour dark cycle with *ad libitum* access to food and water. All procedures were conducted in accordance with the National Institute of Health Guide for the Use and Care of Laboratory Animals and were approved by the University of Washington Institutional Animal Care and Use Committee.

Primary Cell Culture

Cerebellar granule neurons (CGNs) were prepared from PND 7 mice, as described by Giordano et al., 2006. Neurons were grown for 10-12 days before treatments. Briefly, cerebellar tissue was collected in chilled HBSS medium (No Ca2+) and 10 mM HEPES. Tissues were digested for 30 min in HBSS containing papain (1 mg/ml) and DNAse I (40 μg/ml) and centrifuged at 300 × *g* for 7 min at room temperature. The supernatant (containing papain) was removed, and the pellet was gently triturated in Neurobasal-A Medium supplemented with B27 (Life Technologies, Carlsbad, CA). Cells were centrifuged at 200 × *g* at 4°C for 10 min and the cell pellet was gently resuspended in medium. Neurons were then counted, seeded on poly-D-lysine coated 6-well plates at a density of 5×10^4 / cm^2, and cultured in Neurobasal-A medium supplemented with B27. After 4 days, media was completely exchanged for Neurobasal-A Medium with B27 minus antioxidants (-AO). For the DRD1 and DRD2 agonist experiments, neurons were treated for 24 hours with fenoldopam mesylate (3 μM) or quinpirole hydrochloride (3 μM). For the DRD2 antagonist experiment, neurons were pre-treated for 1 hour with L-

741,626 (3 μM), the pre-treatment media was removed and followed by a 24-hour co-incubation with L-741,626 (3 μM) and quinpirole (3 μM) together.

Immunoblotting

Immunoblots were carried out as previously described (Garrick et al., 2016). Briefly, 15 μg of protein was mixed with SDS running buffer and sample reducing agent and subjected to sodium dodecyl sulfate-polyacrylamide gel electrophoresis (SDS-PAGE). Following electrophoresis, proteins were transferred to polyvinylidene difluoride membranes and the membrane blocked for 1-3 hours with 5% nonfat milk. Membranes were then probed with the following diluted primary antibodies: PON2 1:2000, DRD1 1:10000, DRD2 1:2500, DRD5 1:2500, TH 1:3000, VMAT2 1:1500, DAT 1:1000, MAOB 1:2000, HO-1 1:5000, HO-2 1:3000 and NOX2 1:12000. Following primary antibody incubation, membranes were washed with Tris-buffered saline with 0.1% Tween-20 (pH = 7.5) and incubated with horseradish peroxidase-conjugated anti-rabbit secondary antibody at the following dilutions: PON2, DRD1 1:5000, DRD2 1:5000, DRD5 1:5000, TH 1:3000, VMAT2 1:3000, DAT 1:5000, MAOB 1:5000, HO-1 1:4000, HO-2 1:3000 and NOX2 1:4000. Membranes were stripped with Restore™ Western Blot Stripping Buffer (Thermo Fisher Scientific, Waltham, MA) and re-probed for β-actin using a dilution of 1:2500 for the β-actin primary antibody and 1:2500 for the horseradish peroxidase-conjugated anti-mouse secondary antibody. Intensity of bands was measured by densitometry using ImageJ software (NIH), with the band intensity normalized to β-actin expression.

RT-PCR

Total RNA was extracted from striatal tissue using the RNeasy Mini Kit (Qiagen, Hilden, Germany) according to manufacturer's established protocol. Target mRNA levels were measured by RT-PCR, see Table 4.1 below for sequences of primer pairs. cDNA was generated from 1 µg total RNA using the iScript cDNA Synthesis Kit (Bio-Rad Laboratories, Hercules, CA) according to the manufacture's established protocol. The cDNA samples were diluted to a concentration of 6.25ng/µL with nuclease-free water and subsequently used for quantitative polymerase chain reaction (qPCR) using iTaq Universal SYBR Green Supermix in a CFX384 Real-Time Detection System (Bio-Rad Laboratories, Hercules, CA). 6 µL of diluted cDNA were included in a PCR reaction mastermix containing 15 µL Universal SYBR Green Supermix (2x), 1.5 µL each forward and reverse primers (10 µM stock), and 6 µL nuclease-free water (30 µL final volume). The reaction mixture was then aliquoted in triplicate, 8 µL per reaction per sample. The thermal cycling conditions were as follows: A single denaturing step at 95°C for 30 seconds, 40 cycles of 95°C for 15 seconds, 60°C for 30 seconds and 72°C for 30 seconds. dCq values (referenced as "relative mRNA") for each target were calculated by subtracting Cq values of housekeeping gene GAPDH.

Statistical Analysis

Data are expressed as the mean ± SEM of at least three independent experiments. One-way ANOVA followed by the Holm-Šídák test for multiple comparisons was utilized for statistical analysis, while Student's t-test was utilized for comparing two groups.

Table 4.1 – qPCR Primer Pairs

Target	Forward Primer (5’ – 3’)	Reverse Primer (5’ – 3’)
PON2	GCACGCTGGTGGACAATTTATC	TGTCACTGATGGCTTCTCGGAT
DRD1	TCTTTGTCATCTCTTTAGCTGTGTC	TTCGGAGTCATCTTCCTCTCA
DRD2	ATCTCTTGCCCACTGCTCTTTGGA	ATAGACCAGCAGGGTGACGATGAA
DRD5	ACCAAGACACGGTCTTCCAC	CCTCCTCCTCACAGTCAAGC
TH	CAGCTGGAGGATGTGTCTCA	GGCATGACGGATGTACTGTG
VMAT2	TCATCGCTGCAGGCTCCATCT	AGCTGCCACTTTCGGGAACAC
DAT	GGGTGGCCTGGTTCTACG	CAGCATAGCCGCCAGTACAG
MAOB	AAGCGATGTGATCGTGGTGG	ACACTGAGGCCACAATCATGC
HO-1	GCCGAGAATGCTGAGTTCATG	TGGTACAAGGAAGCCATCACC
HO-2	TACTTCACATACTCAGCCCT	ATGGGCCACCAGCAGCTCTG
NOX2	CAGGAACCTCACTTTCCATAAGATG	AACGTTGAAGAGATGTGCAATTGT

4.6 – Acknowledgements

This work was supported in part by the Superfund Research Program (SRP) grant P42ES004696 and the Environmental Pathology/Toxicology training grant T32 ES007032-37 from the National Institute of Environmental Health Sciences. We thank Judit Marsillach and Clement Furlong for their input on experimental protocols.

Chapter 5

Paraoxonase 2 Deficiency in Aging Mice: Measuring Neuroinflammatory and Neurodegenerative Targets

5.1 – Introduction

The aging population is the fastest growing demographic in developed countries, specifically those who are over 80 years old and termed the "super old" (United Nations Report 2015). As the population ages, diseases of aging will have an increasing impact on public health and national healthcare spending, with annual costs associated with Alzheimer's disease (AD) estimated at $305 billion in 2020 and projected to reach more than $1 trillion by 2050 (Wong 2020). While aging affects every organ in the body, neurodegenerative diseases of the brain are most notable for their impact on activities of daily living and subsequent quality of life. As such, further study of these diseases is warranted to understand their etiology and work towards the development of preventative measures as well as better treatment options. Presently, only five medications are approved by the U.S. Food and Drug Administration (FDA) for the treatment of AD and dementia, and less than 20 are approved for Parkinson's disease (PD). Although useful in treating symptoms, these medications are unable to slow progression or reverse disease, and no medication is currently approved for disease prevention (Kiaei 2013; Alzheimer's Association 2019).

One important avenue of study regarding neurodegenerative diseases is the role of genetics. In the preceding decades, numerous genes have been found associated with the risk of developing neurodegenerative disease. Notably, except in the case of rare familial forms, no one gene defect has been found to directly cause dementia or PD (Paulson & Igo 2013; Klein &

Westenberger 2012). To supplement studies on genetics, work has shifted to determine environmental risk factors, with the current consensus that gene-environment interactions play an important role in disease etiology (Spires & Hannan 2005; Elbaz et al., 2007). Environmental factors such as air pollution, metals, pesticides, and vitamin deficiencies have all been linked to the development of neurodegenerative diseases (Chin-Chan et al., 2015). Although these associated risk factors appear vastly different, a common mechanism of action shared by many of these compounds is the ability to generate oxidative stress. Oxidative stress is proposed as a mechanism of neurodegenerative disease etiology and attention has focused recently on antioxidants as therapeutics and potential preventative measures (Liu et al., 2017). PON2, acting as an antioxidant in the brain, may play a protective role in mitigating neurodegenerative disease development and/or progression and could serve as an important therapeutic target. PON2 polymorphism studies have been mixed, with some studies finding no association with PON2 and dementia (Klimkowicz-Mrowiec et al., 2011; Mu et al., 2013), and others identifying a higher proportion of patients with dementia as Ser311Cys allele carriers (Janka et al., 2002; Shi et al., 2004; Nie et al., 2017). PON2 mRNA has also been found to be upregulated in the brains of AD patients upon post-mortem investigation (Leduc et al., 2011).

As no studies to date have examined PON2 deficiency in the aged brain, we sought to investigate numerous neurodegenerative targets at the transcriptional and protein level in 18 – 24 month-old mice to determine if PON2 deficiency affects the expression of these targets and may impact neurodegenerative pathways.

5.2 – Results

Weight Measurement

All mice were weighed at the end of the study prior to sacrifice, with no weight changes noted between the WT and PON2-def mice (Figure 5.1).

Ulcerative Dermatitis in PON2-def Mice

An incidental finding in our study was a significantly higher occurrence of ulcerative dermatitis (UD) in the aged PON2-def mice compared to WT (Figure 5.2). All mice that developed UD were evaluated by a veterinarian and found to have no infectious cause of the condition and no underlying commonality, beyond PON2 deficiency, could be determined.

Oxidative Stress Measured by Lipid Peroxidation

Levels of malondialdehyde (MDA), a byproduct of lipid peroxidation, were quantified as a surrogate measurement of oxidative stress levels. Given that lipid peroxidation is the product of oxidative damage when free radicals interact with lipids, MDA levels are expected to correlate with oxidative stress. When comparing WT and PON2-def mice, no differences in MDA were observed in the cortex (Figure 5.3). MDA levels were also measured in a younger control group of 3-month-old mice, where a similar pattern was observed. The aged mice, both WT and PON2-def, had higher levels of MDA than the younger control group, although this was only statistically significant in the PON2-def groups. Looking exclusively at PON2-def mice and stratifying on ulcer status, no difference in MDA levels were observed between animals that developed ulcerative dermatitis and those that did not (Figure 5.4).

RT-PCR Measurement of Neurodegenerative Targets

Neuroinflammation

To assess whether PON2 deficiency impacts neurodegenerative pathways, transcripts of select targets were measured by qPCR and compared in WT and PON2-def cerebral cortex. Looking at cytokines of neuroinflammatory interest, PON2-def mice had significantly lower transcript levels of tumor necrosis factor alpha (TNF-α) (Figure 5.5A), interferon gamma (IFγ) (Figure 5.5B), interleukin 1-beta (IL-β) (Figure 5.5C) and interleukin 6 (IL-6) (Figure 5.5D). No changes were observed in interleukin 4 (IL-4) (Figure 5.5E).

Glial Activation

Transcript of the microglial activation marker cluster of differentiation 68 (CD68), astrocytic chemokine C-C Motif Chemokine Ligand 2 (CCL2), and astrocytic inflammatory protein S100 calcium binding protein B (S100B) were all significantly lower in PON2-def mice compared to WT (Figures 5.6A, 5.6B and 5.6C respectively).

Glucose Transport

Glucose transport was selectively impacted at the transcript level in PON2-def mice, with PON2 deficiency leading to an increase in glucose transporter 4 (GLUT4) (Figure 5.7B) and no change in glucose transporter 1 (GLUT1) (Figure 5.7A). Insulin receptor (INSR) transcript, from which both insulin receptors A (IR-A) and B (IR-B) alternatively splice, was increased in PON2-def mice (Figure 5.7C).

Neurodegeneration

Neurodegenerative targets were impacted by PON2 deficiency, with Tau (Figure 5.8A) transcript significantly higher in PON2-def mice compared to WT. Serpin Family A Member 3 (SERPINA3), a protease inhibitor whose upregulation is associated with Alzheimer's disease (Kamboh et al., 2006), was significantly lower in PON2-def female mice compared to WT, while no difference was observed in males (Figure 5.8B). Notably, this was the only transcript change to display a sex difference in this study. Presenilin 1 (PSEN1) and 2 (PSEN2), components of the catalytic domain of the γ-secretase complex which cleaves a specific region of amyloid precursor protein (APP), were unchanged with PON2 deficiency (Figures 5.8C and D). Similarly, transcript of beta-secretase 1 (BACE1), which cleaves a different site of APP, was unchanged (Figure 5.8E). Finally, transcript of neuropilin-1 (NRP1), a transmembrane protein found to be important for endothelial homeostasis by regulating mitochondrial iron levels (Issitt et al., 2019), was unchanged with PON2 deficiency (Figure 5.8F).

Cholinesterases

In the brain, the neurotransmitter acetylcholine (ACh) is co-regulated through degradation by acetylcholinesterase (AchE) and butyrylcholinesterase (BuChE). AchE transcript levels were found to be unchanged with PON2 deficiency (Figure 5.9A), however a significant reduction in BuChE transcript was found (Figure 5.9B).

Stress Pathway Targets

Glucose regulated protein 78 (GRP78), an endoplasmic-stress response protein, was significantly higher in PON2-def mice compared to WT (Figure 5.10A). Conversely, protein levels of nuclear factor erythroid 2-related factor 2 (NRF2), an oxidative stress sensitive protein that is ubiquitinated and degraded under basal conditions and maintained during stress, was downregulated with PON2 deficiency (Figure 5.10B).

5.3 – Figures

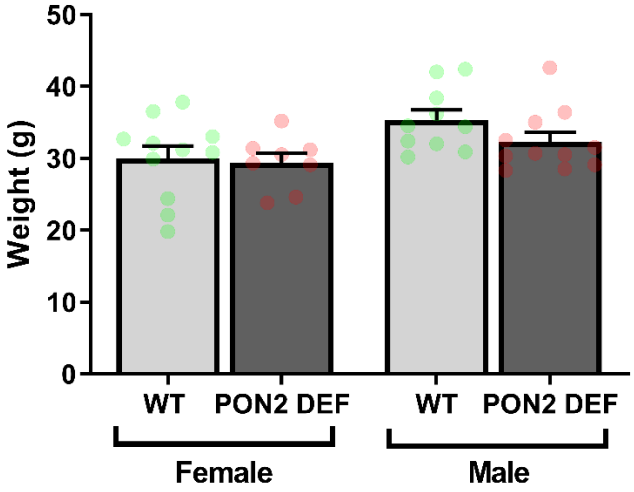

Figure 5.1 – Weight of Aged Mice. Weight in grams of wildtype (WT) and PON2 deficient (PON2-def) aged mice. N = 10 – 12 per group.

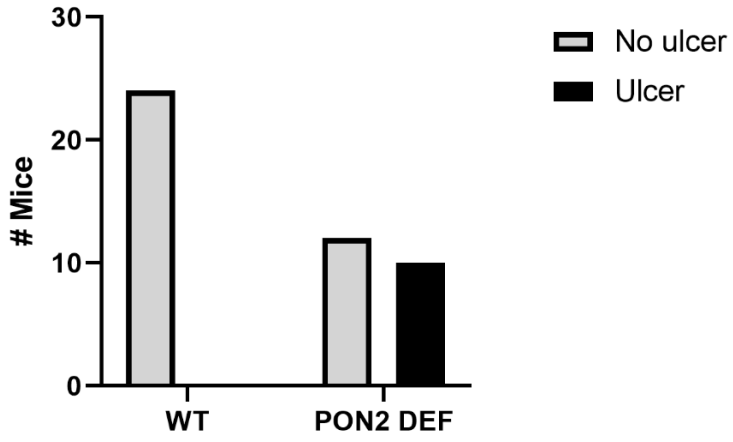

Figure 5.2 – Mice with Ulcerative Dermatitis. Number of wildtype (WT) and PON2 deficient (PON2-def) mice that developed ulcerative dermatitis (UD).

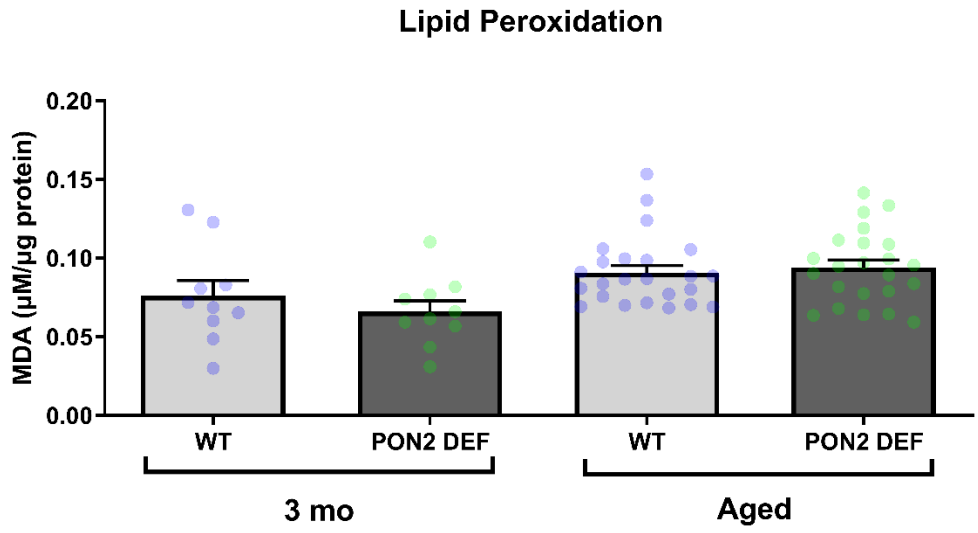

Figure 5.3 – Lipid Peroxidation in Cerebrl Cortex of Wildtype and PON2 deficient Aged Mice and Young Controls. MDA levels, corrected for total protein, in wildtype (WT) and PON2 deficient (PON2-def) aged mice and younger (3 month old) control mice. N = 10 – 25 per group.

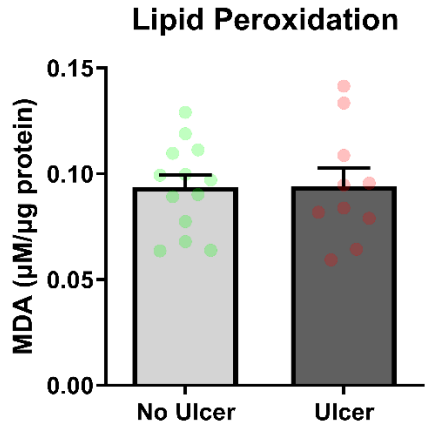

Figure 5.4 – Lipid Peroxidation in Cerebral Cortex of PON2 deficient Aged Mice. MDA levels, corrected for total protein, in PON2 deficient (PON2-def) aged mice with or without ulcerative dermatitis (UD). N = 10 – 13 per group.

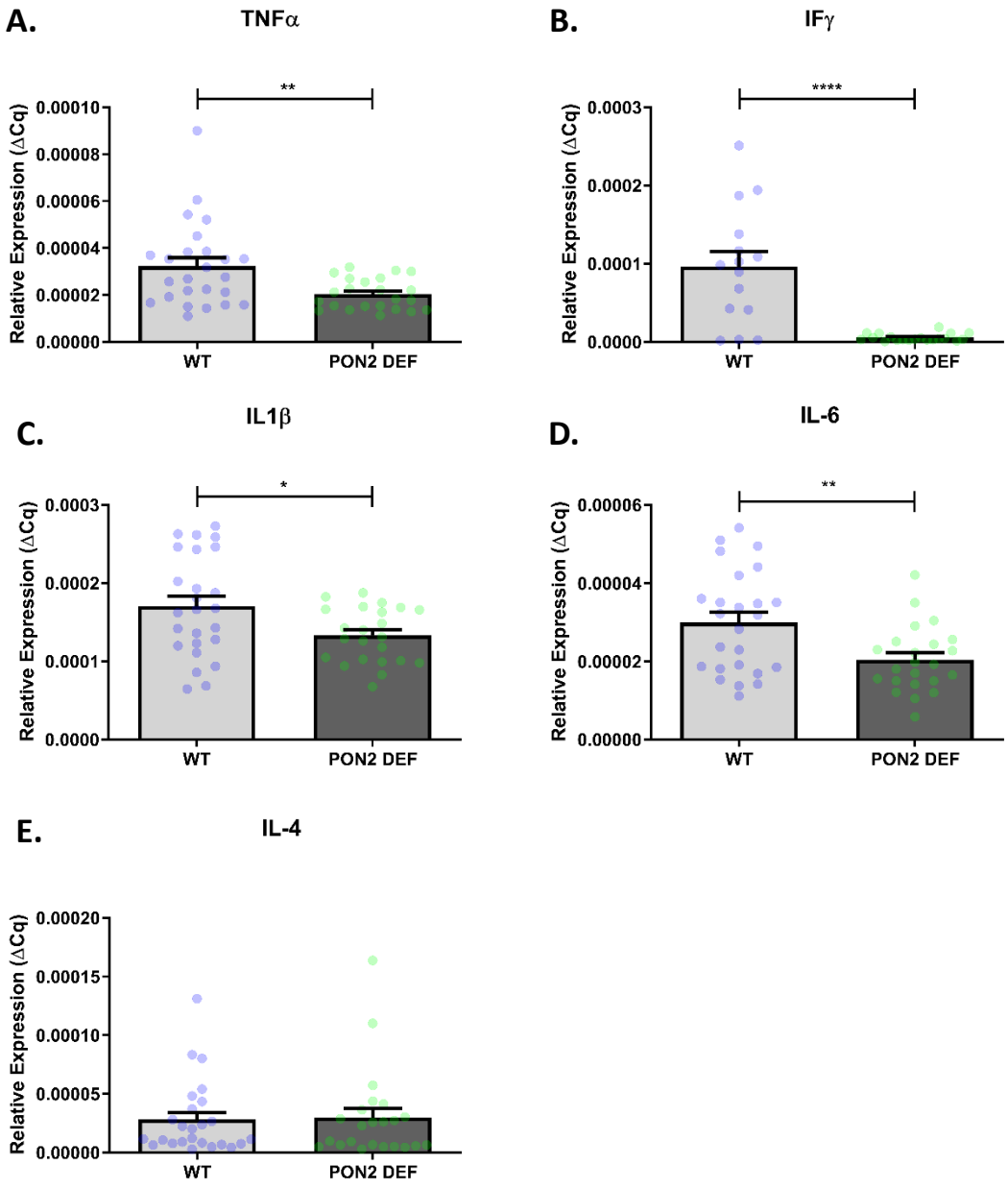

Figure 5.5 - mRNA Expression of Cytokines in Wildtype and PON2 deficient Cerebral Cortex of Aged Mice. A. Quantification of tumor necrosis factor alpha (TNFα) mRNA normalized to GAPDH, mean (± SEM), n = 20 - 24 per group, ** $p < 0.01$. **B.** Quantification of interferon gamma (IFγ) mRNA normalized to GAPDH, mean (± SEM), n = 11 - 13 per group, **** $p < 0.0001$. **C.** Quantification of interleukin 1 beta (IL1β) mRNA normalized to GAPDH, mean (± SEM), n = 20 - 24 per group, * $p < 0.05$. **D.** Quantification of interleukin 6 (IL-6) mRNA normalized to GAPDH, mean (± SEM), n = 20 - 24 per group, ** $p < 0.01$. **E**. Quantification of interleukin 4 (IL-4) mRNA normalized to GAPDH, mean (± SEM), n = 20 - 24 per group.

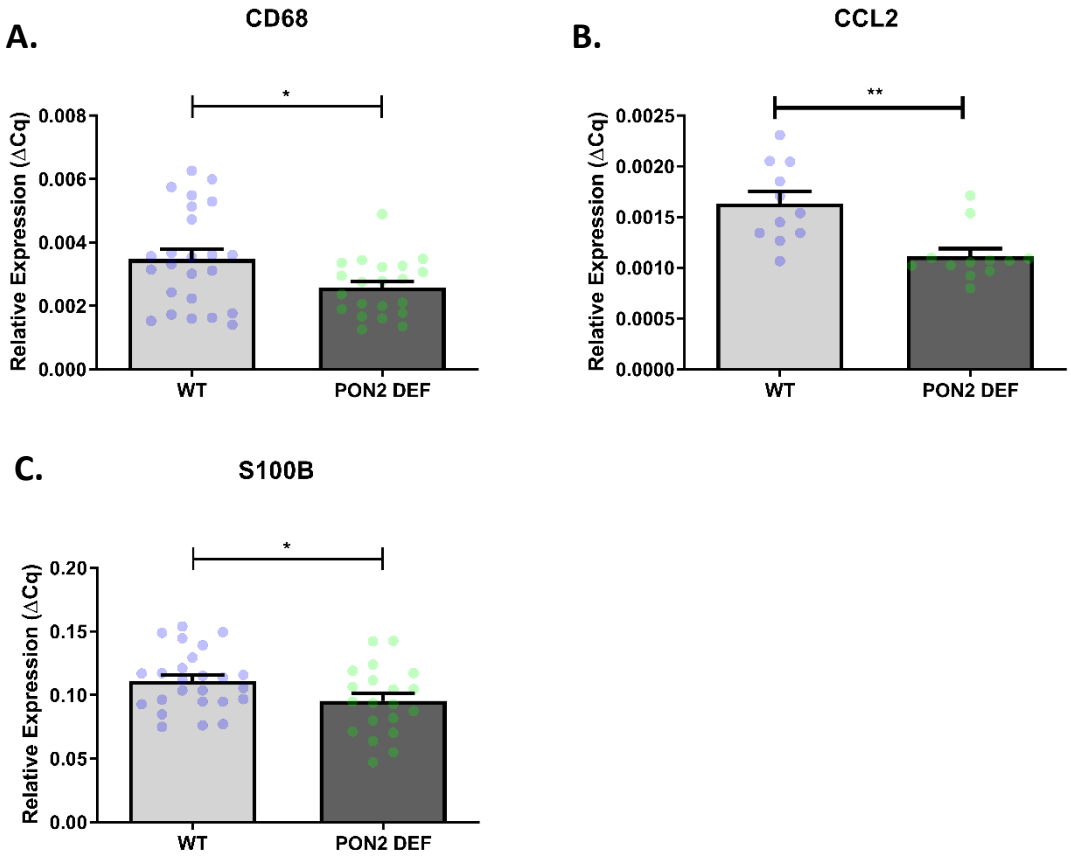

Figure 5.6 - mRNA Expression of Glial Activation Markers in Wildtype and PON2 deficient Cerebral Cortex of Aged Mice. A. Quantification of CD68 mRNA normalized to GAPDH, mean (± SEM), n = 20 - 24 per group, * $p < 0.05$. **B.** Quantification of C-C Motif Chemokine Ligand 2 (CCL2) mRNA normalized to GAPDH, mean (± SEM), n = 11 - 13 per group, ** $p < 0.01$. **C.** Quantification of S100 calcium binding protein B (S100B) mRNA normalized to GAPDH, mean (± SEM), n = 20 - 24 per group, * $p < 0.05$.

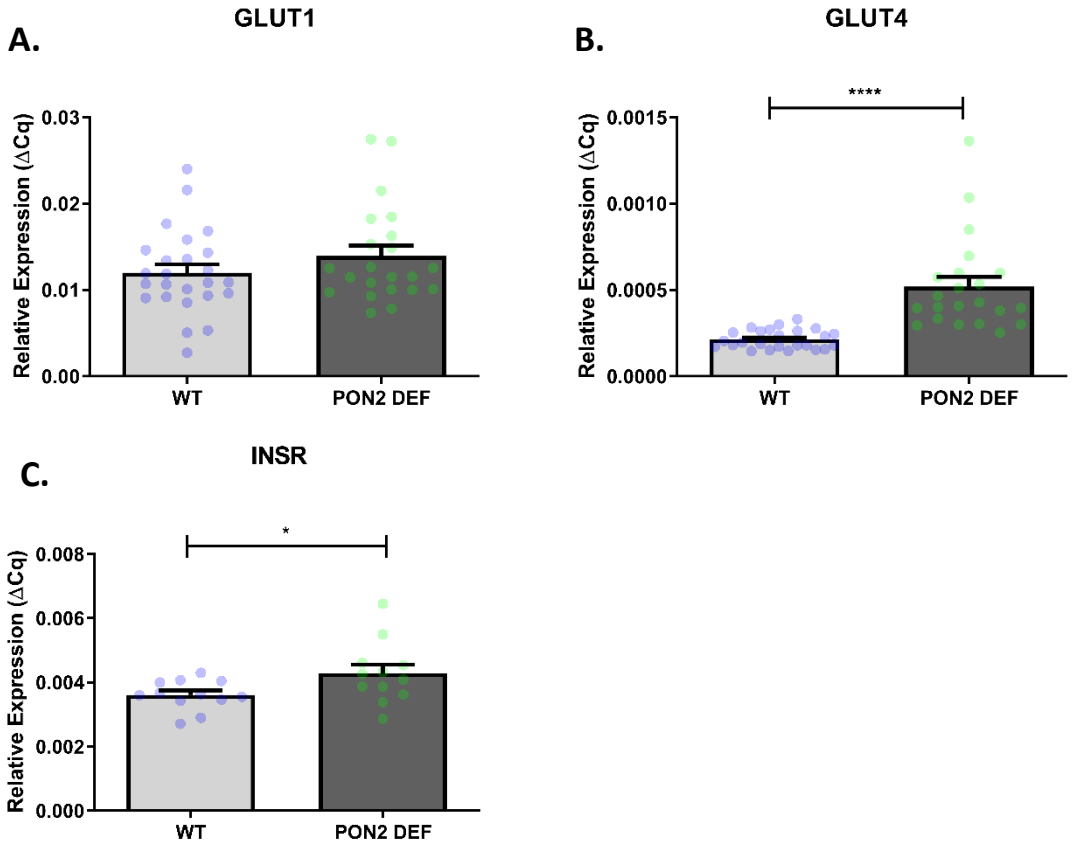

Figure 5.7 - mRNA Expression of Glucose Transporters in Wildtype and PON2 deficient Cerebral Cortex of Aged Mice. A. Quantification of glucose transporter 1 (GLUT1) mRNA normalized to GAPDH, mean (± SEM), n = 20 - 24 per group. **B.** Quantification of glucose transporter 4 (GLUT4) mRNA normalized to GAPDH, mean (± SEM), n = 20 - 24 per group, **** $p < 0.0001$. **C.** Quantification of insulin receptor (INSR) mRNA normalized to GAPDH, mean (± SEM), n = 12 per group, * $p < 0.05$.

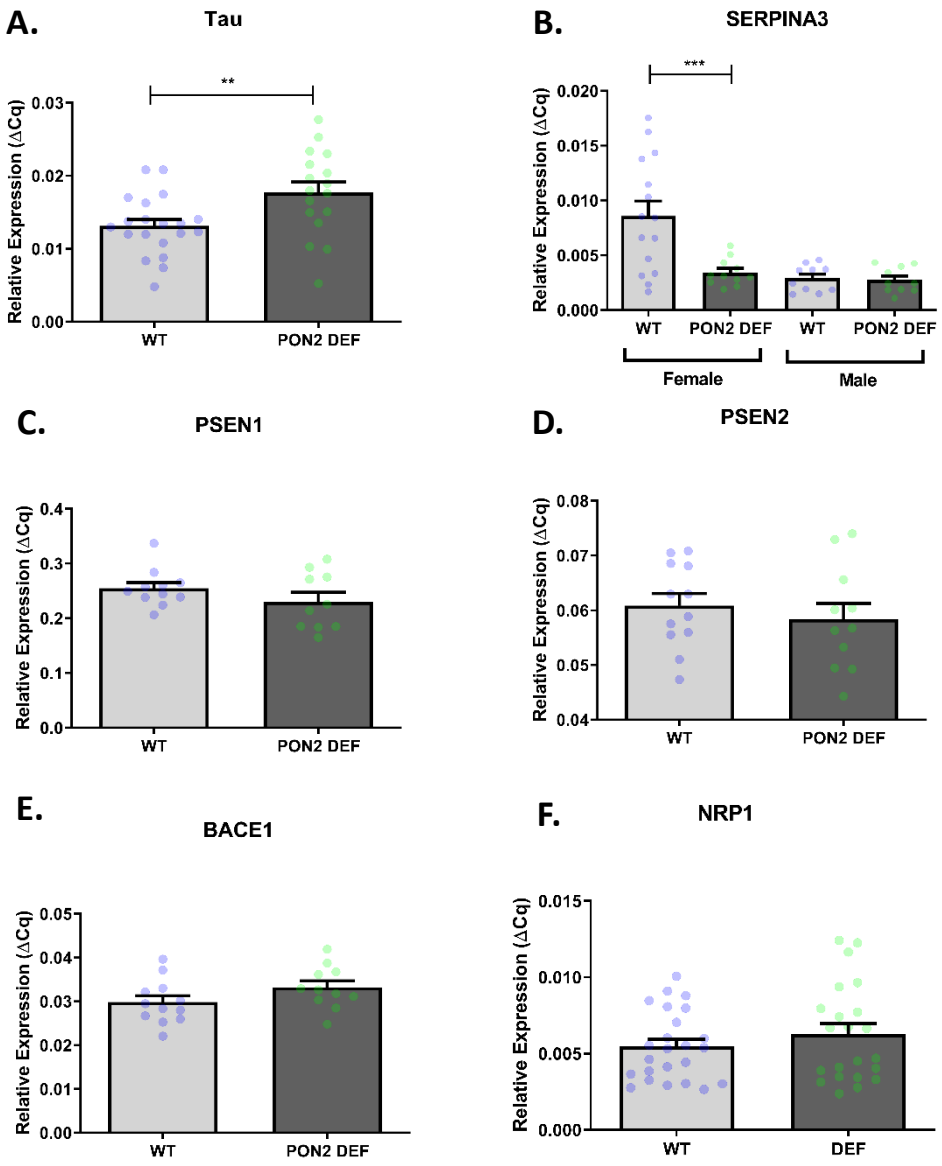

Figure 5.8 - mRNA Expression of Neurodegenerative Markers in Wildtype and PON2 deficient Cerebral Cortex of Aged Mice. A. Quantification of Tau mRNA normalized to GAPDH, mean (± SEM), n = 20 - 24 per group, ** $p < 0.01$. **B.** Quantification of Alpha 1-antichymotrypsin (SERPINA3) mRNA normalized to GAPDH, mean (± SEM), n = 10 - 17 per group, *** $p < 0.001$. **C.** Quantification of presenilin 1 (PSEN1) mRNA normalized to GAPDH, mean (± SEM), n = 9 - 10 per group. **D.** Quantification of presenilin 2 (PSEN2) mRNA normalized to GAPDH, mean (± SEM), n = 11 - 12 per group. **E.** Quantification of beta-secretase 1 (BACE1) mRNA normalized to GAPDH, mean (± SEM), n = 9 - 10 per group. **F.** Quantification of neuropilin-1 (NRP1) mRNA normalized to GAPDH, mean (± SEM), n = 20 - 24 per group.

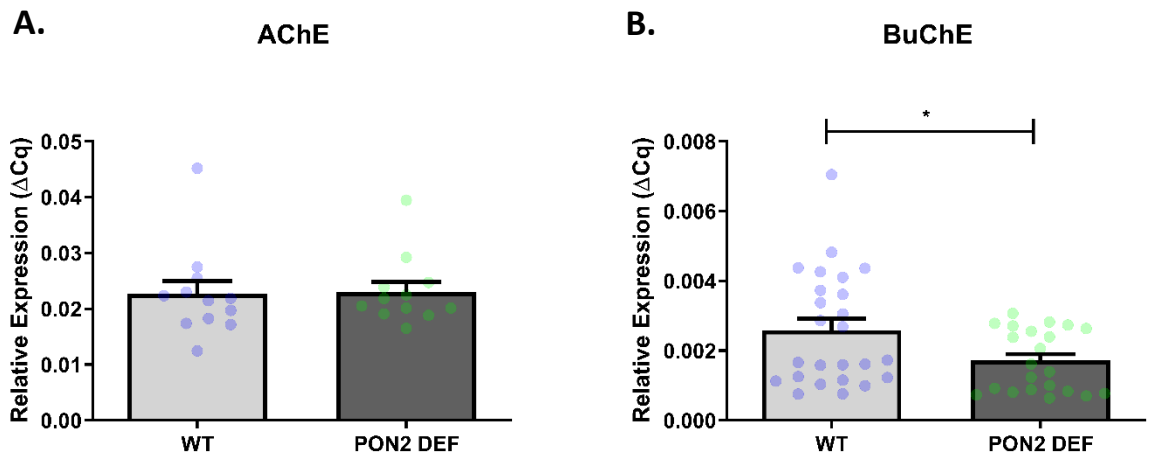

Figure 5.9 - mRNA Expression of Cholinesterases in Wildtype and PON2 deficient Cerebral Cortex of Aged Mice. A. Quantification of acetylcholinesterase (AChE) mRNA normalized to GAPDH, mean (± SEM), n = 12 per group. **B.** Quantification of butyrylcholinesterase (BuChE) mRNA normalized to GAPDH, mean (± SEM), n = 20 - 24 per group, * $p < 0.05$.

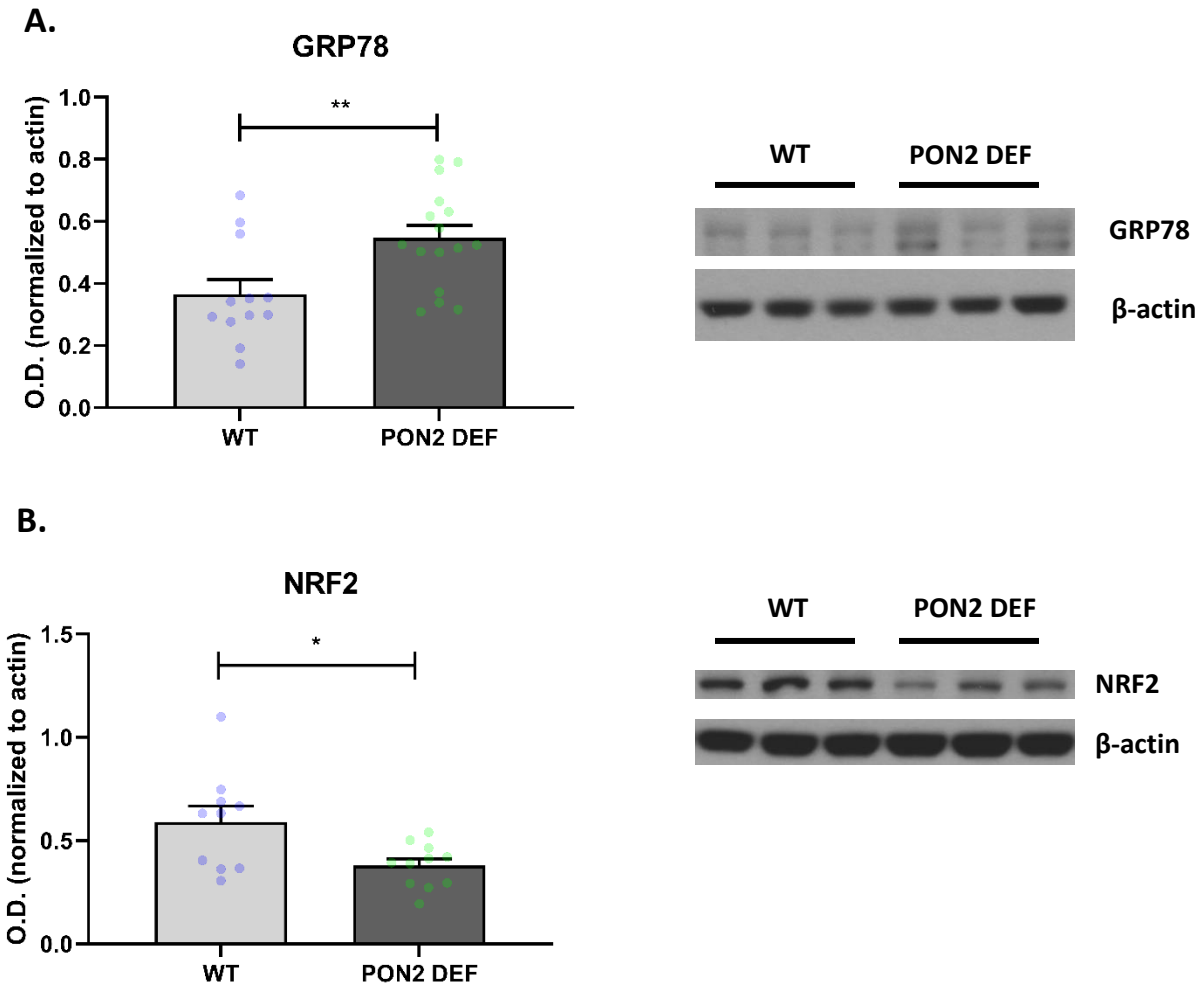

Figure 5.10 - Protein Expression of Stress Response Targets in Wildtype and PON2 deficient Cerebral Cortex of Aged Mice. A. Quantification of glucose regulatory protein 78 (GRP78) protein normalized to β-actin, mean (± SEM), n = 12 per group, ** $p < 0.01$. **B** Quantification of nuclear factor erythroid 2-related factor 2 (NRF2) protein normalized to β-actin, mean (± SEM), n = 9 - 10 per group, * $p < 0.05$.

5.4 – Discussion

As the aging population increases, treating and preventing diseases of aging are a growing concern. Current treatment options for neurodegenerative diseases are limited and only address symptoms, with no treatment options available to reverse or prevent disease (Kiaei 2013). To move beyond the realm of symptom management in future therapeutics, understanding the underlying mechanism of neurodegeneration is crucial. To that end, we sought to investigate PON2 in the aging nervous system, as oxidative stress has been identified as a principle mechanism for neurodegeneration.

Obesity is strongly correlated with neurodegenerative disease, among a host of other morbidities, and is increasing worldwide (Mazon et al., 2017). PON2 deficiency has been linked to diet-induced obesity, where PON2-def mice on a high fat diet gain more weight and exhibit glucose intolerance compared to controls. This was due to a suspected reduction in energy expenditure and not energy intake, as food intake was equal among PON2-def and control animals (Shih et al., 2019). As most animals age, activity levels decrease and body composition changes, with fat redistributing to the viscera (Villareal et al., 2012). Feasibly, we anticipated that PON2-def mice would gain more weight than WT mice as they age due to their reported reduction in energy expenditure. However, no significant weight difference between PON2-def and WT mice was noted in this study, where mice were fed a standard laboratory chow diet (Figure 5.1). This suggests that PON2 deficiency alone is not sufficient to cause weight gain and requires a dietary intervention. Further analysis of PON2 deficiency in aging mice on a high fat diet would be of interest to determine if aging exacerbates the weight gain and metabolic disruptions observed by Shih et al., and if a high fat diet influences other neurodegenerative metrics.

An unexpected finding in this study was the higher incidence of ulcerative dermatitis (UD) in PON2-def mice (Figure 5.2). UD is a debilitating condition which causes large, irregular ulcerated lesions on the skin that are generally unresponsive to treatment (Hampton et al., 2012). This finding in PON2-def mice has never been reported in the literature, likely due to the advanced age of onset ($\geq$ 1 year) and most studies focusing on younger cohorts. C57BL/6 mice, the background of both the WT and PON2-def mice in our study, have a reported higher incidence of idiopathic UD (Hampton et al., 2012). However, no WT mice developed UD in our study and as such this increased incidence appears to be unrelated to the C57BL/6 background. Although the exact cause of UD is unknown, numerous factors have been found to predispose animals to the disease, such as old age (Kastenmayer et al., 2006), female sex (Kastenmayer et al., 2006), diet (Turturro et al., 2002), genetics (Andrews et al., 1994; Kastenmayer et al., 2006; Sundberg et al., 2011), immune complex vasculitis (Andrews et al., 1994), deficiencies in vitamin A metabolism (Sundberg et al., 2011) and chronic inflammation (Duarte-Vogel & Lawson 2011). While our study did not find elevated inflammation in the aged PON2 deficient brain as measured by cytokines, we did not measure systemic or localized dermal inflammation, which would be more appropriate in addressing whether the UD noted in the PON2-def mice was inflammatory mediated. PON2 may play a direct role in maintaining dermal integrity, or PON2 deficiency affecting a gene necessary for prevention of UD. Although genetic studies of this condition have been limited, deficiency in nitric oxide synthase (iNOS) (Kastenmayer et al., 2006) and mutations in alcohol dehydrogenase 4 (ADH4) which reduce its enzymatic activity have been associated with development of UD in mice (Sundberg et al., 2011), while insulin receptor substrate 1 (IRS1) knockout mice are fully resistant to UD (Neuhaus et al., 2012). In the RNA-Seq study discussed in chapter 3, alcohol dehydrogenase 5 (Adh5) was significantly

downregulated in PON2-def female striatum (Figure 3.9E). As well, PON2-def male mice in the cortex had significantly higher levels of insulin receptor substrate 2 (Irs2), a similarly important mediator of insulin signaling as ISR1 (Appendix Table AB.1). Although outside the scope of this dissertation, these RNA-Seq findings combined with the higher UD incidence in aged PON2-def mice suggest novel pathways disrupted by PON2 deficiency with pathological implications in the skin. Further research would be of interest to determine if the downregulation of ADH5 and upregulation of ISR2 persist dermally and are related to UD in PON2-def mice. Rescue studies supplementing ulcerative mice with purified PON2 would also be of interest to determine if exogenous PON2 supplementation reverses disease progression. For future work in this area, systemic and dermal expression should be evaluated in PON2-def mice, as the transcriptional results in the brain discussed in this dissertation are likely not reflective of the expression profile of the skin.

When measuring oxidative stress by lipid peroxidation, PON2-def mice did not exhibit higher levels in the brain compared to controls (Figure 5.3A). As well, PON2-def mice with UD did not have higher levels of oxidative stress in the brain compared to mice without ulcers (Figure 5.3B), suggesting the condition is not due to globally elevated oxidative stress. These findings were surprising, as PON2 deficiency has been reported to increase oxidative stress in multiple systems by numerous investigators (Devarajan et al., 2011; Giordano et al., 2013; Yang et al., 2015; Sulaiman et al., 2019). Our original hypothesis was that age would exacerbate the oxidative stress phenotype of PON2 deficiency; instead, no increase in oxidative stress was observed in either young or aged PON2-def animals. While inconsistent with existing literature, this finding is consistent with the RNA-Seq data discussed in chapter 3, where minimal perturbation of oxidative stress pathways and no upregulation of compensatory antioxidant genes

was found. Potentially, a mutation has arisen in our PON2-def population in a gene that segregates with PON2, or PON2 catalytic activity can be modulated to make up for a reduction in protein, making these animals functionally less deficient than expected. Additional discussion on the deficient model and how this may impact future research directions is offered in chapter 6.

Looking at the expression of select neuroinflammatory cytokines, PON2 deficiency reduced the transcript levels of TNF-α (Figure 5.5A), IF-γ (Figure 5.5B), IL-β (Figure 5.5C) and IL-6 (Figure 5.5D), while levels of IL-4 were unchanged (Figure 5.5E). This was also a surprising finding akin to the lack of lipid peroxidation, as PON2 deficiency has been associated with elevated inflammation in other studies (Ng et al., 2006). Cytokines play a dual role in the brain, both acting as pro-inflammatory agents and signaling molecules for physiological processes, such as the host immune response and cellular differentiation and maturation (Mousa & Bakhiet 2013). IF-γ expression was found to be remarkably reduced in PON2-def mice (Figure 5.5B) and is known to play a role in cell cycle control and viral clearance in addition to inflammatory signaling (Kulkarni et al., 2016). IF-γ production has been found to be regulated positively by cytokines IL-12 and IL-18 (Schroder et al., 2003) as well as transcription factors such as nuclear factor κB (NF-κB) (Sica et al., 1997), and negatively regulated by IL-4, IL-10, transforming growth factor-β (TGF- β), glucocorticoids, and suppressor of cytokine signaling 1 (SOCS1) (Schroder et al., 2003; Starr et al., 2009). From our dataset in aim 3, PON2-def male mice had significant upregulation of NFKB Inhibitor Delta (Nfkbid) in the cortex (Table AB.1), which may reduce NF-κB and impact IF-γ levels in PON2-def mice. Additionally, suppressor of cytokine signaling 5 (Socs5) was noted to be upregulated in the cortex of PON2-def mice (Table AB.1). Although it is unclear whether SOCS5 plays a direct inhibitory role for IF-γ in a similar manner to SOCS1, it would be of further interest to investigate this in relation to the overall

decreased cytokine expression observed with PON2 deficiency. Further, IF-γ is recognized as part of a major tumor surveillance system, where IF-γ receptor null mice, insensitive to the signaling action of IF-γ, develop tumors more rapidly and with higher frequency upon carcinogen challenge (Kaplan et al., 1998). Recent work has also identified IF-γ as a mediator of social behavior and neuronal connectivity, where IF-γ knockout mice display social deficits (Filiano et al., 2016). In macrophages, IF- γ has been shown to regulate the expression of CD68 (Chistiakov et al., 2017), CCL2 (Lin et al., 2009), and S100B (Adami et al., 2001), which were all notably downregulated in PON2-def mice in our study (Figure 5.6). Although PON2 deficiency may not promote inflammation in the brain, the significant reduction in these cytokines, specifically IF-γ, could inhibit their physiological signaling role and have downstream implications for the host immune response, cell differentiation, tumor surveillance and behavior. Exploring whether these downregulated cytokines impact brain immunity and social behavior in aged mice would be of future interest and could prove to be an exciting new area of study.

Altered glucose metabolism and transport are noted in patients with AD (Shah et al., 2012) and associated with epilepsy (Klepper 2008). Four glucose transporter (GLUT) subtypes are expressed in the brain with both overlapping and distinct expression patterns, and are either insulin independent (GLUT1, 2, 3) or dependent (GLUT4) (Koepsell 2020). In our study, we evaluated the transcript expression of GLUT1 (Figure 5.7A) and GLUT4 (Figure 5.7B), finding no changes in GLUT1 with PON2 deficiency and significant upregulation of GLUT4, suggesting a possible perturbation to insulin dependent glucose signaling in the cortex of PON2 deficient aged mice. Additionally, insulin receptor (INSR) transcript was moderately higher in PON2-def mice (Figure 5.7C), providing supplemental evidence for perturbation of insulin related signaling. In the brain, GLUT4 is recruited by firing neurons for additional metabolic energy

and is important for insulin-dependent regulation of neuronal circuits involved in mood and memory (Lee et al., 2016; Koepsell 2020). An increase in GLUT4 could feasibly point to an increase in neuronal activity in PON2-def mice as well as alterations in behavior, although further investigation to support this is necessary. Additional analysis of this system by measuring insulin levels and signaling pathway genes in aged, as well as younger, PON2-def mice would be of interest to identify changes in glucose pathways. While this study is the first to identify glucose transporter and insulin receptor changes with PON2 deficiency in the brain, PON2 deficiency in the liver has been noted to impair insulin signaling (Bourquard et al., 2011). Additionally, the Ser311Cys allele has been found to be associated with insulin resistance in a small Iranian cohort (Qujeg et al., 2018). Taken in summary with the results of our study, further investigation of both systemic and brain-specific insulin signaling with PON2 deficiency would be of value.

Multiple genes have been identified as potential mediators of neurodegenerative disease. In AD, neurotoxic tangles of hyperphosphorylated tau protein and plaques of aggregated amyloid beta (Aβ) deposited in the brain are the primary markers of disease. These plaques and tangles interfere with the function of healthy neurons, causing them to die and leading to progressive and irreversible memory loss and cognitive impairment (DeTure and Dickson 2019). We evaluated the expression of multiple tangle and plaque-related targets in the cortex, finding tau transcript significantly higher in PON2-def mice (Figure 5.8A). Although measurement of phosphorylated tau protein is needed to confirm tangle-related pathology, an increase in tau transcript may point to tau dysregulation. Presenilin 1 and 2 (PSEN1/2) and beta secretase 1 (BACE1), all involved in the processing of amyloid precursor protein (APP), were unchanged with PON2 deficiency (Figure 5.8C – E). Separate from tangles and plaques, the serine protease inhibitor serpin family

member A member 3 (SERPINA3) and mitochondrial iron homeostasis mediator neuropilin-1 (NRP1) have been associated with AD (Kamboh et al., 2006; Issitt et al., 2019). Our findings show no difference in NRP1 transcript in PON2-def mice (Figure 5.8F), whereas female, but not male, deficient mice had significantly reduced SERPINA3 expression (Figure 5.8B). SERPINA3 was the only gene identified as having a sex-specific expression change in our study of aged mice. As reviewed in chapter 3, PON2 deficiency removed sexual dimorphic expression patterns, bringing female and males to similar expression profiles in a similar pattern to that observed for SERPINA3. One study found higher expression of SERPINA3 in females, although the authors could not explain a reason for the expression difference (Zhou et al., 2017). In general, the role of SERPINA3 is still under investigation.

Acetylcholine (ACh) is the principle neurotransmitter of the peripheral parasympathetic nervous system. In the brain it is proposed to also act as a neuromodulator, where it changes the state of neurons without being directly excitatory (via glutamate receptors) or inhibitory (via GABA receptors) (Picciotto et al., 2012). A high density of cholinergic synapses exists in the striatum, neocortex, thalamus, and limbic system, suggesting cholinergic signaling is critical to learning, memory and other higher-order functions performed in these regions (Hampel et al., 2018). Cholinergic dysfunction has been linked to AD pathophysiology, where the cerebral cortex of AD patients has been found depleted of presynaptic cholinergic markers (Bowen et al., 1976) and several cortical cholinergic regions undergo intense neurodegeneration with AD (Whitehouse et al., 1981). To this end, acetylcholinesterase (AChE), responsible for breaking down ACh, has been targeted for therapeutic use to minimize ACh loss. Of the five pharmaceuticals approved by the U.S. FDA, three of them are cholinesterase inhibitors (Alzheimer's Association 2019). In our study, AChE transcript was not altered with PON2

deficiency (Figure 5.9A). However, a reduction in butyrylcholinesterase (BuChE) was found in PON2-def mice (Figure 5.9B). BuChE co-regulates ACh levels along with AChE and has been identified as an emerging target for AD (Geula and Darvesh 2004, Darvesh 2016). These findings were unexpected, as a reduction in BuChE would be anticipated as protective for neurodegeneration and our hypothesis was that PON2 deficiency would increase cholinesterase levels. Additional experiments are necessary to address the role of PON2 in the cholinergic system, such as measuring ACh levels and exploring whether targeted PON2 knockdown can rescue ACh loss. Although these results are preliminary, they provide further evidence for PON2 as a potential therapeutic target for neurodegenerative disease.

Further supporting an absence of oxidative stress, nuclear factor erythroid 2-related factor 2 (NRF2) protein was significantly lower in PON2-def mice (Figure 5.10B). However, this result is somewhat unexpected, as a lack of oxidative stress would be expected to show no difference between WT and PON2-def mice, not a decrease, as WT mice should not be under any substantial oxidative burden. As such, this finding may point to dysregulation of the NRF2-KEAP pathway, potentially impacting a host of NRF2-mediated genes, although further investigation is needed to determine this. While oxidative stress findings were consistently null, a modest increase in GRP78 protein, upregulated during endoplasmic reticulum (ER) stress and disruptions to calcium homeostasis, was seen in PON2-def mice (Figure 5.10A). This finding supports PON2 deficiency increases ER stress in the aged cortex, but this is independent of oxidative stress; analyzing these targets further would be of interest.

The present study was not exhaustive, and many questions remain on PON2 in the aging nervous system. The results described in this chapter support a potential impact on a variety of genes relevant to cytokine signaling and neurodegeneration, but further validation at the protein

level is required, as is the investigation of many other related targets to provide a clear picture on how PON2 deficiency impacts these pathways. As many of these pathways are proposed to affect memory and mood, behavioral investigation would be of value. Numerous unexpected results were obtained that complicate the interpretation of these findings and, in combination with the results of chapter 3, suggest that one-by-one measurements of targets may not be an ideal approach, considering global RNA machinery appears to be impacted by PON2 deficiency. Instead, whole-tissue and cell-specific proteomic studies, paired with RNA-Seq, may provide a better picture of the consequences of PON2 deficiency within the context of neurodegenerative disease, with targeted analysis done as a secondary follow up to omics.

5.5 – Materials and Methods

Materials

TBARS Assay Kit was purchased from Cayman Chemical (Ann Arbor, MI, USA). Anti-NRF2 and GRP78 antibodies were purchased from Abcam (Cambridge, MA, USA). β-actin antibody was purchased from MilliporeSigma (Burlington, MA, USA). Anti-rabbit IgG HRP-linked antibody and Cell Lysis Buffer 10x were purchased from Cell Signaling Technology (Danvers, MA, USA). HRP Goat Anti-Mouse IgG was purchased from BD Biosciences (San Jose, CA, USA). XCell II Blot Module, XCell SureLock Electrophoresis Cell, NuPAGE MOPS SDS Running Buffer 20x, NuPAGE LDS Sample Buffer 4x, NuPAGE Antioxidant, NuPAGE Sample Reducing Agent 10x and NuPAGE 10% Bis-Tris Protein Gels were purchased from Life Technologies (Carlsbad, CA, USA). Immobilon-P Transfer Membrane was purchased from Millipore Corporation (Billerica, MA, USA). Restore Western Blot Stripping Buffer, PageRuler Prestained Protein Ladder and SuperSignal West Pico Chemiluminescent Substrate were

purchased from Thermo Fisher Scientific (Waltham, MA, USA). RNeasy Mini Kit was purchased from Qiagen (Hilden, Germany). iScript cDNA Synthesis Kit, iTaq Universal SYBR Green Supermix and CFX384 Real-Time Detection System were purchases from Bio-Rad Laboratories (Hercules, CA, USA). All qPCR primers were purchased from Integrated DNA Technologies (Newark, NJ, USA).

Animals and Tissue

Male and female wildtype (WT) and PON2-deficient (PON2-def) mice (Ng et al., 2006) on a C57BL/6J background were used for this study. Mice were kept until they reached 'aged' status (18 - 24 months as defined by The Jackson Laboratory). 15 - 20 animals per sex per genotype were assigned to the aged cohort, with an expectation that the final cohort numbers would be lower due to natural attrition from aging. The final cohort size was 10 – 15 mice per sex per genotype. Upon reaching aged status, mice were sacrificed and brain regions (cortex, cerebellum, striatum, hippocampus) and organs were collected and stored at -80°C. Mice were housed in a specific pathogen-free facility on a 14-hour light/ 10-hour dark cycle with *ad libitum* access to food and water. All procedures were conducted in accordance with the National Institute of Health Guide for the Use and Care of Laboratory Animals and were approved by the University of Washington Institutional Animal Care and Use Committee.

Assessment of Lipid Peroxidation

Lipid peroxidation was measured by quantifying the levels of malondialdehyde (MDA), a byproduct of lipid peroxidation, utilizing the Thiobarbituric Acid Reactive Substances (TBARS)

Assay Kit (Cayman Chemical, Ann Arbor, MI) and following the manufacturer's protocol. For preparation of the samples, frozen brain-region powder (~30 mg) was aliquoted and thawed into 1x RIPA buffer (50mM Tris HCl pH 8, 150 mM NaCl, 1% NP-40, 0.5% sodium deoxycholate, 0.1% SDS) containing protease inhibitors (Pierce Protease Inhibitor Mini Tablet, EDTA-free, Thermo-Fisher Scientific, Waltham, MA) and sonicated for 20 – 30 seconds for homogenization. Total protein was measured using the Pierce Bicinchoninic Acid (BCA) Assay Kit (Thermo-Fisher Scientific, Waltham, MA) with bovine serum albumin (BSA) as a standard and conducted according to the manufacturer's protocol. TBARS assay samples were diluted to a total protein concentration of 1µg/µL, with 100µL of sample used for the assay.

Immunoblotting

Immunoblots were carried out as previously described (Garrick et al., 2016). Briefly, 15 µg of protein was mixed with SDS running buffer and sample reducing agent and subjected to sodium dodecyl sulfate-polyacrylamide gel electrophoresis (SDS-PAGE). Following electrophoresis, proteins were transferred to polyvinylidene difluoride membranes and the membrane blocked for 1-3 hours with 5% nonfat milk. Membranes were then probed with the following diluted primary antibodies GRP78 (1:2500) and NRF2 (1:4000). Following primary antibody incubation, membranes were washed with Tris-buffered saline with 0.1% Tween-20 (pH = 7.5) and incubated with horseradish peroxidase-conjugated anti-rabbit secondary antibody at a dilution of 1:5000 and 1:2500 for GRP78 and NRF2, respectively. Membranes were stripped with Restore™ Western Blot Stripping Buffer (Thermo Fisher Scientific, Waltham, MA) and re-probed for β-actin using a dilution of 1:2500 for the β-actin primary antibody and 1:2500 for the horseradish peroxidase-conjugated anti-mouse secondary antibody. Intensity of bands was

measured by densitometry using ImageJ software (NIH), with the band intensity normalized to β-actin expression.

RT-PCR

Target mRNA levels were measured by RT-PCR, see Table 5.1 below for primer pairs. Total RNA was extracted from striatal tissue using the RNeasy Mini Kit (Qiagen, Hilden, Germany) according to manufacturer's established protocol. cDNA was generated from 1µg total RNA using the iScript cDNA Synthesis Kit (Bio-Rad Laboratories, Hercules, CA) according to the manufacture's established protocol. The cDNA samples were diluted to a concentration of 6.25ng/µL with nuclease-free water and subsequently used for quantitative polymerase chain reaction (qPCR) using iTaq Universal SYBR Green Supermix in a CFX384 Real-Time Detection System (Bio-Rad Laboratories, Hercules, CA). 6µL of diluted cDNA were included in a PCR reaction mastermix containing 15µL Universal SYBR Green Supermix (2x), 1.5µL each forward and reverse primers (10µM stock), and 6µL nuclease-free water (30µL final volume). The reaction mixture was then aliquoted in triplicate, 8µL per reaction per sample. The thermal cycling conditions were as follows: A single denaturing step at 95°C for 30 seconds, 40 cycles of 95°C for 15 seconds, 60°C for 30 seconds and 72°C for 30 seconds. dCq values (referenced as "relative mRNA") for each target were calculated by subtracting Cq values of housekeeping gene GAPDH.

Statistical Analysis

Data are expressed as the mean ± SEM of at least three independent experiments. Student's t-test was utilized for comparing two groups, while One-way ANOVA followed by the Bonferroni correction for multiple comparisons was utilized for multiple groups as noted.

Table 5.1 – qPCR Primer Pairs

Target	Forward Primer (5' – 3')	Reverse Primer (5' – 3')
TNF-α	GCCTCTTCTCATTCCTGCTTG	CTGATGAGAGGGAGGCCATT
IF-γ	TCAAGTGGCATAGATGTGGAAGAA	TGGCTCTGCAGGATTTTCATG
IL1-β	CAACCAACAAGTGATATTCTCCATG	ATCCACACTCTCCAGCTGCA
IL-6	GAGGATACCACTCCCAACAGACC	AAGTGCATCATCGTTGTTCATACA
IL-4	ACAGGAGAAGGGACGCCAT	GAAGCCCTACAGACGAGCTCA
CD68	ACTGGTGTAGCCTAGCTGGT	CCTTGGGCTATAAGCGGTCC
CCL2	ACTGAAGCCAGCTCTCTCTTCCTC	TTCCTTCTTGGGGTCAGCACAGAC
S100B	GGGTGACAAGCACAAGCTGA	TCCACCACTTCCTGCTCCTT
GLUT1	TCTCTGTCGGCCTCTTTGTT	GCAGAAGGGCAACAGGATAC
GLUT4	AAAAGTGCCTGAAACCAGAG	TCACCTCCTGCTCTAAAAGG
INSR	TTTGTCATGGATGGAGGCTA	CCTCATCTTGGGGTTGAACT
Tau	GAACCACCAAAATCCGGAGA	CTCTTACTAGCTGATGGTGAC
SERPINA3	GGGATGATCAAGGAACTGGTCT	CCGCGTAGAACTCAGACTTGAA
PSEN1	TGCACCTTTGTCCTACTTCC	GCTCAGGGTTGTCAAGTCTCTG
PSEN2	GAGCTGACCCTCAAGTATGG	GTGAAGGGCGTGTAGATGAG
BACE1	CTGTGCGTGCCAACATTGC	TCACCAGGGAGTCAAAGAAGG
NRP1	GGCTGTGAAGTGGAAGCACC	AGTGGTGCCTCCTGTGAGC
AChE	GAGAGGATCTTTGCTCAGCGAC	GAGAAAGCGATTCCAGAAGGC
BuChE	TAGCACAATGTGGCCTGTCT	ATTGCTCCAGCGATGAAATC

5.6 Acknowledgements

This work was supported in part by the Superfund Research Program (SRP) grant P42ES004696 and the Environmental Pathology/Toxicology training grant T32 ES007032-37 from the National Institute of Environmental Health Sciences.

Chapter 6

Conclusions and Future Directions

This dissertation contributes to the current scientific body of knowledge regarding PON2 in the CNS by characterizing its developmental expression in the brain (aim 1, chapter 2), identifying a behavioral phenotype and transcriptional profile of PON2 deficiency in multiple brain regions (aim 2, chapter 3), demonstrating dopamine receptor modulation of PON2 expression and transcriptional changes of dopaminergic targets (aim 3, chapter 4), and providing preliminary work supporting PON2 deficiency transcriptionally alters the expression of genes relevant to neurodegeneration in aged mice (aim 1, chapter 5).

In chapter 2, PON2 expression in the brain and liver was measured over multiple age points to identify potential windows of susceptibility to oxidative stress. This study revealed that PON2 is developmentally regulated and displayed a bell-shaped expression profile in the brain, with expression peaking at PND21 (Chapter 2, Figure 2.2). As well, the brain expression profile differs significantly from that of the liver, where PON2 expression increased persistently in a linear fashion and follows the pattern of other paraoxonases (Chapter 2, Figure 2.4). This work identified tissue-specific expression profiles of PON2 and suggests that both younger and older mice may be more susceptible to oxidative damage in the CNS due to lower PON2 levels. Additionally, PON2 may be playing a signaling role in the developing nervous system. At PND21, the rodent brain is undergoing significant restructuring through synaptic pruning (Semple et al., 2013). PON2 may be functioning as an apoptotic protector to maintain the pathways designated for maintenance or playing another signaling role during maturation. Further examination of this age point would be of interest to determine what purpose elevated PON2 expression serves and investigate whether PON2 deficiency alters CNS maturation.

Additionally, examination of other tissues over development, such as the kidneys, lung, and heart, would be of interest to understand the tissue-specificity of developmental regulation.

Chapter 3 describes the behavioral and transcriptional phenotype of PON2 deficient mice. These mice displayed hyperactivity and motor coordination deficits compared to their WT littermates, identifying a previously unreported behavioral phenotype for this deficient strain. Looking at transcript expression changes in the brain, PON2 deficiency significantly altered RNA processing pathways in a highly regional and sex-specific manner. Furthermore, PON2 deficiency abolished sex differences such that female and male mice had similar transcript profiles, compared to WT mice where females and males had vastly different expression. To my knowledge, this is the first transcriptional analysis of PON2 deficiency in any organ system. As such, these findings provide exciting new avenues of study for PON2 research, particularly when considering the impacted pathways were ones with global implications for the organism. These pathways were unexpected, as no overt oxidative stress pathways were noted in the deficient mice and no compensatory antioxidant genes were upregulated. Further targeted study of the afflicted pathways would be of interest and determining which are directly linked to the observed motor phenotype.

The role of PON2 in the dopaminergic system was investigated in chapter 4. Significant transcript changes in multiple dopaminergic pathway genes were found in PON2 deficient mice, although many of these changes were not observed at the protein level. PON2 was also found to be modulated by dopamine receptor activity in a receptor-specific manner, with protein and transcript upregulated in neurons upon exposure to a dopamine receptor 2 agonist, but not an agonist for dopamine receptor 1. Further building from this dissertation work, examining the interactions of PON2 in the dopaminergic system in more detail would be of interest and may

have clinical implications. Many transcriptional changes were observed in dopaminergic pathway genes which could have consequences if translational controls breakdown. As well, this work demonstrates that dopamine receptor signaling modulates the expression of PON2, supporting that it plays a role in dopamine signaling. However, this work was limited in determining the mechanism by which PON2 expression is modulated and what role it plays, leaving many questions left to address. It is unclear if there is direct interaction between PON2 and the dopamine receptor at the synaptic membrane, or whether it plays a role further downstream. Additionally, it is unclear if the role of PON2 is to act as an antioxidant in this pathway or plays an unidentified signaling role, as many findings in this dissertation support a non-antioxidant role for PON2. Where in the cell are PON2 levels increasing after dopamine receptor binding is also of interest, as there is speculation that cytosolic and mitochondrial-bound PON2 may have functional differences. Looking at more translational aspects, determining if dopaminergic neurons have impaired dopamine signaling and functional impacts in the absence of PON2 would provide evidence for a role in dopaminergic pathologies such as PD and addiction behaviors.

Building off chapter 3, where PON2 was observed to be lower in adult mice, I sought to characterize PON2 deficiency in the aging nervous system in chapter 5. While the results of this chapter are preliminary and many targets still need to be addressed, the findings support a lack of oxidative stress in the aged brain with potential impacts to endogenous signaling and host immunity through a reduction in cytokine expression. Furthermore, transcripts of glucose transporter 4, insulin receptor and tau were upregulated in PON2-def mice, while butyrylcholinesterase was significantly downregulated, potentially having neurodegenerative consequences that require further examination.

As with all projects, there were limitations and challenges experienced while completing this work. One of the biggest challenges lies with the mouse model, as a deficient model was utilized that has reduced, but not eliminated, expression of PON2; transcript levels measure around 30x lower and protein levels 3x lower in the deficient mice compared to WT (Chapter 3, Figure 3.5A and Chapter 4, Figure 4.1). To answer further questions about the role of PON2 with minimal ambiguity, a full knockout should be utilized going forward. It is unclear what the expression threshold for dysfunction is regarding PON2, and this threshold may be different for different cell types, tissues and pathways. It would be of interest to repeat some of the work in this dissertation with a full knockout model, particularly the behavioral and transcriptional phenotype work, to determine if the motor phenotype exacerbates and/or if the transcriptional profile changes when PON2 is entirely absent.

Furthermore, the PON2-def model in our lab was not routinely backcrossed prior to the start of this project, and certain experiments (chapter 4, chapter 5) utilized mice that had been inter-bred with their own genotype for many years. This could have resulted in an undesired strain difference, where random mutations arising in either the WT or PON2-def colonies could persist and create a difference between the genotypes other than the expression of PON2. This makes the comparison of WT and PON2-def mice difficult, as the observed differences may not be due to PON2, but an acquired mutation. This issue was corrected for other experiments (chapter 2) and mice were backcrossed and kept as heterozygotes. Future researchers should maintain all transgenic colonies as heterozygotes and use littermates when possible to eliminate colony-driven variables.

An additional challenge presented during this work was the non-specificity of commercially available PON2 antibodies. Out of 5 antibodies available, only 1 was found to be

specific to PON2 and able to detect expression differences between WT and PON2-def tissue. As many of these antibodies are polyclonal, this may present a challenge for future PON2 research, as lot-to-lot variability may influence the specificity and quality of the product. Careful validation of all antibodies used should be conducted before a study and the same lot of antibody should be utilized for as much of the work as possible.

The work presented in this dissertation has identified previously unknown pathways affected by PON2 deficiency and raises many additional questions as to the role of PON2 in the CNS. A multitude of novel directions have been revealed for future research, such as investigation of mood disorders and circadian disruptions, like those observed in shift work sleep disorder. Minimal attention has been given to behavioral studies in the PON2 field, leaving much to be learned in this area. As well, there are many mechanistic studies left to be done with PON2 in the dopaminergic system and further probing of the aging nervous system, both having implications for movement disorders and diseases of aging. It is my hope that this work has provided a foundation for future researchers to refer to when investigating PON2 in the brain, and that this work has brought us one step closer to fully understanding the function of this curious enzyme.

References

Adami, C., Sorci, G., Blasi, E., Agneletti, A. L., Bistoni, F., & Donato, R. (2001). S100B expression in and effects on microglia. *Glia*, *33*(2), 131–142.

Alexa, A., Rahnenführer, J., & Lengauer, T. (2006). Improved scoring of functional groups from gene expression data by decorrelating GO graph structure. *Bioinformatics (Oxford, England)*, *22*(13), 1600–1607.

Aliev, G., Priyadarshini, M., Reddy, V. P., Grieg, N. H., Kaminsky, Y., Cacabelos, R., Ashraf, G. M., Jabir, N. R., Kamal, M. A., Nikolenko, V. N., Zamyatnin, A. A., Benberin, V. V., & Bachurin, S. O. (2014). Oxidative stress mediated mitochondrial and vascular lesions as markers in the pathogenesis of Alzheimer disease. *Current Medicinal Chemistry*, *21*(19), 2208–2217.

Altenhöfer, S., Witte, I., Teiber, J. F., Wilgenbus, P., Pautz, A., Li, H., Daiber, A., Witan, H., Clement, A. M., Förstermann, U., & Horke, S. (2010). One enzyme, two functions: PON2 prevents mitochondrial superoxide formation and apoptosis independent from its lactonase activity. *The Journal of Biological Chemistry*, *285*(32), 24398–24403.

Alzheimer's Association. (2019). *FDA-approved treatments for Alzheimer's*. www.alz.org. https://www.alz.org/media/documents/fda-approved-treatments-alzheimers-ts.pdf

Andrews, A. G., Dysko, R. C., Spilman, S. C., Kunkel, R. G., Brammer, D. W., & Johnson, K. J. (1994). Immune complex vasculitis with secondary ulcerative dermatitis in aged C57BL/6NNia mice. *Veterinary Pathology*, *31*(3), 293–300.

Anisimova, A. S., Alexandrov, A. I., Makarova, N. E., Gladyshev, V. N., & Dmitriev, S. E. (2018). Protein synthesis and quality control in aging. *Aging*, *10*(12), 4269–4288.

Aryal, R. P., Kwak, P. B., Tamayo, A. G., Gebert, M., Chiu, P.-L., Walz, T., & Weitz, C. J. (2017). Macromolecular assemblies of the mammalian circadian clock. *Molecular Cell*, *67*(5), 770-782.e6.

Asmat, U., Abad, K., & Ismail, K. (2016). Diabetes mellitus and oxidative stress—A concise review. *Saudi Pharmaceutical Journal*, *24*(5), 547–553.

Bacchetti, T., Salvolini, E., Pompei, V., Campagna, R., Molinelli, E., Brisigotti, V., Togni, L., Lucarini, G., Sartini, D., Campanati, A., Mattioli-Belmonte, M., Rubini, C., Ferretti, G., Offidani, A., & Emanuelli, M. (2020). Paraoxonase-2: A potential biomarker for skin cancer aggressiveness. *European Journal of Clinical Investigation*, e13452.

Bacchetti, T., Sartini, D., Pozzi, V., Cacciamani, T., Ferretti, G., & Emanuelli, M. (2017). Exploring the role of paraoxonase-2 in bladder cancer: Analyses performed on tissue samples, urines and cell cultures. *Oncotarget*, *8*(17), 28785–28795.

Bangasser, D. A., & Valentino, R. J. (2014). Sex differences in stress-related psychiatric disorders: Neurobiological perspectives. *Frontiers in Neuroendocrinology*, *35*(3), 303–319.

Bar-Rogovsky, H., Hugenmatter, A., & Tawfik, D. S. (2013). The Evolutionary Origins of Detoxifying Enzymes: THE MAMMALIAN SERUM PARAOXONASES (PONs) RELATE TO BACTERIAL HOMOSERINE LACTONASES*. Journal of Biological Chemistry, 288(33), 23914–23927.

Blesa, J., Trigo-Damas, I., Quiroga-Varela, A., & Jackson-Lewis, V. R. (2015). Oxidative stress and Parkinson's disease. *Frontiers in Neuroanatomy*, *9*, 91.

Bourquard, N., Ng, C. J., & Reddy, S. T. (2011). Impaired hepatic insulin signalling in PON2-deficient mice: A novel role for the PON2/apoE axis on the macrophage inflammatory response. *The Biochemical Journal*, *436*(1), 91–100.

Bowen, D. M., Smith, C. B., White, P., & Davison, A. N. (1976). Neurotransmitter-related enzymes and indices of hypoxia in senile dementia and other abiotrophies. *Brain: A Journal of Neurology*, *99*(3), 459–496.

Branca, J. J. V., Pacini, A., Gulisano, M., Taddei, N., Fiorillo, C., & Becatti, M. (2020). Cadmium-Induced Cytotoxicity: Effects on Mitochondrial Electron Transport Chain. *Frontiers in Cell and Developmental Biology*, *8*, 1428.

Bruckner, J. V. (2000). Differences in Sensitivity of Children and Adults to Chemical Toxicity: The NAS Panel Report. *Regulatory Toxicology and Pharmacology*, *31*(3), 280–285.

Caligioni, C. S. (2009). Assessing reproductive status/stages in mice. *Current Protocols in Neuroscience, Appendix 4*, Appendix 4I.

Chen, Q., Reis, S. E., Kammerer, C. M., McNamara, D. M., Holubkov, R., Sharaf, B. L., Sopko, G., Pauly, D. F., Merz, C. N. B., Kamboh, M. I., & WISE Study Group. (2003). Association between the severity of angiographic coronary artery disease and paraoxonase gene polymorphisms in the National Heart, Lung, and Blood Institute-sponsored Women's Ischemia Syndrome Evaluation (WISE) study. *American Journal of Human Genetics*, *72*(1), 13–22.

Chen, S., Ren, Q., Zhang, J., Ye, Y., Zhang, Z., Xu, Y., Guo, M., Ji, H., Xu, C., Gu, C., Gao, W., Huang, S., & Chen, L. (2014). N-acetyl-L-cysteine protects against cadmium-induced neuronal apoptosis by inhibiting ROS-dependent activation of Akt/mTOR pathway in mouse brain. *Neuropathology and Applied Neurobiology*, *40*(6), 759–777.

Cheng, X., & Klaassen, C. D. (2012). Hormonal and chemical regulation of paraoxonases in mice. *The Journal of Pharmacology and Experimental Therapeutics*, *342*(3), 688–695.

Chin-Chan, M., Navarro-Yepes, J., & Quintanilla-Vega, B. (2015). Environmental pollutants as risk factors for neurodegenerative disorders: Alzheimer and Parkinson diseases. *Frontiers in Cellular Neuroscience*, *9*.

Chistiakov, D. A., Killingsworth, M. C., Myasoedova, V. A., Orekhov, A. N., & Bobryshev, Y. V. (2017). CD68/macrosialin: Not just a histochemical marker. *Laboratory Investigation; a Journal of Technical Methods and Pathology*, *97*(1), 4–13.

Cole, T. B., Jampsa, R. L., Walter, B. J., Arndt, T. L., Richter, R. J., Shih, D. M., Tward, A., Lusis, A. J., Jack, R. M., Costa, L. G., & Furlong, C. E. (2003). Expression of human paraoxonase (PON1) during development. *Pharmacogenetics*, *13*(6), 357–364.

Costa, L. G., Tait, L., de Laat, R., Dao, K., Giordano, G., Pellacani, C., Cole, T. B., & Furlong, C. E. (2013). Modulation of paraoxonase 2 (PON2) in mouse brain by the polyphenol quercetin: A mechanism of neuroprotection? *Neurochemical Research*, *38*(9), 1809–1818.

Danysz, W., & Parsons, C. G. (2012). Alzheimer's disease, β-amyloid, glutamate, NMDA receptors and memantine—Searching for the connections. *British Journal of Pharmacology*, *167*(2), 324–352.

Darvesh, S. (2016). Butyrylcholinesterase as a Diagnostic and Therapeutic Target for Alzheimer's Disease. *Current Alzheimer Research*, *13*(10), 1173–1177.

Dasgupta, S., Demirci, F. Y., Dressen, A. S., Kao, A. H., Rhew, E. Y., Ramsey-Goldman, R., Manzi, S., Kammerer, C. M., & Kamboh, M. I. (2011). Association analysis of PON2 genetic variants with serum paraoxonase activity and systemic lupus erythematosus. *BMC Medical Genetics*, *12*(1), 7.

D'Autréaux, B., & Toledano, M. B. (2007). ROS as signalling molecules: Mechanisms that generate specificity in ROS homeostasis. *Nature Reviews. Molecular Cell Biology*, *8*(10), 813–824.

Deakin, S., Leviev, I., Gomaraschi, M., Calabresi, L., Franceschini, G., & James, R. W. (2002). Enzymatically active paraoxonase-1 is located at the external membrane of producing cells and released by a high affinity, saturable, desorption mechanism. *The Journal of Biological Chemistry*, *277*(6), 4301–4308.

Deavall, D. G., Martin, E. A., Horner, J. M., & Roberts, R. (2012). Drug-Induced Oxidative Stress and Toxicity. *Journal of Toxicology*, *2012*, 645460.

DeTure, M. A., & Dickson, D. W. (2019). The neuropathological diagnosis of Alzheimer's disease. *Molecular Neurodegeneration*, *14*(1), 32.

Devarajan, A., Bourquard, N., Grijalva, V. R., Gao, F., Ganapathy, E., Verma, J., & Reddy, S. T. (2013). Role of PON2 in innate immune response in an acute infection model. *Molecular Genetics and Metabolism*, *110*(3), 362–370.

Devarajan, A., Bourquard, N., Hama, S., Navab, M., Grijalva, V. R., Morvardi, S., Clarke, C. F., Vergnes, L., Reue, K., Teiber, J. F., & Reddy, S. T. (2011). Paraoxonase 2 Deficiency Alters

Mitochondrial Function and Exacerbates the Development of Atherosclerosis. *Antioxidants & Redox Signaling*, *14*(3), 341–351.

Devarajan, A., Su, F., Grijalva, V., Yalamanchi, M., Yalamanchi, A., Gao, F., Trost, H., Nwokedi, J., Farias-Eisner, G., Farias-Eisner, R., Fogelman, A. M., & Reddy, S. T. (2018). Paraoxonase 2 overexpression inhibits tumor development in a mouse model of ovarian cancer. *Cell Death & Disease*, *9*(3), 392.

Di Dalmazi, G., Hirshberg, J., Lyle, D., Freij, J. B., & Caturegli, P. (2016). Reactive oxygen species in organ-specific autoimmunity. *Auto- Immunity Highlights*, *7*(1), 11.

Donato, M., Xu, Z., Tomoiaga, A., Granneman, J. G., MacKenzie, R. G., Bao, R., Than, N. G., Westfall, P. H., Romero, R., & Draghici, S. (2013). Analysis and correction of crosstalk effects in pathway analysis. *Genome Research*, *23*(11), 1885–1893.

Draganov, D. I., & La Du, B. N. (2004). Pharmacogenetics of paraoxonases: A brief review. *Naunyn-Schmiedeberg's Archives of Pharmacology*, *369*(1), 78–88.

Draganov, Dragomir I., Teiber, J. F., Speelman, A., Osawa, Y., Sunahara, R., & La Du, B. N. (2005). Human paraoxonases (PON1, PON2, and PON3) are lactonases with overlapping and distinct substrate specificities. *Journal of Lipid Research*, *46*(6), 1239–1247.

Duarte-Vogel, S. M., & Lawson, G. W. (2011). Association between Hair-Induced Oronasal Inflammation and Ulcerative Dermatitis in C57BL/6 Mice. *Comparative Medicine*, *61*(1), 13–19.

Elbaz, A., Dufouil, C., & Alpérovitch, A. (2007). Interaction between genes and environment in neurodegenerative diseases. *Comptes Rendus Biologies*, *330*(4), 318–328.

Erikson, K. M., & Aschner, M. (2003). Manganese neurotoxicity and glutamate-GABA interaction. *Glutamine, Glutamate and GABA in the CNS: Transport and Metabolism in Health and Disease*, *43*(4), 475–480.

Filiano, A. J., Xu, Y., Tustison, N. J., Marsh, R. L., Baker, W., Smirnov, I., Overall, C. C., Gadani, S. P., Turner, S. D., Weng, Z., Peerzade, S. N., Chen, H., Lee, K. S., Scott, M. M., Beenhakker, M. P., Litvak, V., & Kipnis, J. (2016). Unexpected role of interferon-γ in regulating neuronal connectivity and social behavior. *Nature*, *535*(7612), 425–429.

Fortunato, G., Di Taranto, M. D., Bracale, U. M., Del Guercio, L., Carbone, F., Mazzaccara, C., Morgante, A., D'Armiento, F. P., D'Armiento, M., Porcellini, M., Sacchetti, L., Bracale, G., & Salvatore, F. (2008). Decreased paraoxonase-2 expression in human carotids during the progression of atherosclerosis. *Arteriosclerosis, Thrombosis, and Vascular Biology*, *28*(3), 594–600.

Furlong, C. E. (2007). Genetic variability in the cytochrome P450-paraoxonase 1 (PON1) pathway for detoxication of organophosphorus compounds. *Journal of Biochemical and Molecular Toxicology*, *21*(4), 197–205.

Furlong, C. E., Holland, N., Richter, R. J., Bradman, A., Ho, A., & Eskenazi, B. (2006). PON1 status of farmworker mothers and children as a predictor of organophosphate sensitivity. *Pharmacogenetics and Genomics*, *16*(3), 183–190.

Furlong, C. E., Marsillach, J., Jarvik, G. P., & Costa, L. G. (2016). Paraoxonases-1, -2 and -3: What are their functions? *Chemico-Biological Interactions*, *259*(Pt B), 51–62.

Gaki, G. S., & Papavassiliou, A. G. (2014). Oxidative stress-induced signaling pathways implicated in the pathogenesis of Parkinson's disease. *Neuromolecular Medicine*, *16*(2), 217–230.

Garrick, J. M., Dao, K., de Laat, R., Elsworth, J., Cole, T. B., Marsillach, J., Furlong, C. E., & Costa, L. G. (2016). Developmental expression of paraoxonase 2. *Chemico-Biological Interactions*, *259*(Pt B), 168–174.

Gery, S., Komatsu, N., Baldjyan, L., Yu, A., Koo, D., & Koeffler, H. P. (2006). The Circadian Gene Per1 Plays an Important Role in Cell Growth and DNA Damage Control in Human Cancer Cells. *Molecular Cell*, *22*(3), 375–382.

Geula, C., & Darvesh, S. (2004). Butyrylcholinesterase, cholinergic neurotransmission and the pathology of Alzheimer's disease. *Drugs of Today (Barcelona, Spain: 1998)*, *40*(8), 711–721.

Giordano, G., Tait, L., Furlong, C. E., Cole, T. B., Kavanagh, T. J., & Costa, L. G. (2013a). Gender differences in brain susceptibility to oxidative stress are mediated by levels of paraoxonase-2 expression. *Free Radical Biology & Medicine*, *58*, 98–108.

Giordano, G., Tait, L., Furlong, C. E., Cole, T. B., Kavanagh, T. J., & Costa, L. G. (2013b). GENDER DIFFERENCES IN BRAIN SUSCEPTIBILITY TO OXIDATIVE STRESS ARE MEDIATED BY LEVELS OF PARAOXONASE-2 (PON2) EXPRESSION. *Free Radical Biology & Medicine*, *58*, 98–108.

Giordano, G., White, C. C., McConnachie, L. A., Fernandez, C., Kavanagh, T. J., & Costa, L. G. (2006). Neurotoxicity of Domoic Acid in Cerebellar Granule Neurons in a Genetic Model of Glutathione Deficiency. *Molecular Pharmacology*, *70*(6), 2116.

Giordano, Gennaro, Cole, T. B., Furlong, C. E., & Costa, L. G. (2011). Paraoxonase 2 (PON2) in the mouse central nervous system: A neuroprotective role? *Toxicology and Applied Pharmacology*, *256*(3), 369–378.

Gochfeld, M. (2017). Sex Differences in Human and Animal Toxicology: Toxicokinetics. *Toxicologic Pathology*, *45*(1), 172–189.

Grosch, J., Winkler, J., & Kohl, Z. (2016). Early Degeneration of Both Dopaminergic and Serotonergic Axons – A Common Mechanism in Parkinson's Disease. *Frontiers in Cellular Neuroscience*, *10*.

Gu, L., Cui, T., Fan, C., Zhao, H., Zhao, C., Lu, L., & Yang, H. (2009). Involvement of ERK1/2 signaling pathway in DJ-1-induced neuroprotection against oxidative stress. *Biochemical and Biophysical Research Communications*, *383*(4), 469–474.

Hagmann, H., Kuczkowski, A., Ruehl, M., Lamkemeyer, T., Brodesser, S., Horke, S., Dryer, S., Schermer, B., Benzing, T., & Brinkkoetter, P. T. (2014). Breaking the chain at the membrane: Paraoxonase 2 counteracts lipid peroxidation at the plasma membrane. *The FASEB Journal*, *28*(4), 1769–1779.

Hampton, A. L., Hish, G. A., Aslam, M. N., Rothman, E. D., Bergin, I. L., Patterson, K. A., Naik, M., Paruchuri, T., Varani, J., & Rush, H. G. (2012). Progression of Ulcerative Dermatitis Lesions in C57BL/6Crl Mice and the Development of a Scoring System for Dermatitis Lesions. *Journal of the American Association for Laboratory Animal Science : JAALAS*, *51*(5), 586–593.

Harris, R. C., & Zhang, M.-Z. (2012). Dopamine, the kidney, and hypertension. *Current Hypertension Reports*, *14*(2), 138–143.

Harrison, D. G., & Gongora, M. C. (2009). Oxidative stress and hypertension. *The Medical Clinics of North America*, *93*(3), 621–635.

Hershey, J. W. B., Sonenberg, N., & Mathews, M. B. (2012). Principles of translational control: An overview. *Cold Spring Harbor Perspectives in Biology*, *4*(12), a011528.

Higgins, G. C., Beart, P. M., Shin, Y. S., Chen, M. J., Cheung, N. S., & Nagley, P. (2010). Oxidative stress: Emerging mitochondrial and cellular themes and variations in neuronal injury. *Journal of Alzheimer's Disease: JAD*, *20 Suppl 2*, S453-473.

Horke, S., Witte, I., Altenhöfer, S., Wilgenbus, P., Goldeck, M., Förstermann, U., Xiao, J., Kramer, G. L., Haines, D. C., Chowdhary, P. K., Haley, R. W., & Teiber, J. F. (2010). Paraoxonase 2 is down-regulated by the Pseudomonas aeruginosa quorumsensing signal N-(3-oxododecanoyl)-L-homoserine lactone and attenuates oxidative stress induced by pyocyanin. *The Biochemical Journal*, *426*(1), 73–83.

Horke, S., Witte, I., Wilgenbus, P., Krüger, M., Strand, D., & Förstermann, U. (2007). Paraoxonase-2 reduces oxidative stress in vascular cells and decreases endoplasmic reticulum stress-induced caspase activation. *Circulation*, *115*(15), 2055–2064.

Inden, M., Taira, T., Kitamura, Y., Yanagida, T., Tsuchiya, D., Takata, K., Yanagisawa, D., Nishimura, K., Taniguchi, T., Kiso, Y., Yoshimoto, K., Agatsuma, T., Koide-Yoshida, S., Iguchi-Ariga, S. M. M., Shimohama, S., & Ariga, H. (2006). PARK7 DJ-1 protects against degeneration of nigral dopaminergic neurons in Parkinson's disease rat model. *Neurobiology of Disease*, *24*(1), 144–158.

Issitt, T., Bosseboeuf, E., De Winter, N., Dufton, N., Gestri, G., Senatore, V., Chikh, A., Randi, A. M., & Raimondi, C. (2019). Neuropilin-1 Controls Endothelial Homeostasis by Regulating Mitochondrial Function and Iron-Dependent Oxidative Stress. *IScience*, *11*, 205–223.

Janka, Z., Juhász, A., Rimanóczy A, A., Boda, K., Márki-Zay, J., & Kálmán, J. (2002). Codon 311 (Cys—> Ser) polymorphism of paraoxonase-2 gene is associated with apolipoprotein E4 allele in both Alzheimer's and vascular dementias. *Molecular Psychiatry*, *7*(1), 110–112.

Juhas, M., Eberl, L., & Tümmler, B. (2005). Quorum sensing: The power of cooperation in the world of Pseudomonas. *Environmental Microbiology*, *7*(4), 459–471.

Kamboh, M. I., Minster, R. L., Kenney, M., Ozturk, A., Desai, P. P., Kammerer, C. M., & DeKosky, S. T. (2006). Alpha-1-antichymotrypsin (ACT or SERPINA3) polymorphism may affect age-at-onset and disease duration of Alzheimer's disease. *Neurobiology of Aging*, *27*(10), 1435–1439.

Kaplan, D. H., Shankaran, V., Dighe, A. S., Stockert, E., Aguet, M., Old, L. J., & Schreiber, R. D. (1998). Demonstration of an interferon gamma-dependent tumor surveillance system in immunocompetent mice. *Proceedings of the National Academy of Sciences of the United States of America*, *95*(13), 7556–7561.

Kastenmayer, R. J., Fain, M. A., & Perdue, K. A. (2006). A retrospective study of idiopathic ulcerative dermatitis in mice with a C57BL/6 background. *Journal of the American Association for Laboratory Animal Science: JAALAS*, *45*(6), 8–12.

Kehrer, J. P., & Klotz, L.-O. (2015). Free radicals and related reactive species as mediators of tissue injury and disease: Implications for Health. *Critical Reviews in Toxicology*, *45*(9), 765–798.

Kellendonk, C., Simpson, E. H., Polan, H. J., Malleret, G., Vronskaya, S., Winiger, V., Moore, H., & Kandel, E. R. (2006). Transient and Selective Overexpression of Dopamine D2 Receptors in the Striatum Causes Persistent Abnormalities in Prefrontal Cortex Functioning. *Neuron*, *49*(4), 603–615.

Khan, J. Y., & Black, S. M. (2003). Developmental changes in murine brain antioxidant enzymes. *Pediatric Research*, *54*(1), 77–82.

Khan, Z., & Ali, S. A. (2018). Oxidative stress-related biomarkers in Parkinson's disease: A systematic review and meta-analysis. *Iranian Journal of Neurology*, *17*(3), 137–144.

Kiaei, M. (2013). New hopes and challenges for treatment of neurodegenerative disorders: Great opportunities for young neuroscientists. *Basic and Clinical Neuroscience*, *4*(1), 3–4.

Kim, G. H., Kim, J. E., Rhie, S. J., & Yoon, S. (2015). The Role of Oxidative Stress in Neurodegenerative Diseases. *Experimental Neurobiology*, *24*(4), 325–340.

Klein, C., & Westenberger, A. (2012). Genetics of Parkinson's Disease. *Cold Spring Harbor Perspectives in Medicine*, *2*(1).

Klepper, J. (2008). Glucose transporter deficiency syndrome (GLUT1DS) and the ketogenic diet. *Epilepsia*, *49*(s8), 46–49.

Klimkowicz-Mrowiec, A., Marona, M., Wolkow, P., Witkowski, A., Maruszak, A., Styczynska, M., Barcikowska, M., Szczudlik, A., & Slowik, A. (2011). Paraoxonase gene polymorphism and the risk for Alzheimer's disease in the polish population. *Dementia and Geriatric Cognitive Disorders*, *31*(6), 417–423.

Koepsell, H. (2020). Glucose transporters in brain in health and disease. *Pflugers Archiv : European Journal of Physiology*, *472*(9), 1299–1343.

Krüger, M., Amort, J., Wilgenbus, P., Helmstädter, J. P., Grechowa, I., Ebert, J., Tenzer, S., Moergel, M., Witte, I., & Horke, S. (2016). The anti-apoptotic PON2 protein is Wnt/β-catenin-regulated and correlates with radiotherapy resistance in OSCC patients. *Oncotarget*, *7*(32), 51082–51095.

Krüger, M., Pabst, A. M., Al-Nawas, B., Horke, S., & Moergel, M. (2015). Paraoxonase-2 (PON2) protects oral squamous cell cancer cells against irradiation-induced apoptosis. *Journal of Cancer Research and Clinical Oncology*, *141*(10), 1757–1766.

Kulkarni, A., Ganesan, P., & O'Donnell, L. A. (2016). Interferon Gamma: Influence on Neural Stem Cell Function in Neurodegenerative and Neuroinflammatory Disease. *Clinical Medicine Insights. Pathology*, *9*(Suppl 1), 9–19.

Kumari, S., Badana, A. K., G, M. M., G, S., & Malla, R. (2018). Reactive Oxygen Species: A Key Constituent in Cancer Survival. *Biomarker Insights*, *13*, 1177271918755391–1177271918755391.

Landriscina, M., Maddalena, F., Laudiero, G., & Esposito, F. (2009). Adaptation to oxidative stress, chemoresistance, and cell survival. *Antioxidants & Redox Signaling*, *11*(11), 2701–2716.

Law, C. W., Chen, Y., Shi, W., & Smyth, G. K. (2014). voom: Precision weights unlock linear model analysis tools for RNA-seq read counts. Genome biology, 15(2), R29.

Leduc, V., Legault, V., Dea, D., & Poirier, J. (2011). Normalization of gene expression using SYBR green qPCR: A case for paraoxonase 1 and 2 in Alzheimer's disease brains. *Journal of Neuroscience Methods*, *200*(1), 14–19.

Lee, S.-H., Zabolotny, J. M., Huang, H., Lee, H., & Kim, Y.-B. (2016). Insulin in the nervous system and the mind: Functions in metabolism, memory, and mood. *Molecular Metabolism*, *5*(8), 589–601.

Levy, E., Trudel, K., Bendayan, M., Seidman, E., Delvin, E., Elchebly, M., Lavoie, J.-C., Precourt, L.-P., Amre, D., & Sinnett, D. (2007). Biological role, protein expression, subcellular localization, and oxidative stress response of paraoxonase 2 in the intestine of humans and rats. *American Journal of Physiology. Gastrointestinal and Liver Physiology*, *293*(6), G1252-1261.

Li, B., Xia, M., Zorec, R., Parpura, V., & Verkhratsky, A. (2021). Astrocytes in Heavy Metal Neurotoxicity and Neurodegeneration. *Brain Research*, 147234.

Li, B.-H., Zhang, L.-L., Yin, Y.-W., Pi, Y., Yang, Q.-W., Gao, C.-Y., Fang, C.-Q., Wang, J.-Z., & Li, J.-C. (2012). Association between paraoxonase 2 Ser311Cys polymorphism and ischemic stroke risk: A meta-analysis involving 5,008 subjects. *Molecular Biology Reports*, *39*(5), 5623–5630.

Li, W. F., Matthews, C., Disteche, C. M., Costa, L. G., & Furlong, C. E. (1997). Paraoxonase (PON1) gene in mice: Sequencing, chromosomal localization and developmental expression. *Pharmacogenetics*, *7*(2), 137–144.

Li, W., Kennedy, D., Shao, Z., Wang, X., Kamdar, A. K., Weber, M., Mislick, K., Kiefer, K., Morales, R., Agatisa-Boyle, B., Shih, D. M., Reddy, S. T., Moravec, C. S., & Tang, W. H. W. (2018). Paraoxonase 2 prevents the development of heart failure. *Free Radical Biology & Medicine*, *121*, 117–126.

Lin, A. A., Tripathi, P. K., Sholl, A., Jordan, M. B., & Hildeman, D. A. (2009). Gamma interferon signaling in macrophage lineage cells regulates central nervous system inflammation and chemokine production. *Journal of Virology*, *83*(17), 8604–8615.

Liu, Y., Beyer, A., & Aebersold, R. (2016). On the Dependency of Cellular Protein Levels on mRNA Abundance. *Cell*, *165*(3), 535–550.

Liu, Z., Zhou, T., Ziegler, A. C., Dimitrion, P., & Zuo, L. (2017). Oxidative Stress in Neurodegenerative Diseases: From Molecular Mechanisms to Clinical Applications. *Oxidative Medicine and Cellular Longevity*, *2017*, 2525967.

Mackness, B., McElduff, P., & Mackness, M. I. (2005). The paraoxonase-2-310 polymorphism is associated with the presence of microvascular complications in diabetes mellitus. *Journal of Internal Medicine*, *258*(4), 363–368.

Madamanchi, N. R., Vendrov, A., & Runge, M. S. (2005). Oxidative stress and vascular disease. *Arteriosclerosis, Thrombosis, and Vascular Biology*, *25*(1), 29–38.

Maier, T., Güell, M., & Serrano, L. (2009). Correlation of mRNA and protein in complex biological samples. *FEBS Letters*, *583*(24), 3966–3973.

Marchegiani, F., Spazzafumo, L., Provinciali, M., Cardelli, M., Olivieri, F., Franceschi, C., Lattanzio, F., & Antonicelli, R. (2009). Paraoxonase2 C311S polymorphism and low levels of HDL contribute to a higher mortality risk after acute myocardial infarction in elderly patients. *Molecular Genetics and Metabolism*, *98*(3), 314–318.

Maritim, A. C., Sanders, R. A., & Watkins, J. B. (2003). Diabetes, oxidative stress, and antioxidants: A review. *Journal of Biochemical and Molecular Toxicology*, *17*(1), 24–38.

Marsillach, J., Mackness, B., Mackness, M., Riu, F., Beltrán, R., Joven, J., & Camps, J. (2008). Immunohistochemical analysis of paraoxonases-1, 2, and 3 expression in normal mouse tissues. *Free Radical Biology & Medicine*, *45*(2), 146–157.

Masri, S., & Sassone-Corsi, P. (2018). The emerging link between cancer, metabolism, and circadian rhythms. *Nature Medicine*, *24*(12), 1795–1803.

Mazon, J. N., de Mello, A. H., Ferreira, G. K., & Rezin, G. T. (2017). The impact of obesity on neurodegenerative diseases. *Life Sciences*, *182*, 22–28.

Meiser, J., Weindl, D., & Hiller, K. (2013). Complexity of dopamine metabolism. *Cell Communication and Signaling : CCS*, *11*(1), 34–34.

Milatovic, D., Gupta, R. C., Yu, Y., Zaja-Milatovic, S., & Aschner, M. (2011). Protective effects of antioxidants and anti-inflammatory agents against manganese-induced oxidative damage and neuronal injury. *Toxicology and Applied Pharmacology*, *256*(3), 219–226.

Miyazaki, I., & Asanuma, M. (2008). Dopaminergic neuron-specific oxidative stress caused by dopamine itself. *Acta Medica Okayama*, *62*(3), 141–150.

Mochizuki, H., Scherer, S. W., Xi, T., Nickle, D. C., Majer, M., Huizenga, J. J., Tsui, L. C., & Prochazka, M. (1998). Human PON2 gene at 7q21.3: Cloning, multiple mRNA forms, and missense polymorphisms in the coding sequence. *Gene*, *213*(1–2), 149–157.

Morresi, C., Cianfruglia, L., Sartini, D., Cecati, M., Fumarola, S., Emanuelli, M., Armeni, T., Ferretti, G., & Bacchetti, T. (2019). Effect of High Glucose-Induced Oxidative Stress on Paraoxonase 2 Expression and Activity in Caco-2 Cells. *Cells*, *8*(12), 1616.

Morrow, B. A., Roth, R. H., Redmond, D. E., Diano, S., & Elsworth, J. D. (2012). Susceptibility to a parkinsonian toxin varies during primate development. *Experimental Neurology*, *235*(1), 273–281.

Morrow, B. A., Roth, R. H., Redmond, D. E., & Elsworth, J. D. (2011). Impact of methamphetamine on dopamine neurons in primates is dependent on age: Implications for development of Parkinson's disease. *Neuroscience*, *189*, 277–285.

Mousa, A., & Bakhiet, M. (2013). Role of Cytokine Signaling during Nervous System Development. *International Journal of Molecular Sciences*, *14*(7), 13931–13957.

Mu, N., Xu, S. C., Chang, Q., Rao, D. P., Chen, J. P., & Ma, C. (2013). Study of lipids, insulin metabolism, and paraoxonase-2-311 polymorphism in patients with different subtypes of Alzheimer's disease (translated version). *East Asian Archives of Psychiatry: Official Journal of the Hong Kong College of Psychiatrists = Dong Ya Jing Shen Ke Xue Zhi: Xianggang Jing Shen Ke Yi Xue Yuan Qi Kan*, *23*(3), 114–119.

Nagarajan, A., Dogra, S. K., Sun, L., Gandotra, N., Ho, T., Cai, G., Cline, G., Kumar, P., Cowles, R. A., & Wajapeyee, N. (2017). Paraoxonase 2 Facilitates Pancreatic Cancer Growth and Metastasis by Stimulating GLUT1-Mediated Glucose Transport. *Molecular Cell*, *67*(4), 685-701.e6.

Neavin, D. R., Liu, D., Ray, B., & Weinshilboum, R. M. (2018). The Role of the Aryl Hydrocarbon Receptor (AHR) in Immune and Inflammatory Diseases. *International Journal of Molecular Sciences*, *19*(12).

Neuhaus, B., Niessen, C. M., Mesaros, A., Withers, D. J., Krieg, T., & Partridge, L. (2012). Experimental analysis of risk factors for ulcerative dermatitis in mice. *Experimental Dermatology*, *21*(9), 712–713.

Ng, C. J., Wadleigh, D. J., Gangopadhyay, A., Hama, S., Grijalva, V. R., Navab, M., Fogelman, A. M., & Reddy, S. T. (2001). Paraoxonase-2 is a ubiquitously expressed protein with antioxidant properties and is capable of preventing cell-mediated oxidative modification of low density lipoprotein. *The Journal of Biological Chemistry*, *276*(48), 44444–44449.

Ng, Carey J., Bourquard, N., Grijalva, V., Hama, S., Shih, D. M., Navab, M., Fogelman, A. M., Lusis, A. J., Young, S., & Reddy, S. T. (2006). Paraoxonase-2 deficiency aggravates atherosclerosis in mice despite lower apolipoprotein-B-containing lipoproteins: Anti-atherogenic role for paraoxonase-2. *The Journal of Biological Chemistry*, *281*(40), 29491–29500.

Nie, Y., Luo, D., Yang, M., Wang, Y., Xiong, L., Gao, L., Liu, Y., & Liu, H. (2017). A Meta-Analysis on the Relationship of the PON Genes and Alzheimer Disease. *Journal of Geriatric Psychiatry and Neurology*, *30*(6), 303–310.

Nyarko-Danquah, I., Pajarillo, E., Digman, A., Soliman, K. F. A., Aschner, M., & Lee, E. (2020). Manganese Accumulation in the Brain via Various Transporters and Its Neurotoxicity Mechanisms. *Molecules (Basel, Switzerland)*, *25*(24), 5880.

Ousman, S. S., Tomooka, B. H., van Noort, J. M., Wawrousek, E. F., O'Connor, K. C., Hafler, D. A., Sobel, R. A., Robinson, W. H., & Steinman, L. (2007). Protective and therapeutic role for alphaB-crystallin in autoimmune demyelination. *Nature*, *448*(7152), 474–479.

Panth, N., Paudel, K. R., & Parajuli, K. (2016). Reactive Oxygen Species: A Key Hallmark of Cardiovascular Disease. *Advances in Medicine*, *2016*, 9152732–9152732.

Park, H. R., Lee, J. M., Moon, H. E., Lee, D. S., Kim, B.-N., Kim, J., Kim, D. G., & Paek, S. H. (2016). A Short Review on the Current Understanding of Autism Spectrum Disorders. *Experimental Neurobiology*, *25*(1), 1–13.

Parsanejad, M., Bourquard, N., Qu, D., Zhang, Y., Huang, E., Rousseaux, M. W. C., Aleyasin, H., Irrcher, I., Callaghan, S., Vaillant, D. C., Kim, R. H., Slack, R. S., Mak, T. W., Reddy, S. T., Figeys, D., & Park, D. S. (2014). DJ-1 interacts with and regulates paraoxonase-2, an enzyme critical for neuronal survival in response to oxidative stress. *PloS One*, *9*(9), e106601.

Patro, R., Duggal, G., & Kingsford, C. (2015). Salmon: Accurate, Versatile and Ultrafast Quantification from RNA-seq Data using Lightweight-Alignment. *BioRxiv*, 021592.

Paulson, H. L., & Igo, I. (2011). Genetics of Dementia. *Seminars in Neurology*, *31*(5), 449–460.

Picciotto, M. R., Higley, M. J., & Mineur, Y. S. (2012). Acetylcholine as a neuromodulator: Cholinergic signaling shapes nervous system function and behavior. *Neuron*, *76*(1), 116–129.

Pizzino, G., Irrera, N., Cucinotta, M., Pallio, G., Mannino, F., Arcoraci, V., Squadrito, F., Altavilla, D., & Bitto, A. (2017). Oxidative Stress: Harms and Benefits for Human Health. *Oxidative Medicine and Cellular Longevity*, *2017*.

Primo-Parmo, S. L., Sorenson, R. C., Teiber, J., & La Du, B. N. (1996). The human serum paraoxonase/arylesterase gene (PON1) is one member of a multigene family. *Genomics*, *33*(3), 498–507.

Quiñonez-Flores, C. M., González-Chávez, S. A., Del Río Nájera, D., & Pacheco-Tena, C. (2016). Oxidative Stress Relevance in the Pathogenesis of the Rheumatoid Arthritis: A Systematic Review. *BioMed Research International*, *2016*.

Qujeq, D., Mahrooz, A., Alizadeh, A., & Boorank, R. (2018). Paraoxonase-2 variants potentially influence insulin resistance, beta-cell function, and their interrelationships with alanine aminotransferase in type 2 diabetes. *Journal of Research in Medical Sciences : The Official Journal of Isfahan University of Medical Sciences*, *23*, 107.

Reddy, S. T., Wadleigh, D. J., Grijalva, V., Ng, C., Hama, S., Gangopadhyay, A., Shih, D. M., Lusis, A. J., Navab, M., & Fogelman, A. M. (2001). Human paraoxonase-3 is an HDL-associated enzyme with biological activity similar to paraoxonase-1 protein but is not regulated by oxidized lipids. *Arteriosclerosis, Thrombosis, and Vascular Biology*, *21*(4), 542–547.

Ripperger, J. A., Jud, C., & Albrecht, U. (2011). The daily rhythm of mice. *Circadian Rhythms*, *585*(10), 1384–1392.

Roels, H. A., Bowler, R. M., Kim, Y., Henn, B. C., Mergler, D., Hoet, P., Gocheva, V. V., Bellinger, D. C., Wright, R. O., Harris, M. G., Chang, Y., Bouchard, M. F., Riojas-Rodriguez, H., Menezes-Filho, J. A., & Téllez-Rojo, M. M. (2012). Manganese exposure and cognitive deficits: A growing concern for manganese neurotoxicity. *Neurotoxicology*, *33*(4).

Rosenblat, M., Coleman, R., Reddy, S. T., & Aviram, M. (2009). Paraoxonase 2 attenuates macrophage triglyceride accumulation via inhibition of diacylglycerol acyltransferase 1. *Journal of Lipid Research*, *50*(5), 870–879.

Rothem, L., Hartman, C., Dahan, A., Lachter, J., Eliakim, R., & Shamir, R. (2007). Paraoxonases are associated with intestinal inflammatory diseases and intracellularly localized to the endoplasmic reticulum. *Free Radical Biology & Medicine*, *43*(5), 730–739.

Sanders, A. P., Henn, B. C., & Wright, R. O. (2015). Perinatal and Childhood Exposure to Cadmium, Manganese, and Metal Mixtures and Effects on Cognition and Behavior: A Review of Recent Literature. *Current Environmental Health Reports*, *2*(3), 284–294.

Sayre, L. M., Perry, G., & Smith, M. A. (2008). Oxidative Stress and Neurotoxicity. *Chemical Research in Toxicology*, *21*(1), 172–188.

Scheuplein, R., Charnley, G., & Dourson, M. (2002). Differential Sensitivity of Children and Adults to Chemical Toxicity: I. Biological Basis. *Regulatory Toxicology and Pharmacology*, *35*(3), 429–447.

Semple, B. D., Blomgren, K., Gimlin, K., Ferriero, D. M., & Noble-Haeusslein, L. J. (2013). Brain development in rodents and humans: Identifying benchmarks of maturation and vulnerability to injury across species. *Progress in Neurobiology*, *0*, 1–16.

Seol, W., Choi, H.-S., & Moore, D. D. (1996). An Orphan Nuclear Hormone Receptor That Lacks a DNA Binding Domain and Heterodimerizes with Other Receptors. *Science*, *272*(5266), 1336.

Shah, K., DeSilva, S., & Abbruscato, T. (2012). The Role of Glucose Transporters in Brain Disease: Diabetes and Alzheimer's Disease. *International Journal of Molecular Sciences*, *13*(10), 12629–12655.

Shakhparonov, M. I., Antipova, N. V., Shender, V. O., Shnaider, P. V., Arapidi, G. P., Pestov, N. B., & Pavlyukov, M. S. (2018). Expression and Intracellular Localization of Paraoxonase 2 in Different Types of Malignancies. *Acta Naturae*, *10*(3), 92–99.

Shao, W., Zhang, S., Tang, M., Zhang, X., Zhou, Z., Yin, Y., Zhou, Q., Huang, Y., Liu, Y., Wawrousek, E., Chen, T., Li, S., Xu, M., Zhou, J., Hu, G., & Zhou, J. (2013). Suppression of neuroinflammation by astrocytic dopamine D2 receptors via αB-crystallin. *Nature*, *494*(7435), 90–94.

Schroder, K., Hertzog, P. J., Ravasi, T., & Hume, D. A. (2004). Interferon-γ: An overview of signals, mechanisms and functions. *Journal of Leukocyte Biology*, *75*(2), 163–189.

Shi, J., Zhang, S., Tang, M., Liu, X., Li, T., Han, H., Wang, Y., Guo, Y., Zhao, J., Li, H., & Ma, C. (2004). Possible association between Cys311Ser polymorphism of paraoxonase 2 gene and late-onset Alzheimer's disease in Chinese. *Brain Research. Molecular Brain Research*, *120*(2), 201–204.

Shih, D. M., & Lusis, A. J. (2009). The roles of PON1 and PON2 in cardiovascular disease and innate immunity. *Current Opinion in Lipidology*, *20*(4).

Shih, D. M., Meng, Y., Sallam, T., Vergnes, L., Shu, M. L., Reue, K., Tontonoz, P., Fogelman, A. M., Lusis, A. J., & Reddy, S. T. (2019). PON2 Deficiency Leads to Increased Susceptibility to Diet-Induced Obesity. *Antioxidants (Basel, Switzerland)*, *8*(1), Article 1.

Shih, D. M., Xia, Y.-R., Yu, J. M., & Lusis, A. J. (2010). Temporal and tissue-specific patterns of Pon3 expression in mouse: In situ hybridization analysis. *Advances in Experimental Medicine and Biology*, *660*, 73–87.

Sica, A., Dorman, L., Viggiano, V., Cippitelli, M., Ghosh, P., Rice, N., & Young, H. A. (1997). Interaction of NF-κB and NFAT with the Interferon-γ Promoter *. *Journal of Biological Chemistry*, *272*(48), 30412–30420.

Sidoryk-Wegrzynowicz, M., & Aschner, M. (2013). Manganese toxicity in the central nervous system: The glutamine/glutamate-γ-aminobutyric acid cycle. *Journal of Internal Medicine*, *273*(5), 466–477.

Soneson, C., Love, M. I., & Robinson, M. D. (2015). Differential analyses for RNA-seq: Transcript-level estimates improve gene-level inferences. *F1000Research*, *4*, 1521.

Sorenson, R. C., Primo-Parmo, S. L., Camper, S. A., & La Du, B. N. (1995). The genetic mapping and gene structure of mouse paraoxonase/arylesterase. *Genomics*, *30*(3), 431–438.

Spijker, S. (2011). *Dissection of Rodent Brain Regions* (Vol. 57, pp. 13–26).

Spires, T. L., & Hannan, A. J. (2005). Nature, nurture and neurology: Gene–environment interactions in neurodegenerative disease. *The FEBS Journal*, *272*(10), 2347–2361.

Starr, R., Fuchsberger, M., Lau, L. S., Uldrich, A. P., Goradia, A., Willson, T. A., Verhagen, A. M., Alexander, W. S., & Smyth, M. J. (2009). SOCS-1 Binding to Tyrosine 441 of IFN-γ Receptor Subunit 1 Contributes to the Attenuation of IFN-γ Signaling In Vivo. *The Journal of Immunology*, *183*(7), 4537–4544.

Stoltz, D. A., Ozer, E. A., Ng, C. J., Yu, J. M., Reddy, S. T., Lusis, A. J., Bourquard, N., Parsek, M. R., Zabner, J., & Shih, D. M. (2007). Paraoxonase-2 deficiency enhances Pseudomonas aeruginosa quorum sensing in murine tracheal epithelia. *American Journal of Physiology. Lung Cellular and Molecular Physiology*, *292*(4), L852-860.

Stoltz, D. A., Ozer, E. A., Recker, T. J., Estin, M., Yang, X., Shih, D. M., Lusis, A. J., & Zabner, J. (2009). A common mutation in paraoxonase-2 results in impaired lactonase activity. *The Journal of Biological Chemistry*, *284*(51), 35564–35571.

Sulaiman, D., Li, J., Devarajan, A., Cunningham, C. M., Li, M., Fishbein, G. A., Fogelman, A. M., Eghbali, M., & Reddy, S. T. (2019). Paraoxonase 2 protects against acute myocardial ischemia-reperfusion injury by modulating mitochondrial function and oxidative stress via the PI3K/Akt/GSK-3β RISK pathway. *Journal of Molecular and Cellular Cardiology*, *129*, 154–164.

Sundberg, J. P., Taylor, D., Lorch, G., Miller, J., Silva, K. A., Sundberg, B. A., Roopenian, D., Sperling, L., Ong, D., King, L. E., & Everts, H. (2011). Primary Follicular Dystrophy with Scarring Dermatitis in C57BL/6 Mouse Substrains Resembles Central Centrifugal Cicatricial Alopecia in Humans. *Veterinary Pathology*, *48*(2), 513–524.

Teiber, J. F., Horke, S., Haines, D. C., Chowdhary, P. K., Xiao, J., Kramer, G. L., Haley, R. W., & Draganov, D. I. (2008). Dominant role of paraoxonases in inactivation of the Pseudomonas

aeruginosa quorum-sensing signal N-(3-oxododecanoyl)-L-homoserine lactone. *Infection and Immunity*, *76*(6), 2512–2519.

Teiber, J. F., Xiao, J., Kramer, G. L., Ogawa, S., Ebner, C., Wolleb, H., Carreira, E. M., Shih, D. M., & Haley, R. W. (2018). Identification of biologically active δ-lactone eicosanoids as paraoxonase substrates. *Biochemical and Biophysical Research Communications*, *505*(1), 87–92.

Thanan, R., Oikawa, S., Hiraku, Y., Ohnishi, S., Ma, N., Pinlaor, S., Yongvanit, P., Kawanishi, S., & Murata, M. (2014). Oxidative stress and its significant roles in neurodegenerative diseases and cancer. *International Journal of Molecular Sciences*, *16*(1), 193–217.

Turturro, A., Duffy, P., Hass, B., Kodell, R., & Hart, R. (2002). Survival Characteristics and Age-Adjusted Disease Incidences in C57BL/6 Mice Fed a Commonly Used Cereal-Based Diet Modulated by Dietary Restriction. *The Journals of Gerontology: Series A*, *57*(11), B379–B389.

Ullah, M. F., Ahmad, A., Bhat, S. H., Abu-Duhier, F. M., Barreto, G. E., & Ashraf, G. M. (2019). Impact of sex differences and gender specificity on behavioral characteristics and pathophysiology of neurodegenerative disorders. *Neuroscience & Biobehavioral Reviews*, *102*, 95–105.

United Nations Department of Economic and Social Affairs Population Division. (2015). *World Population Ageing 2015*. Report ST/ESA/SER.A/390.

Varçin, M., Bentea, E., Michotte, Y., & Sarre, S. (2012). Oxidative stress in genetic mouse models of Parkinson's disease. *Oxidative Medicine and Cellular Longevity*, *2012*, 624925–624925.

Vega, A., Martinot, E., Baptissart, M., De Haze, A., Saru, J.-P., Baron, S., Caira, F., Schoonjans, K., Lobaccaro, J.-M. A., & Volle, D. H. (2015). Identification of the Link Between the Hypothalamo-Pituitary Axis and the Testicular Orphan Nuclear Receptor NR0B2 in Adult Male Mice. *Endocrinology*, *156*(2), 660–669.

Villareal, D. T., Apovian, C. M., Kushner, R. F., & Klein, S. (2005). Obesity in Older Adults: Technical Review and Position Statement of the American Society for Nutrition and NAASO, The Obesity Society. *Obesity Research*, *13*(11), 1849–1863.

Wang, B., & Du, Y. (2013). Cadmium and its neurotoxic effects. *Oxidative Medicine and Cellular Longevity*, *2013*, 898034.

Wang, Xiaohua, Xu, G., Zhang, J., Wang, S., Ji, M., Mo, L., Zhu, M., Li, J., Zhou, G., Lu, J., & Chen, C. (2019). The clinical and prognostic significance of paraoxonase-2 in gastric cancer patients: Immunohistochemical analysis. *Human Cell*, *32*(4), 487–494.

Wang, Xinkun, & Michaelis, E. K. (2010). Selective neuronal vulnerability to oxidative stress in the brain. *Frontiers in Aging Neuroscience*, *2*, 12–12.

Whitehouse, P. J., Price, D. L., Clark, A. W., Coyle, J. T., & DeLong, M. R. (1981). Alzheimer disease: Evidence for selective loss of cholinergic neurons in the nucleus basalis. *Annals of Neurology*, *10*(2), 122–126.

Wirdefeldt, K., Adami, H.-O., Cole, P., Trichopoulos, D., & Mandel, J. (2011). Epidemiology and etiology of Parkinson's disease: A review of the evidence. *European Journal of Epidemiology*, *26 Suppl 1*, S1-58.

Witte, I, Altenhöfer, S., Wilgenbus, P., Amort, J., Clement, A. M., Pautz, A., Li, H., Förstermann, U., & Horke, S. (2011). Beyond reduction of atherosclerosis: PON2 provides apoptosis resistance and stabilizes tumor cells. *Cell Death & Disease*, *2*(1), e112.

Witte, Ines, Foerstermann, U., Devarajan, A., Reddy, S. T., & Horke, S. (2012). Protectors or Traitors: The Roles of PON2 and PON3 in Atherosclerosis and Cancer. *Journal of Lipids*, *2012*, 342806.

Wong, W. (2020). *Economic Burden of Alzheimer Disease and Managed Care Considerations*. *26*, S177–S183.

Wright, R. O., & Baccarelli, A. (2007). Metals and Neurotoxicology. *The Journal of Nutrition*, *137*(12), 2809–2813.

Wyss-Coray, T. (2016). Ageing, neurodegeneration and brain rejuvenation. *Nature*, *539*(7628), 180–186.

Yang, S., Yang, Y., Yu, P., Yang, J., Jiang, X., Villar, V. a. M., Sibley, D. R., Jose, P. A., & Zeng, C. (2015). Dopamine D1 and D5 receptors differentially regulate oxidative stress through paraoxonase 2 in kidney cells. *Free Radical Research*, *49*(4), 397–410.

Yang, Y., Zhang, Y., Cuevas, S., Villar, V. A., Escano, C., D Asico, L., Yu, P., Grandy, D. K., Felder, R. A., Armando, I., & Jose, P. A. (2012). Paraoxonase 2 decreases renal reactive oxygen species production, lowers blood pressure, and mediates dopamine D2 receptor-induced inhibition of NADPH oxidase. *Free Radical Biology & Medicine*, *53*(3), 437–446.

Zhou, J., Cheng, Y., Tang, L., Martinka, M., & Kalia, S. (2016). Up-regulation of SERPINA3 correlates with high mortality of melanoma patients and increased migration and invasion of cancer cells. *Oncotarget*, *8*(12), 18712–18725.

Appendix A

Expression of PON2 and Measurement of Cellular Death in CGNs after 24-hour Exposure to Heavy Metals Manganese and Cadmium

A.1 – Introduction

Heavy metals manganese and cadmium are widespread environmental pollutants. While manganese is an essential nutrient and serves an important physiological role, exposure to high levels can pose a significant health concern. Conversely, cadmium is non-essential and has no physiological function (Wright & Baccarelli 2007). These metals accumulate in the brain and can impact cognition, memory and motor function (Roels et al., 2012; Wang & Du 2013; Nyarko-Danquah 2020). Both metals have a pronounced oxidative stress component to their proposed toxicity pathways, with manganese disrupting glutamatergic signaling and leading to Ca^{2+} mediated oxidative stress (Erikson & Aschner 2003), and cadmium thought to cause mitochondrial dysfunction by acting as a decoupling agent and inhibiting many of the electron transport chain complexes, leading to cell death as well as ROS generation and oxidative damage (Branca et al., 2020). These mechanisms of action suggest antioxidants as an important defense against metal toxicity. Experimental evidence supports this, with treatment with the antioxidant N-acetyl-L-cysteine (NAC) able to protect neurons from cadmium-induced cell death (Chen et al., 2015). Similarly, antioxidant and anti-inflammatory agents have been demonstrated to protect against manganese-mediated oxidative injury in neurons (Milatovic et al., 2012).

Given the role of PON2 in the mitochondria as an antioxidant and the oxidative stress mechanisms of toxicity for both manganese and cadmium, which are thought to be mitochondrial

mediated, we sought to determine if PON2-def neurons were more sensitive to metal toxicity by manganese and cadmium.

A.2 – Results

Upon 24-hour exposure to manganese at two concentrations, 25 and 100 μM, and cadmium at two concentrations, 0.45 and 3 μM, no increase in PON2 protein expression was observed in WT neurons compared to control (Figures A.2.1A and B).

Cell viability as measured by MTT assay displayed no sensitivity differences between WT and PON2-def neurons when exposed to manganese (Figure A.2.2A) or cadmium (Figure A.2.2B).

A.3 – Figures

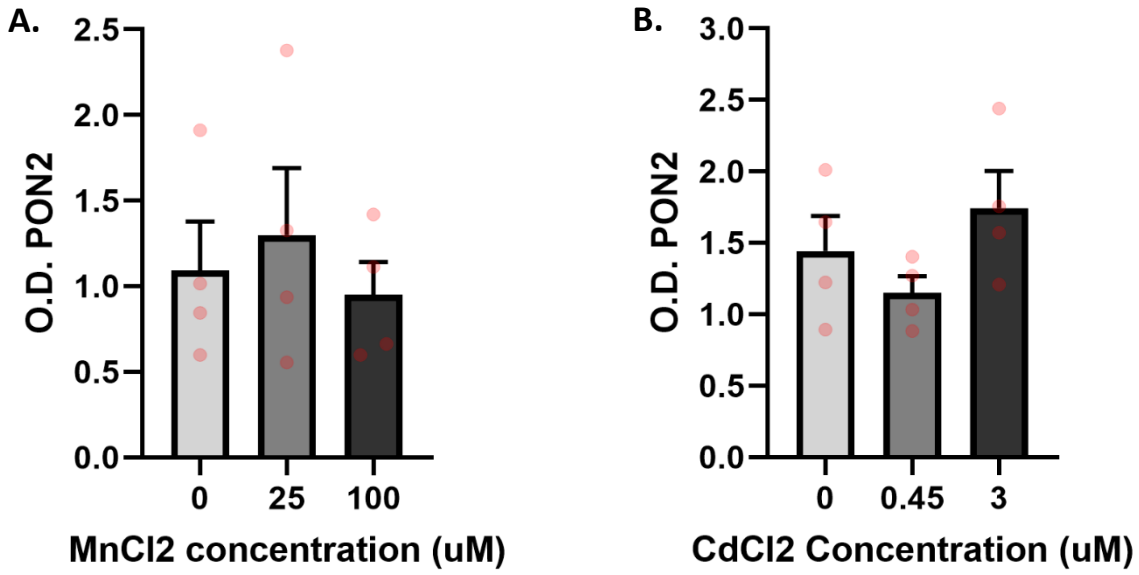

Figure A.2.1 – PON2 Protein Expression in Neurons After 24-hour Exposure to Manganese and Cadmium. A. PON2 protein after 24-hour exposure to 0, 25 and 100μM manganese chloride ($MnCl_2$), n = 4 per group. **B**. PON2 protein after 24-hour exposure to 0, 0.45 and 3 μM cadmium chloride ($CdCl_2$), n = 4 per group.

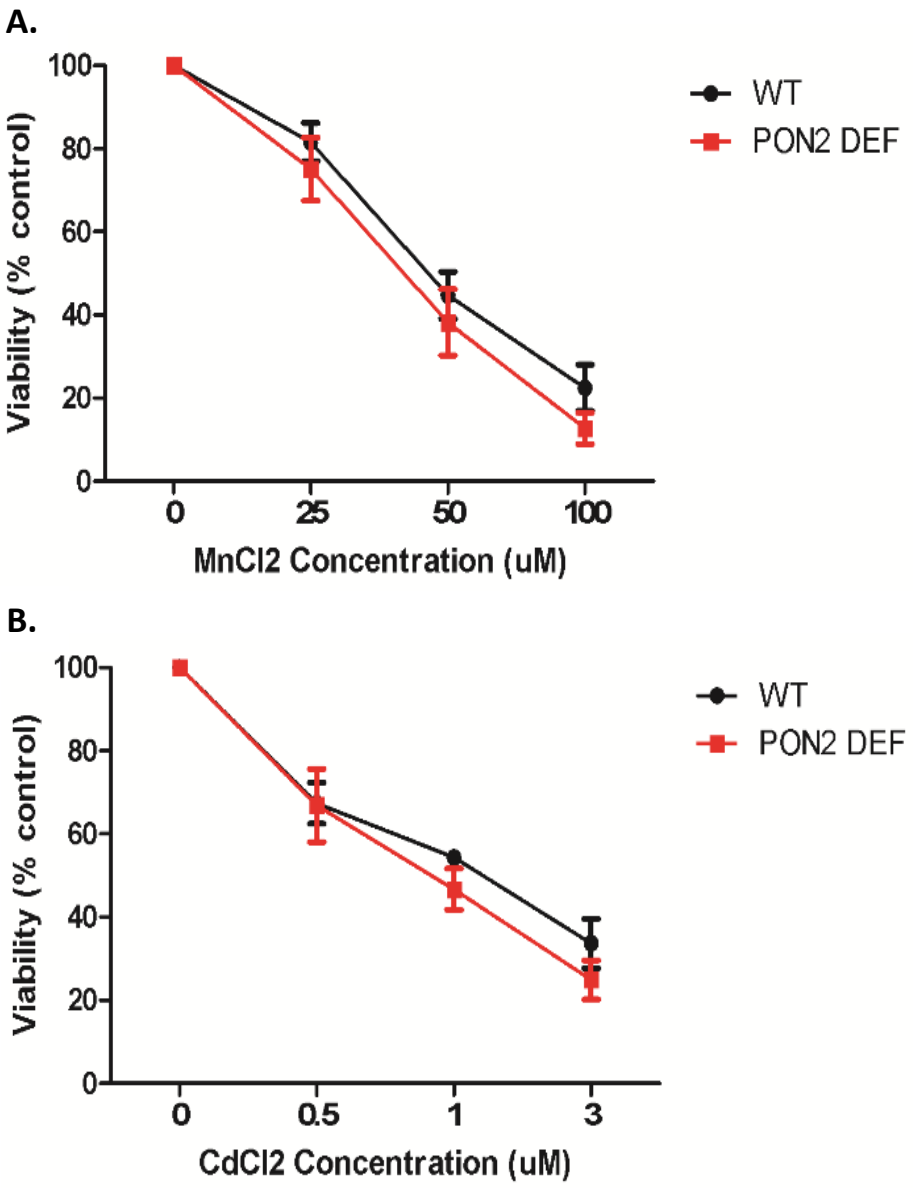

Figure A.2.2 – Viability of WT and PON2-def Neurons after 24-hour Exposure to Manganese and Cadmium. A. Viability as % control measured by MTT assay after 24-hour exposure to 0, 25,50 and 100 μM manganese chloride ($MnCl_2$), n = 4 per group. **B**. Viability as % control measured by MTT assay after 24-hour exposure to 0, 0.5, 1 and 3 μM cadmium chloride ($CdCl_2$), n = 4 per group.

A.4 – Discussion

No differences in PON2 protein level were noted in WT neurons exposed to manganese and cadmium, nor were PON2-def neurons more sensitive to manganese and cadmium compared

to WT cells. These results were unanticipated, as PON2-def neurons are reported to have higher levels of oxidative stress and be sensitive to oxidative compounds (Giordano et al., 2011; Giordano et al., 2013), and it was anticipated that heavy metals would function as oxidative compounds in these cell types. Potentially, our *in-vitro* methods were unable to capture the complex toxicological effects of metals in the nervous system, particularly as they relate to oxidative stress. The brain is comprised of multiple cell types, principally falling into two categories of glial cells and neurons. Our *in-vitro* system utilized pure neuronal cultures, which does not allow for important glial feedback to take place and could impact the functionality of the neurons and alter their transcriptional profile. Astrocytes are known to sequester heavy metals, particularly manganese, and generate oxidative stress feedback loops through glutamate excitotoxicity which contribute to neurological disease (Li et al., 2021). Indeed, a primary mechanism proposed for manganese neurotoxicity is the interruption of the glutamine/glutamate cycling between astrocytes and neurons, leading to perturbations in glutamate metabolism and GABAergic signaling (Sidoryk-Wegrzynowicz & Aschner 2013). To test whether the presence of astrocytes impacts these results, comparing monocultures of neurons and astrocytes to co-culture systems comprised of both neurons and astrocytes would be of value, as well as investigation if *in-vivo* effects of heavy metal toxicity in PON2-def mice. Furthermore, PON2 deficiency may not be sufficient to cause observable differences in survivability upon metal exposure. These experiments should be repeated utilizing primary cells from a full PON2 knockout model with the co-culture system discussed in chapter 6 to determine if the loss of PON2 effects metal sensitivity.

A.2 – Materials and Methods

Materials

Anti-PON2 antibody was purchased from Genscript (Piscataway, NJ, USA). Anti β-actin antibody, papain, poly-D-lysine, DMSO and MTT [3-(4,5-dimethyltiazol-2-yl)-2,5 diphenyltetrazolium bromide] were purchased from MilliporeSigma (Burlington, MA, USA). Anti-rabbit IgG HRP-linked antibody and Cell Lysis Buffer 10x were purchased from Cell Signaling Technology (Danvers, MA, USA). HRP Goat Anti-Mouse IgG was purchased from BD Biosciences (San Jose, CA, USA). XCell II Blot Module, XCell SureLock Electrophoresis Cell, NuPAGE MOPS SDS Running Buffer 20x, NuPAGE LDS Sample Buffer 4x, NuPAGE Antioxidant, NuPAGE Sample Reducing Agent 10x, NuPAGE 10% Bis-Tris Protein Gels, Neurobasal-A medium, B-27 supplement with and without antioxidant, fungizone, HBSS medium (No Ca2+) and 10 mM HEPES were purchased from Life Technologies (Carlsbad, CA, USA). Immobilon-P Transfer Membrane was purchased from Millipore Corporation (Billerica, MA, USA). Restore Western Blot Stripping Buffer, PageRuler Prestained Protein Ladder, SuperSignal West Pico Chemiluminescent Substrate and Costar 6 and 24-well TC plates were purchased from Thermo Fisher Scientific (Waltham, MA, USA).

Primary Cell Culture

Cerebellar granule neurons (CGNs) were prepared from PND 7 mice, as described by Giordano et al., 2006. Neurons were grown for 10-12 days before treatments. Briefly, cerebellar tissue was collected in chilled HBSS medium (No Ca2+) and 10 mM HEPES. Tissues were digested for 30 min in HBSS containing papain (1 mg/ml) and DNAse I (40 μg/ml) and centrifuged at 300 × *g* for 7 min at room temperature. The supernatant (containing papain) was removed, and the pellet was gently triturated in Neurobasal-A Medium supplemented with B27 (Life Technologies,

Carlsbad, CA). Cells were centrifuged at 200 × *g* at 4°C for 10 min and the cell pellet was gently resuspended in medium. Neurons were then counted, seeded on poly-D-lysine coated 6-well or 24-well plates at a density of 5×10^4 / cm^2, and cultured in Neurobasal-A medium supplemented with B27. After 4 days, media was completely exchanged for Neurobasal-A Medium with B27 minus antioxidants (-AO). Cells were incubated with manganese chloride ($MnCl_2$) at concentrations of 25 and 100 μM, or cadmium chloride ($CdCl_2$) at concentrations of 0.45 and 1 μM for 24 hours. After the 24-hour exposure, cells used for immunoblotting were scraped from the culture dish using a rubber policeman and collected in ~100 μL RIPA buffer.

Immunoblotting

Immunoblots were carried out as previously described (Garrick et al., 2016). Briefly, 15 μg of protein was mixed with SDS running buffer and sample reducing agent and subjected to sodium dodecyl sulfate-polyacrylamide gel electrophoresis (SDS-PAGE). Following electrophoresis, proteins were transferred to polyvinylidene difluoride membranes and the membrane blocked for 1-3 hours with 5% nonfat milk. Membranes were then probed with anti-PON2 primary antibody at a dilution of 1:2000. Following primary antibody incubation, membranes were washed with Tris-buffered saline with 0.1% Tween-20 (pH = 7.5) and incubated with horseradish peroxidase-conjugated anti-rabbit secondary antibody at a dilution of 1:5000. Membranes were stripped with Restore Western Blot Stripping Buffer (Thermo Fisher Scientific, Waltham, MA) and re-probed for β-actin using a dilution of 1:2500 for the β-actin primary antibody and 1:2500 for the horseradish peroxidase-conjugated anti-mouse secondary antibody. Intensity of bands was measured by densitometry using ImageJ software (NIH), with the band intensity normalized to β-actin expression.

MTT Cell Viability Assay

Cell viability was quantified using a colormetric assay with metabolic dye MTT [3-(4,5-dimethyltiazol-2-yl)-2,5 diphenyltetrazolium bromide] as previously described (Giordano et al., 2011). In this assay, metabolically active cells uptake the yellow MTT dye and convert it to an insoluble purple formazan which is then spectrophotometrically measured. Cells in 24-well plates were treated with either $MnCl_2$ or $CdCl_2$ for 24 hours at 37 °C. At the end of exposure, media was aspirated and cells were incubated with 500 μL/well of PBS containing 4 μg/mL MTT for 30 minutes. MTT solution was removed, and the precipitated formazan reaction product was dissolved in 250 μL DMSO/well. The absorbance was read at 570 nm in a SpectraMax 190 microplate reader (Molecular Devices, San Jose, CA, USA), and results expressed as percent viability relative to controls.

Appendix B

Differentially Expressed Genes in Paraoxonase 2 Deficient Brain Regions Compared to WT

P < 0.1

Table AB.1 – Differentially Expressed Genes in Male Cortex

Upregulated

Symbol	logFC	adjpv
Gm14288	2.803566	0.054071
4930565N06Rik	2.117063	0.080623
4930573H18Rik	1.868875	0.087124
BC046401	1.057436	0.065347
Sytl5	0.882867	0.061773
Tnfrsf25	0.871722	0.046644
Zfp382	0.814079	0.024591
Arid3b	0.767804	0.001946
Cln8	0.696956	0.054744
Sned1	0.696874	0.087124
Dusp4	0.686816	0.078665
Pou2f1	0.679478	0.05649
Per1	0.667522	0.064305
Frmd6	0.650983	0.012042
Per2	0.644522	0.027458
Tmem104	0.631096	0.054071
Uprt	0.602583	0.068122
Klf10	0.582503	0.054562
Vipr1	0.572082	0.064305
Phf21b	0.550546	0.087686
Zfp366	0.550313	0.097338
Fbxo28	0.549759	0.093814
A730060N03Rik	0.548858	0.046644
Gm14403	0.532902	0.092842
E130308A19Rik	0.531699	0.053706
Htr1b	0.531253	0.092254
Zfp800	0.528057	0.069745
Bhlhe40	0.506137	0.061773
Sntb2	0.502267	0.034144

Downregulated

Symbol	logFC	adjpv
Pon2	-4.10883	0.000001
Gm19918	-3.63213	0.054071
Accsl	-2.60465	0.087124
Nek5	-1.97873	0.077154
1700012B09Rik	-1.95579	0.093083
Dnajb13	-1.9326	0.066295
Cxcl5	-1.85386	0.053706
Gm3752	-1.78233	0.077154
Il2rb	-1.65307	0.05649
Acpp	-1.38592	0.070556
Ebf3	-1.3124	0.093814
0610009E02Rik	-1.18797	0.046644
Calb2	-1.18108	0.082062
Tstd1	-1.16649	0.059953
Gm4349	-1.01594	0.092842
Ppp1r32	-0.98065	0.078665
Best1	-0.9557	0.078665
Cdca7l	-0.9515	0.09792
Dnah7b	-0.90729	0.082065
Gm3252	-0.90543	0.087686
Olfr1192-ps1	-0.86521	0.068002
BC051077	-0.83645	0.053706
Gm10432	-0.80785	0.046978
Btg2	-0.76711	0.054071
A430110L20Rik	-0.76134	0.035644
Ms4a6d	-0.71469	0.064305
Lama4	-0.68894	0.064305
Gm14634	-0.6688	0.087686
Grk4	-0.64629	0.046644

Cdc73	0.498864	0.054562
Btaf1	0.495689	0.068605
Map3k13	0.481276	0.011877
D030047H15Rik	0.475381	0.076114
Dnajb5	0.473951	0.087686
Pcdhb16	0.4688	0.053706
Cpeb3	0.460482	0.096231
Tet3	0.457045	0.000271
Nfkbid	0.448408	0.046644
Drd1	0.443774	0.090172
Wac	0.437395	0.03535
Igsf9b	0.428093	0.024591
Zfp882	0.420827	0.087686
Wdr47	0.407467	0.014388
Cchcr1	0.406605	0.09792
Mn1	0.398008	0.065778
Wdr90	0.394959	0.093814
Zc3h11a	0.391031	0.094699
Nab2	0.387442	0.082062
Atrx	0.38538	0.094699
Fras1	0.380508	0.064305
Ttc39b	0.378577	0.054071
Irs2	0.377014	0.064305
Lss	0.375702	0.065347
Zfp397	0.3755	0.053706
Gtf2ird1	0.36214	0.096806
Kdm3a	0.361975	0.054071
Acap2	0.352268	0.046978
Spred3	0.35167	0.09792
Myt1l	0.346497	0.068605
Ankrd33b	0.338962	0.06901
Mlec	0.336859	0.080692
Ern1	0.335648	0.080692
Tnrc6a	0.33092	0.087686
Hectd2	0.330875	0.068605
Pot1a	0.329066	0.087686
Iws1	0.327681	0.067872
Zfp948	0.326566	0.054642
Pik3c2b	0.323577	0.088275
Fam13b	0.321768	0.068493
Zhx3	0.320652	0.024591

Nrn1l	-0.62795	0.087686
Cd274	-0.6055	0.094699
Rad54l	-0.58614	0.086044
H1f2	-0.51275	0.068683
Phf7	-0.49094	0.065347
A230059L01Rik	-0.48841	0.071539
Ift74	-0.47709	0.093814
1110046J04Rik	-0.47294	0.076114
Txnrd2	-0.47111	0.015056
4930511M06Rik	-0.45724	0.05649
Aldh3b1	-0.44081	0.064305
Gm42418	-0.40577	0.065347
Mthfsl	-0.39055	0.058662
Gm9776	-0.3896	0.064305
Tmem117	-0.38898	0.094699
Gart	-0.3844	0.091214
A230103L15Rik	-0.36422	0.088275
2410006H16Rik	-0.32743	0.090375
Vmn2r115	-0.32711	0.054642
Klf11	-0.32549	0.05332
Cyth4	-0.32523	0.054071
Smim26	-0.32334	0.046644
Rnaset2a	-0.3207	0.068683
Chchd5	-0.31687	0.068605
Pskh1	-0.31565	0.087686
Rps27rt	-0.30754	0.024591
Dalrd3	-0.30688	0.068253
Mex3b	-0.30505	0.068605
Uqcr11	-0.30488	0.046644
Ndufc1	-0.29939	0.077872
Ppp1r14b	-0.29486	0.054861
Tmsb10	-0.29027	0.056107
Med30	-0.28996	0.087124
Olfr338	-0.2892	0.087686
Scand1	-0.28128	0.087686
Nfkbil1	-0.28	0.05649
Nkain4	-0.27988	0.064305
Ccdc166	-0.27081	0.096231
Snrpa	-0.26236	0.067109
Ttc30b	-0.26212	0.094699
Rpl30	-0.26086	0.054861

Lztfl1	0.319384	0.068683
Brwd3	0.319243	0.093814
Ercc6	0.319199	0.024591
Ide	0.314363	0.05649
Aak1	0.314146	0.09792
Atxn7	0.31265	0.05649
Tmem229b	0.306402	0.082062
Skil	0.30541	0.054071
Nufip2	0.303084	0.054071
Tada2b	0.302118	0.054562
Wdr37	0.29799	0.05649
Luc7l	0.297562	0.077363
Plekha6	0.293457	0.035644
Zfp106	0.290872	0.086044
Srpk1	0.290806	0.09792
Apc	0.290362	0.068605
Zfp142	0.28947	0.092842
Dusp11	0.28922	0.097041
Pde7a	0.288795	0.082757
Gxylt1	0.288299	0.046644
Fam193a	0.28742	0.066932
Sec24c	0.286384	0.046978
Prdm2	0.28501	0.047377
Unc13a	0.284214	0.093853
Wnk1	0.284085	0.042156
Itga1	0.282657	0.066932
Mettl17	0.280575	0.092842
Chuk	0.280375	0.053706
Tapt1	0.277174	0.046644
Snap23	0.276414	0.091104
Ube2d3	0.275265	0.073556
Dhx57	0.273873	0.024591
Akap10	0.269404	0.095747
Pspc1	0.268709	0.087686
Kmt2e	0.266613	0.067671
Zbtb26	0.266483	0.093814
Scd1	0.265309	0.090375
Kif21b	0.264706	0.078665
Ccnh	0.263744	0.064305
Ccdc93	0.263294	0.065716
Kmt5a	0.260353	0.067109

Grcc10	-0.25552	0.058662
Akr1b3	-0.25035	0.066295
Marveld1	-0.23813	0.094186
Yipf2	-0.23537	0.077154
Zfp90	-0.23249	0.087124
Fam210b	-0.22843	0.066932
Msrb1	-0.22697	0.09792
Mrps9	-0.22626	0.05649
Spata7	-0.22595	0.073584
Hmgn2	-0.22345	0.046425
Slc12a9	-0.22281	0.084761
Ppp2r1a	-0.22213	0.094699
Dut	-0.21774	0.074968
Inafm1	-0.21434	0.082062
Sox12	-0.2134	0.073409
Rps12	-0.21219	0.064305
Arl2	-0.21125	0.073556
Rps19	-0.20867	0.080623
Rplp2	-0.19997	0.064305
Med28	-0.19358	0.068605
Rpl17	-0.18403	0.061773
Igsf8	-0.17752	0.064305
Pcsk1n	-0.16973	0.087686
Rtl8b	-0.16634	0.06963
Gas5	-0.15922	0.091214
1500011B03Rik	-0.15269	0.082532

Osbpl8	0.260208	0.08111
Epc2	0.259268	0.092842
Map7	0.258841	0.097807
Gm35040	0.258071	0.082757
Pum2	0.257891	0.041146
Arhgef3	0.25779	0.046644
Arih1	0.25695	0.065347
Gng12	0.252819	0.087686
Myh9	0.252172	0.09792
Ric1	0.24946	0.042156
Kmt2a	0.249125	0.078601
Slc25a51	0.247279	0.087686
Trip12	0.24482	0.093814
Acap3	0.243712	0.088275
Zmynd8	0.242687	0.053706
Pou6f1	0.241556	0.054071
Dpp8	0.239289	0.082062
Smg7	0.238705	0.054562
Numb	0.237242	0.097627
Kdm7a	0.236295	0.054562
Tbc1d10b	0.235825	0.084392
Mtmr4	0.235615	0.064305
Oxct1	0.23394	0.076114
1810013L24Rik	0.232943	0.051365
Zfp27	0.232827	0.068683
C2cd5	0.231125	0.084392
Add2	0.230986	0.061773
Ttc3	0.229573	0.05649
Arel1	0.229413	0.094699
Tub	0.226665	0.087686
Specc1	0.225636	0.077363
Pkn2	0.225582	0.087686
Socs5	0.224924	0.053706
Ints10	0.224558	0.041146
Zfp326	0.219806	0.081603
Aopep	0.217817	0.084392
Mpp3	0.217641	0.068605
Arl8b	0.21632	0.061773
Fbrsl1	0.213809	0.068605
Arnt	0.213809	0.087686
Lonrf1	0.212871	0.058662

Cramp1l	0.209105	0.097505
Pdcd6ip	0.2078	0.064305
Capza2	0.202426	0.087124
Bicdl1	0.202029	0.064305
Gramd1b	0.201369	0.046644
Mdm2	0.199333	0.065347
Hnrnpll	0.199108	0.040191
Rnf24	0.198596	0.097338
Otud5	0.197358	0.068122
Phf20l1	0.195697	0.067109
Slc20a1	0.194102	0.054562
Ash1l	0.192972	0.093814
Ccnt2	0.192558	0.082062
Irf2bpl	0.191843	0.054642
Ncoa7	0.19119	0.05649
Rrp12	0.188895	0.065347
Zkscan3	0.188808	0.054562
Gapvd1	0.182549	0.073584
Vps37a	0.181796	0.077363
Ppp1r12a	0.181125	0.064305
Prickle2	0.179671	0.09792
Trim33	0.178273	0.064305
Usp7	0.175984	0.068605
Itch	0.174627	0.068122
Rfx7	0.173934	0.06901
Nsf	0.173151	0.068605
Ccdc47	0.172243	0.093814
Tmem63b	0.170796	0.078266
Wdr48	0.170001	0.077363
Rab6b	0.169411	0.092842
Btbd1	0.16152	0.087124
Usp31	0.155465	0.091214
Mau2	0.151358	0.087686
Mapre2	0.151101	0.084392
Adam9	0.139518	0.087686
Cdc37l1	0.137078	0.087686
Trappc11	0.135323	0.068605
Mia3	0.127157	0.091214
Spin1	0.12659	0.046644

Table AB.2 – Differentially Expressed Genes in Female Striatum

Upregulated

Symbol	logFC	adjpv
Aspm	1.18108	0.042016
St8sia2	0.692292	0.035705
Mex3a	0.609444	0.035705
Gm15328	0.496583	0.0897
Arhgap19	0.458044	0.047729
Dlx6os1	0.404042	0.078437
Slc5a3	0.398034	0.090986
Nup205	0.384648	0.006912
Dusp11	0.34725	0.090986
1700086L19Rik	0.316344	0.046964
C2cd5	0.30559	0.035705
Zdhhc23	0.303638	0.053496
Ophn1	0.302411	0.078437
Ccnt2	0.246125	0.056208

Downregulated

Symbol	logFC	adjpv
Pon2	-3.59774	0.000001
Nr0b2	-2.73571	0.035705
Wnt9b	-2.44427	0.078437
Abhd12b	-2.06668	0.010553
D830039M14Rik	-1.90703	0.042555
4930426L09Rik	-1.31336	0.035705
Rab37	-1.27024	0.026926
Kcng4	-1.11971	0.035705
Pvalb	-1.09676	0.002766
Fzd10	-0.99203	0.04638
Ramp3	-0.96909	0.035705
Plekhd1	-0.79926	0.029861
Lef1	-0.73992	0.035705
Plekhg1	-0.73491	0.055345
Wnt3	-0.72706	0.035705
Nefh	-0.65021	0.035705
Flt3	-0.62243	0.078437
Vamp1	-0.59552	0.035705
Adssl1	-0.53186	0.041246
Esrrg	-0.52263	0.035705
Nr1d1	-0.48598	0.078437
Lhfp	-0.48104	0.035705
Gm13375	-0.37991	0.078437
Kndc1	-0.3592	0.04638
Kcnc3	-0.35729	0.04638
Lgi3	-0.35327	0.003443
Eci1	-0.34268	0.079294
Sgpp2	-0.33578	0.066219
Scrt1	-0.32122	0.078437
Fndc5	-0.31949	0.078437
Abhd11	-0.29654	0.035705
Tmem218	-0.29623	0.085789
Cygb	-0.28856	0.046964
H1f0	-0.28322	0.035705
Chmp6	-0.27357	0.078437

Grsf1	-0.25927	0.078437
Rab4b	-0.25553	0.035705
Diras1	-0.24857	0.035705
Fbxo2	-0.24802	0.078437
Ccdc124	-0.24685	0.082445
Adh5	-0.23367	0.052936
Csrp1	-0.21969	0.047729
Stmn4	-0.218	0.078437
Ubxn1	-0.21649	0.035705
Hepacam	-0.21376	0.041246
Paqr4	-0.21103	0.053154
Cadm4	-0.20986	0.078437
Pfkm	-0.19238	0.01223
Slc25a4	-0.17212	0.079294
Pkm	-0.13308	0.066219

Table AB.3 – Differentially Expressed Genes in Male Cerebellum

Upregulated

Symbol	logFC	adjpv
Gm6013	2.198032	0.063242
Gm12161	1.700806	0.095712
Nr4a3	1.401588	0.044706
Gm30524	1.331487	0.088447
Gimap5	1.139457	0.059976
C4a	1.118585	0.079046
Spry4	1.078767	0.004288
Gm14246	1.010196	0.090335
Dusp4	1.006434	0.010782
Eomes	0.949624	0.028981
Gm30191	0.865738	0.077372
Emilin2	0.839269	0.077372
Gm3294	0.792356	0.000001
Col11a2	0.782132	0.056536
Per2	0.757633	0.004387
Dusp6	0.724955	0.059976
Plk3	0.716809	0.045628
Per1	0.698756	0.056267
Gm17344	0.682392	0.05303
Mapkapk3	0.630401	0.006608
Mfsd2a	0.626945	0.020783
Cln8	0.620173	0.070316
Bcl6	0.613757	1.11E-05
Banp	0.583903	0.06359
Cpt1b	0.581709	0.076419
Frmd6	0.580761	0.024995
Fam227a	0.569012	0.023783
Gm33466	0.553318	0.023078
Spred2	0.550251	0.01944
D11Wsu47e	0.537211	0.079046
Rad51c	0.536018	0.045159
Acrbp	0.515948	0.003746
Prag1	0.507759	0.004234
Atg16l2	0.503815	0.002672
Galnt7	0.474568	0.017183

Downregulated

Symbol	logFC	adjpv
Pon2	-6.03897	0.000001
Xist	-3.12327	0.01944
Rsph14	-1.87994	0.095712
Fut7	-1.65348	0.063133
Asb4	-1.64355	0.088312
G630030J09Rik	-1.42806	0.089834
Cxcr4	-1.30085	0.01502
Gm12977	-1.20417	0.044706
1700020N18Rik	-1.11232	0.088312
Caps2	-0.96099	0.070224
Gm31812	-0.93777	0.046444
Pln	-0.93473	0.062656
Glipr1	-0.88078	0.077461
E430024P14Rik	-0.79254	0.089057
Gm5628	-0.76728	0.033957
Abi3	-0.70864	0.07608
Aacs	-0.64759	0.032444
Lrrc32	-0.6346	0.016541
Il10ra	-0.60613	0.01502
B830017H08Rik	-0.59856	0.069708
Nsl1	-0.57273	0.020783
5330437M03Rik	-0.5352	0.084796
Plin2	-0.53093	0.017183
Rara	-0.4726	0.004438
Galnt15	-0.46168	0.003746
Zfp811	-0.45479	0.00176
Hdac4	-0.44634	0.016122
Lrrc56	-0.43947	0.089834
Zscan2	-0.42328	0.033163
Ehhadh	-0.41015	0.057554
Nrde2	-0.40847	0.06244
Gm42418	-0.40033	0.019615
Ubtd1	-0.39444	0.017673
A930017K11Rik	-0.39023	0.075343
Sstr3	-0.38794	0.077372

Grk4	0.471285	0.082373
Ifrd2	0.467724	0.029054
C2cd3	0.455059	0.063988
Bud13	0.449961	0.060031
Mafg	0.442793	0.002672
Rif1	0.439007	0.001306
A930024E05Rik	0.438862	0.000557
Tbc1d31	0.436604	0.030258
Helz2	0.435793	0.049126
Nrd1	0.412975	0.07795
Pla2g3	0.412864	0.023078
Rpgrip1l	0.412118	0.023078
Tex10	0.411323	0.020783
Spata2l	0.408006	0.070912
Dusp16	0.402908	0.000922
Fv1	0.401344	0.074382
Hps4	0.394212	0.070584
Kifc5b	0.385952	0.089834
Cacna1b	0.380192	0.028949
Rnft1	0.377903	0.059976
Ndor1	0.37489	0.033455
Usp37	0.37158	0.037297
Tjap1	0.370555	0.02517
Cnksr3	0.367821	0.004438
Zfp384	0.361755	0.004988
Abcc8	0.359001	0.012796
Prox1	0.351631	0.070912
Dusp11	0.344771	0.017183
Gls2	0.34197	0.043797
Plat	0.322519	0.016622
Nuak1	0.321138	0.076419
Srpk1	0.314971	0.079738
Cry1	0.313229	0.037357
Dgat1	0.312693	0.021992
Zfp397	0.312277	0.045628
Gtpbp2	0.311019	0.029571
Daam2	0.309177	0.01502
Snx30	0.309043	0.01944
Slc2a8	0.306842	0.017183
Fbrs	0.304182	0.036838
Ikbkb	0.303343	0.018549

Axin2	-0.3866	0.017183
Gm3854	-0.37508	0.025888
Parp16	-0.37473	0.051002
Sox9	-0.36031	0.049698
Elp4	-0.3512	0.07884
Xpa	-0.3504	0.017673
Nusap1	-0.34435	0.075315
Zc3h6	-0.32902	0.079738
Pum3	-0.32546	0.055934
Ripk2	-0.32055	0.081606
Zfp518b	-0.31723	0.05303
Ppp1r18	-0.30967	0.024995
Ccdc34	-0.30651	0.052704
Ptms	-0.29994	0.025888
Zfp867	-0.29363	0.01944
Nupl2	-0.29149	0.088485
E330034L11Rik	-0.29111	0.059976
Ppargc1b	-0.28664	0.073559
Ptk7	-0.28127	0.070584
Zmat2	-0.28071	0.004438
Wdr11	-0.27973	0.041713
Pak4	-0.27159	0.065455
Triobp	-0.26999	0.079738
Nfib	-0.26812	0.062656
Fzd7	-0.26538	0.077431
Chmp6	-0.26345	0.025888
Slc7a8	-0.26277	0.01502
Zcchc17	-0.26119	0.046393
Ing5	-0.26035	0.039764
Lyar	-0.25594	0.061284
Bet1l	-0.25388	0.025888
Kcnq1ot1	-0.24509	0.069708
Lonrf1	-0.24244	0.077372
Acsl1	-0.24005	0.055934
Toe1	-0.23651	0.077461
Pla2g15	-0.23374	0.030258
Nucks1	-0.23256	0.003631
Spata7	-0.22718	0.061284
H1f0	-0.21012	0.043797
Anp32b	-0.20284	0.077372
Elavl3	-0.19064	0.024968

Nsun5	0.299782	0.0753
Eif4g1	0.299119	0.01502
Map3k13	0.298091	0.067777
Rtn4rl1	0.293896	0.039741
Crhr1	0.293392	0.075343
Emsy	0.290976	0.020783
Arrb2	0.290948	0.040248
Itsn2	0.287535	0.077461
Mxi1	0.287349	0.025664
Afap1l2	0.286843	0.044094
Zmym3	0.283283	0.0753
Zgpat	0.282908	0.016629
Abca8b	0.282059	0.004193
Zfp446	0.278302	0.020783
Arl5a	0.273188	0.003746
Zfp324	0.271014	0.04845
Slx4	0.268577	0.029054
Txndc11	0.266173	0.037357
Gdap2	0.265808	0.089333
Leng8	0.263298	0.082373
Traf6	0.262369	0.040997
Car4	0.258892	0.043797
Pdss1	0.257015	0.025664
Aifm3	0.254988	0.077372
Nsd3	0.254765	0.01502
Fgfr1	0.25169	0.020783
Tra2a	0.249946	0.05172
Glt8d1	0.249215	0.085065
Rabggta	0.244522	0.01944
Ascc2	0.244157	0.043035
Extl2	0.24414	0.072543
Sidt2	0.243887	0.01944
Ap1g1	0.241726	0.023078
Chka	0.238388	0.049126
Zdhhc5	0.238196	0.012796
Sec24c	0.236767	0.067028
Ppm1f	0.235426	0.036838
Ypel4	0.231918	0.06359
Eif6	0.231673	0.070316
Zfp946	0.228635	0.04845
Nvl	0.227633	0.012796

Cfap97	-0.17973	0.07795
Kank2	-0.17839	0.054055
Rc3h2	-0.17679	0.074382
Hmgn2	-0.17558	0.095774
Clic1	-0.17519	0.099492
Ak1	-0.17314	0.030405
Slc39a1	-0.17192	0.028975
Zrsr1	-0.17091	0.038969
Gtf3c3	-0.16181	0.070021
Fam131b	-0.15898	0.06359
Actb	-0.15525	0.07795
Rrp1	-0.1502	0.043797
Ambra1	-0.15001	0.01944
Pura	-0.14629	0.074382
Eid1	-0.1332	0.055989
Spop	-0.13283	0.036838
Rab1b	-0.1261	0.05359
Rab11b	-0.11733	0.049698

Lsm8	0.222953	0.089834
Supt20	0.222294	0.07795
Madd	0.221771	0.062656
Foxj2	0.221256	0.056997
Usp19	0.219859	0.092244
Gas2l1	0.218833	0.062656
Cdc23	0.218094	0.029054
Pcgf6	0.217406	0.070224
Jmy	0.217002	0.020783
Zswim8	0.215847	0.057554
Arnt	0.214499	0.05303
Smg7	0.214205	0.06439
Ppp1r12c	0.212439	0.092912
Rrnad1	0.212387	0.062656
Lemd3	0.208881	0.029054
Ints7	0.207599	0.07213
Fcho2	0.206121	0.095712
Capn15	0.203312	0.056997
Tbc1d17	0.20285	0.085065
Trmt1l	0.202617	0.056997
Wrap73	0.202271	0.059976
Ak2	0.20113	0.070021
Zw10	0.199094	0.083418
Ccnt2	0.198965	0.052704
Cdc5l	0.198091	0.045628
Stk16	0.196028	0.057306
Rbm10	0.194641	0.01269
Ints10	0.194238	0.056997
Nelfa	0.192395	0.056997
Anks3	0.19189	0.077372
Pdcd6ip	0.191335	0.066992
Prpsap1	0.190765	0.098488
Mtus1	0.190688	0.082373
Mapk14	0.189888	0.027016
Hbs1l	0.189817	0.073559
Ptpn2	0.188872	0.06359
Taf1a	0.188701	0.07884
Entr1	0.183649	0.088176
Grpel2	0.179335	0.091141
Bag6	0.178469	0.043035
Cog6	0.177936	0.069708

Sybu	0.175636	0.07608
Fut11	0.172245	0.077372
Srsf6	0.16631	0.045628
Bicd2	0.165542	0.07795
Rusc2	0.165193	0.079017
Nampt	0.147658	0.079738
Kansl2	0.136797	0.077506
Ap3d1	0.12235	0.070021